REMOVAL OF SULFAMETHOXAZOLE BY ADSORPTION AND BIODEGRADATION IN THE SUBSURFACE:

BATCH AND COLUMN EXPERIMENTS WITH SOIL AND BIOCHAR AMENDMENTS

by

Wenwen Yao

A Dissertation

Submitted in partial fulfillment
of the requirements for the Degree of

Doctor of Philosophy
in
Civil Engineering

January 2018

APPROVED:

Dr. Paul P. Mathisen, Assoc. Professor, Civil and Environmental Engineering, Worcester Polytechnic Institute, Major Advisor

Dr. Mingjiang Tao, Assoc. Professor, Civil and Environmental Engineering, Worcester Polytechnic Institute

Dr. John A. Bergendahl, Assoc. Professor, Civil and Environmental Engineering, Worcester Polytechnic Institute

Dr. David A. Reckhow, Professor, Civil and Environmental Engineering, University of Massachusetts Amherst

ABSTRACT

The wide use and the incomplete metabolism of antibiotics, along with the poor removal efficiency of current treatment systems, results in the introduction of large quantities of antibiotics to the environment through the discharge of treated and untreated wastewater. If not treated or attenuated near the source of discharge, the antibiotics can be distributed widely in the environment. In this research, sulfamethoxazole (SMX), a common sulfonamide antibiotic, was selected as a model compound due to its presence in the environment and its resistance to remediation and natural attenuation. Among the various entry routes, discharges from on-site disposal systems are of particular interest due to the wide use of these systems. The complex nature of subsurface transport downstream of these systems adds difficulties to the removal of SMX from subsurface discharges. For this research, two processes that impact SMX removal, biodegradation and sorption, were examined to determine the primary factors governing the elimination of SMX from septic effluent discharges in the subsurface.

To characterize the biodegradation of SMX, batch experiments were conducted with SMX in the presence of septic effluent and soil for both aerobic and anoxic conditions. Results showed that SMX removal was limited in the septic effluent but increased in the presence of soil, demonstrating the important role of the soil in SMX removal in both aerobic and anoxic conditions. Addition of external nutrients (ammonium and sulfate) had small effects on SMX removal, although SMX removal was enhanced under aerobic condition with increased dissolved organic carbon.

To overcome the limited sorption of SMX on soil, soil amendments were developed and evaluated using biochar, a green and cost-effective adsorbent. Biochars produced from different types of feedstock were characterized for different pyrolysis temperatures, and their adsorption behaviors were examined and compared with commercial biochar and activated carbon (AC). Adsorption isotherms were developed and adsorption kinetics of soil, biochar and AC were studied. Results showed that adsorption on soil, biochar and AC followed three different kinetics models and their equilibrium isotherms followed the Freunlich model. Higher adsorption rates were achieved with biochars prepared at the higher temperature. A lab-engineered biochar with pine sawdust at 500 ˚C achieved comparable sorption capacity to AC.

SMX transport in subsurface was also explored with saturated soil columns filled with soil that was mixed with biochar at different percentages. Significant SMX removal (including complete elimination at a low flowrate and over 90 % elimination at a high flowrate) for all cases was primarily attributed to biodegradation. These results provide insight into the transport and transformations affecting SMX, and then provide a basis for developing low-cost approaches for the mitigation of SMX.

I dedicate this thesis to

My Mother Xiuping, my Father Jinlong, my husband Chi and my beloved son Yubo

for their constant support and unconditional love.

ACKNOWLEDGEMENTS

I would like to sincerely thank my advisor Professor Paul Mathisen for his guidance, insights, support and friendship throughout my PhD years in WPI. I would also like to thank my committee members Professor John Bergendahl, Professor Mingjiang Tao and Professor David Reckhow for their acceptance in being part of my PhD committee, and for their time and priceless insights.

I would like to sincerely thank Donald Pellegrino. We spent a lot of time together in the lab and he is professional, knowledgeable and always helpful. I would also like to thank Russell Lang for his friendship and it's been a joy working with him.

I would like to give special thanks to Agata Lajoie, Marylou Horazny, Cynthia Bergeron and Maryann Watts. They were always there when I needed. I would like to thank my fellow graduate students for their feedback, cooperation and of course friendship. It was great sharing laboratory with all of you during last four years. Many thanks go to Professor Tahar El-Korchi. He can always cheer you up with his warm smiles and big hugs.

I would like to thank the Department of Civil and Environmental Engineering at WPI for giving me the chance to pursue my doctorate and for providing the financial support with a teaching assistantship.

More than all, I would like to thank my family, especially my husband, this could not be done without his support. I am grateful to my mon and my dad, who have provided me through moral and emotional support in my life. I am also grateful to my other family members and friends who have supported me along the way.

TABLE OF CONTENTS

LIST OF FIGURES

LIST OF TABLES

Chapter I. Introduction

Antibiotics are widely used to treat disease in humans and promote animal growth in livestock (Gelband et al. 2015). However, the metabolism of antibiotics is incomplete within human bodies and animals (Hirsch et al. 1999; Boxall and Sinclair 2001; Boxall et al. 2002). Therefore, significant amounts of antibiotics and their metabolites are excreted and end up in environment. Their occurrence has been detected worldwide in water and soil media (Heberer 2002; Kolpin et al. 2002; Barnes et al. 2008; Focazio et al. 2008).

As one of the most commonly used antibiotics, Sulfamethoxazole (SMX) is one of the most commonly detected antibiotics in the environment. Its occurrence has been reported in different water bodies throughout the world (Furlong et al. 2002; Kolpin et al. 2002; Gros et al. 2007; Barnes et al. 2008; Focazio et al. 2008; Barber et al. 2009; Munoz et al. 2009). SMX contamination is of public concern because SMX can build up antibiotic resistance in bacteria and develop antibiotic resistant infections in humans by contacting resistant organisms or by having resistant microbes in the body (Lewis 1995; Reinthaler et al. 2003; Laville et al. 2004). Overall the concentrations of SMX detected in environment are low. To our knowledge, the highest surface water concentration reported was 4.33 μg/L, which was lower than reported effective concentrations to human health (Segura et al. 2009; Phan Thi Phuong et al. 2011). Nevertheless, it can still potentially affect the most sensitive species, such as bacteria (Reinthaler et al. 2003; Laville et al. 2004; Segura et al. 2009). Underwood et al. (2011) studied the influence of SMX at low concentrations. They showed that the presence of SMX could alter the enriched nitrate-reducing microcosms and decrease nitrate reduction potential by 47% for a concentration as low as 1.3 μg/L. These findings raise concerns to humans and ecology for the long-term dispersion of SMX even at low concentrations.

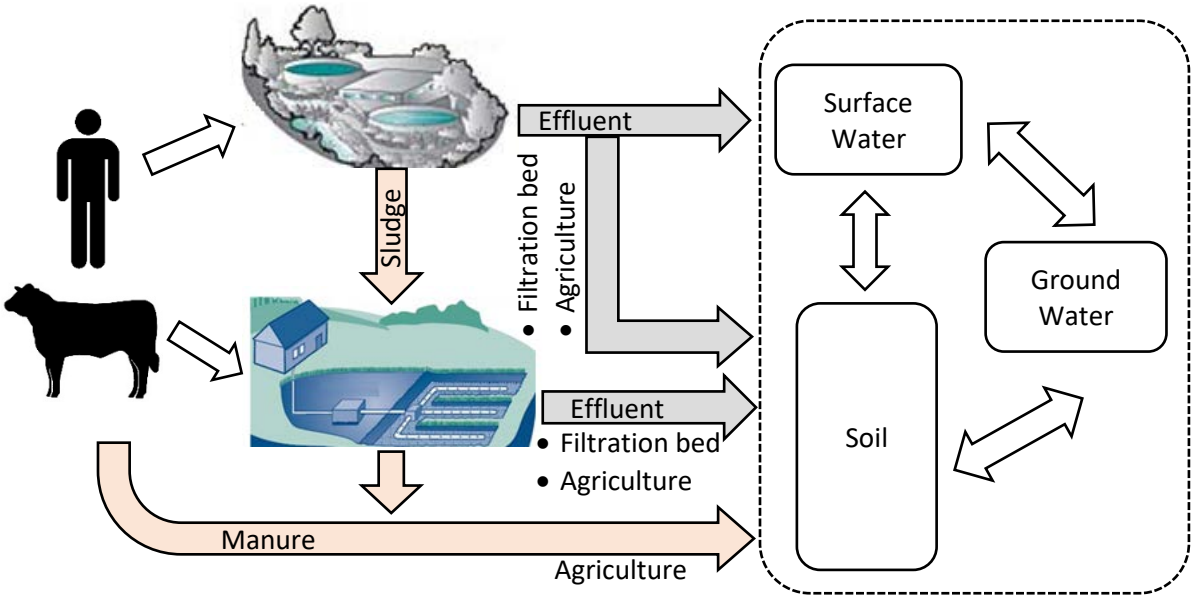

Figure I-1. Sources and fates of antibiotics in the environment.

Antibiotics and their metabolites excreted by waste enter the environment through various routes (figure I-1). They could be released via municipal treatment plants or onsite treatment systems. These systems are not designed to treat antibiotics. Their efficiencies are usually low, highly dependent on the environmental temperature, and require long retention times (Castiglioni et al. 2006; Du et al. 2014). Discharges from municipal treatment plants and seepage from onsite septic systems are identified as major point sources of antibiotics contamination (Ternes 1998; Heberer 2002; Gros et al. 2007). In addition to the direct discharge to surface water, a large portion of antibiotics enters the environment through the subsurface via discharges of the antibiotic-contaminated effluent to the filtration beds and farmland (irrigation with reclaimed water). Another route is through contaminated solid wastes, such as manure and sludge. The untreated antibiotics enriched in these solid wastes can be leached to the subsurface when they are used as fertilizer. Therefore, transport in the subsurface is a crucial strep for the spread of antibiotics in the environment, and the study of the related processes is needed for contamination management.

However, the physicochemical properties of SMX make it a challenge to attenuate in the subsurface. SMX is a water-soluble compound with low pKa, poor chelating ability and low biodegradability, which makes it persistent and mobile in the subsurface (Alexy et al. 2004; Holtge and Kreuzig 2007; Benotti and Brownawell 2009). As a result, point source

contamination could potentially lead to long term exposure due to wide spread contamination plumes, which has been reported in Cape Cod, US, where SMX was detected in a subsurface plume over kilometers and decades (Barber et al. 2009).

Among the various entering routes to the subsurface, discharge of septic effluent is of particular interest due to its relevance to the large population and the removal difficulties added by the nature of septic effluent. In 2015, one out of 4.3 people, meaning 1.3 billion population, relies on septic system in the world (WHO 2017). In developed countries, like Australia, approximately 13 % of the population don't have municipal sewage connection (Thomas et al. 1997). In U.S., the estimated portion is even higher – about 20 % of U.S. population (Bureau 2013). In less developed countries, this percentage can be even higher (WHO 2017). The complexity of septic effluent, which usually enriched with nutrients (such as nitrogen, sulfur, and organic carbon), could have significant influence and add difficulties to both adsorptive removal and biodegradation of SMX in the subsurface. However, to our knowledge, no studies on the SMX removal from septic effluent have been reported.

Research objective and specific aims

Because of the wide spread concern of SMX and the relevance of septic systems, innovative treatment technologies are needed to remove SMX in septic effluent from the subsurface. The overall goal of this research is to design a low-cost but effective treatment technology to remove SMX in the septic effluent and prevent its spread in the subsurface. To accomplish this goal, a systematic study is needed to understand the processes and identify the influential factors governing the transport, transformation and removal of SMX in the subsurface. This research used well-controlled batch experiments to explore two main removal mechanisms for SMX: biodegradation and adsorption. In addition, the extrapolation of batch experiments to larger scales was examined using soil column studies. The specific aims of this work are listed below:

Specific aims:

- To study the degradation of SMX in different matrices and nutrient amendments to determine the factors influencing the degradation of SMX in the subsurface.

- To evaluate the effectiveness of SMX adsorption on soil in the subsurface and the effectiveness of biochar amendment.
- To determine the effectiveness of biochar amendment on the scale-up of batch scale to soil columns.

The main body of this dissertation consists of four chapters, including one chapter of research background and the other three addressing each specific aim respectively.

References

Alexy, R., Kumpel, T. and Kummerer, K. (2004). "Assessment of degradation of 18 antibiotics in the Closed Bottle Test." *Chemosphere* 57(6), 505-512.

Barber, L. B., Keefe, S. H., Leblanc, D. R., Bradley, P. M., Chapelle, F. H., Meyer, M. T., Loftin, K. A., Kolpin, D. W. and Rubio, F. (2009). "Fate of Sulfamethoxazole, 4-Nonylphenol, and 17 beta-Estradiol in Groundwater Contaminated by Wastewater Treatment Plant Effluent." *Environmental Science & Technology* 43(13), 4843-4850.

Barnes, K. K., Kolpin, D. W., Furlong, E. T., Zaugg, S. D., Meyer, M. T. and Barber, L. B. (2008). "A national reconnaissance of pharmaceuticals and other organic wastewater contaminants in the United States - I) Groundwater." *Science of the Total Environment* 402(2-3), 192-200.

Benotti, M. J. and Brownawell, B. J. (2009). "Microbial degradation of pharmaceuticals in estuarine and coastal seawater." *Environmental Pollution* 157(3), 994-1002.

Boxall, A. B. A., Blackwell, P., Cavallo, R., Kay, P. and Tolls, J. (2002). "The sorption and transport of a sulphonamide antibiotic in soil systems." *Toxicology Letters* 131(1-2), 19-28.

Boxall, A. B. A. and Sinclair, C. J. (2001). "Assessment of the environmental properties and effects of pesticide degradation products." *Pesticide Behaviour in Soils and Water*(78), 113-118.

Bureau, U. S. C. (2013). "American housing survey for the United States: 2011." Current Housing Reports Sereis H150/11. [Accessed

Castiglioni, S., Bagnati, R., Fanelli, R., Pomati, F., Calamari, D. and Zuccato, E. (2006). "Removal of pharmaceuticals in sewage treatment plants in Italy." *Environmental Science & Technology* 40(1), 357-363.

Du, B., Price, A. E., Scott, W. C., Kristofco, L. A., Ramirez, A. J., Chambliss, C. K., Yelderman, J. C. and Brooks, B. W. (2014). "Comparison of contaminants of emerging concern removal, discharge, and water quality hazards among centralized and on-site wastewater treatment

system effluents receiving common wastewater influent." *Science of the Total Environment* 466, 976-984.

Focazio, M. J., Kolpin, D. W., Barnes, K. K., Furlong, E. T., Meyer, M. T., Zaugg, S. D., Barber, L. B. and Thurman, M. E. (2008). "A national reconnaissance for pharmaceuticals and other organic wastewater contaminants in the United States - II) Untreated drinking water sources." *Science of the Total Environment* 402(2-3), 201-216.

Furlong, E. T., Ferrer, I., Zaugg, S. D. and Kolpin, D. W. (2002). "Antimicrobial surfactants in water and sediment: Determination and environmental distribution." *Abstracts of Papers of the American Chemical Society* 223, U515-U516.

Gelband, H., Miller-Petrie, M., Pant, S., Grandra, S., Levinson, J., Barter, D., White, A. and Laxminarayan, R. (2015). "State of the World's Antibiotics, 2015" Available: [Accessed

Gros, M., Petrovic, M. and Barcelo, D. (2007). "Wastewater treatment plants as a pathway for aquatic contamination by pharmaceuticals in the ebro river basin (northeast spain)." *Environmental Toxicology and Chemistry* 26(8), 1553-1562.

Heberer, T. (2002). "Occurrence, fate, and removal of pharmaceutical residues in the aquatic environment: a review of recent research data." *Toxicology Letters* 131(1-2), 5-17.

Hirsch, R., Ternes, T., Haberer, K. and Kratz, K. L. (1999). "Occurrence of antibiotics in the aquatic environment." *Science of the Total Environment* 225(1-2), 109-118.

Holtge, S. and Kreuzig, R. (2007). "Laboratory testing of sulfamethoxazole and its metabolite acetyl-sulfamethoxazole in soil." *Clean-Soil Air Water* 35(1), 104-110.

Kolpin, D. W., Furlong, E. T., Meyer, M. T., Thurman, E. M., Zaugg, S. D., Barber, L. B. and Buxton, H. T. (2002). "Pharmaceuticals, hormones, and other organic wastewater contaminants in US streams, 1999-2000: A national reconnaissance." *Environmental Science & Technology* 36(6), 1202-1211.

Laville, N., Ait-Aissa, S., Gomez, E., Casellas, C. and Porcher, J. M. (2004). "Effects of human pharmaceuticals on cytotoxicity, EROD activity and ROS production in fish hepatocytes." *Toxicology* 196(1-2), 41-55.

Lewis, R. (1995). "The rise of antibiotic-resistant infections." *FDA consumer magazine* 29(1).

Munoz, I., Gomez-Ramos, M. J., Aguera, A., Garcia-Reyes, J. F., Molina-Diaz, A. and Fernandez-Alba, A. R. (2009). "Chemical evaluation of contaminants in wastewater effluents and the environmental risk of reusing effluents in agriculture." *Trac-Trends in Analytical Chemistry* 28(6), 676-694.

Phan Thi Phuong, H., Managaki, S., Nakada, N., Takada, H., Shimizu, A., Duong Hong, A., Pham Hung, V. and Suzuki, S. (2011). "Antibiotic contamination and occurrence of antibiotic-resistant bacteria in aquatic environments of northern Vietnam." *Science of the Total Environment* 409(15), 2894-2901.

Reinthaler, F. F., Posch, J., Feierl, G., Wust, G., Haas, D., Ruckenbauer, G., Mascher, F. and Marth, E. (2003). "Antibiotic resistance of E-coli in sewage and sludge." *Water Research* 37(8), 1685-1690.

Segura, P. A., Francois, M., Gagnon, C. and Sauve, S. (2009). "Review of the Occurrence of Anti-infectives in Contaminated Wastewaters and Natural and Drinking Waters." *Environmental Health Perspectives* 117(5), 675-684.

Ternes, T. A. (1998). "Occurrence of drugs in German sewage treatment plants and rivers." *Water Research* 32(11), 3245-3260.

Thomas, J. F., Gomboso, J., Oliver, J. E. and Ritchie, V. A. (1997). "Wastewater re-use, stormwater management, and the National Water Reform Agenda." *CSIRO Land and Water*.

Underwood, J. C., Harvey, R. W., Metge, D. W., Repert, D. A., Baumgartner, L. K., Smith, R. L., Roane, T. M. and Barber, L. B. (2011). "Effects of the Antimicrobial Sulfamethoxazole on Groundwater Bacterial Enrichment." *Environmental Science & Technology* 45(7), 3096-3101.

WHO (2017). "Progress on Drinking Water, Sanitation and Hygiene: 2017 Update and SDG Baselines" Geneva: World Health Organization (WHO) and the United Nations Children's Fund (UNICEF). Available: http://www.who.int/mediacentre/news/releases/2017/launch-version-report-jmp-water-sanitation-hygiene.pdf [Accessed Nov. 1, 2017]

Chapter II. Background

This chapter provides a literature review on the background on the SMX in the subsurface. Basic properties of SMX are introduced. The sources and occurrence are summarized. The reported negative effects of the SMX exposure to nature and humans are presented. Two remediation processes that are crucial to SMX removal in subsurface biodegradation and adsorption, are discussed in detail. Reported findings for SMX biodegradation in terms of kinetic modeling, mechanisms and influential effects are presented and discussed. The limitation of SMX adsorption to soil is pointed out and biochar is introduced as a green and cost-effective adsorbent that could be applied in soil remediation. Adsorption mechanisms and influential factors proposed by researchers are summarized. Finally, models commonly used for analyzing adsorption kinetics and isotherms are introduced.

2.1 Definition of sulfamethoxazole (SMX)

SMX is a broad-spectrum antibiotic drug first introduced to US in 1961 (Crasto 2016). It prevents the formation of folic acid, a compound that the bacteria have to produce to generate nucleic acid. SMX is prescribed to treat respiratory, urinary tract, skin and gastrointestinal infections for humans and animals. It is also widely used in aquaculture and livestock breeding for promoting growth (Drillia et al. 2005a). The SMX can be metabolized in human bodies forming at least five metabolites, the N4-acetyl-, N4-hydroxy-, N4-acetyl-5-methylhydroxy-, 5-methylhydroxy-sulfamethoxazole metabolites, and an N1-glucuronide conjugate. However, the metabolism of SMX in human and animal bodies are incomplete. Approximately 43 % of the SMX is decomposed to N4-acetyl-sulfamethoxazole, 9-15 % to sulfamethoxazole N1-glucuronide, and 15-25 % is excreted unchanged (Holtge and Kreuzig 2007; Radke et al. 2009).

SMX is a sulfonamide compound attached with an aniline group and an isoxazole group. It can undergo intramolecular hydrogen transfer to form isoamide and imide (figure II-1). The physicochemical properties of SMX is summarized in table II-1. SMX is water soluble and hydrophilic with a low log K_{OC} and Log P values. It is also an amphoteric compound. The protonation of aniline group has a pK_a of 1.6 and the hydrogen of amide dissociates with a pK_a value of 5.7 (figure II-2) (Boreen et al. 2004).

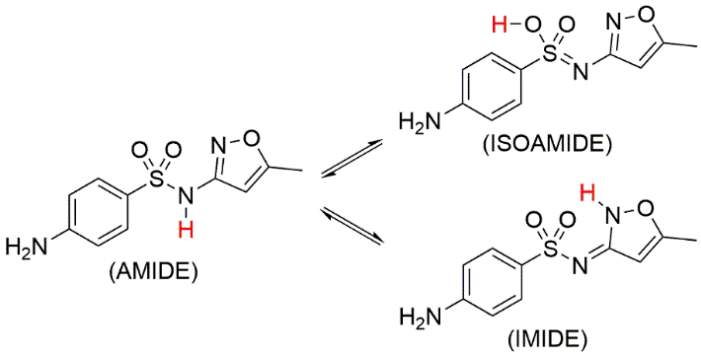

Figure II-1. Molecular structure of SMX and the two isomers of intramolecular hydrogen transfer.

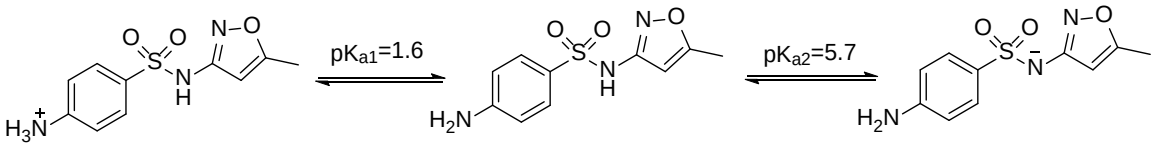

Figure II-2. Dissociation reaction of SMX and its dissociation constants (Boreen et al. 2004).

Table II-1. Properties of Sulfamethoxazole

Properties	Value	Reference
Molecular formula	C10H11N3O3S	
Molecular weight	253.38 g/mol	
Water solubility	610 mg/L	Yalkowsky (2003)
Log P	0.89	Hansch et al. (1995)
Log K_{OC}	1.21-1.87	Srinivasan et al. (2010)
pK_a's	1.6; 5.7	Boreen et al. (2004)

2.2 Sources, fate and occurrence of SMX in the environment

The SMX that is not metabolized in human and animal bodies is treated in onsite and municipal wastewater treatment systems. However, the treatment of SMX in wastewater systems is not satisfactory and wastewater treatment systems have been recognized as hotspots for the release of SMX (Michael et al. 2013). The removal efficiencies of conventional treatment plants vary significantly, depending on types of treatment processes and operation conditions (table II-2) (Clara et al. 2005; Castiglioni et al. 2006; Karthikeyan and Meyer 2006; Gros et al. 2010; Michael et al. 2013; Du et al. 2014). Complete removal of SMX was reported in treatment

plant in China when the influent concentrations was as high as 5.45-7.91 μg/L (Peng et al. 2006). However, in other studies, low removal percentages (< 20 %) were also reported (Brown et al. 2006; Xu et al. 2007; Michael et al. 2013). Application of advanced treatment techniques such as advanced oxidation processes and membrane processes have been reported to be able to increase the removal rates of SMX. However, the increased capital and operation costs, along with other side effects limited the prevalence of these techniques (Michael et al. 2013). Therefore, the untreated SMX was frequently detected in the effluent and sludge of treatment systems (Michael et al. 2013; Du et al. 2014).

Table II-2. Removal percentage of SMX in treatment systems

	Removal Percentage (%)	Reference
STS	11±10, Oct.	Du et al. (2014)
	7.7±5, Jan.	
STS-WET	48±30, Oct.	
	27±10, Jan.	
STS-ATS	31±20, Oct.	
	17±7, Jan.	
MTP	57±40, Oct.	Du et al. (2014)
	81±30, Jan.	
MTP	17-71	Castiglioni et al. (2006)
MTP	6-64	Xu et al. (2007)
MTP	55.6-70	Lee (2009)
MTP-ATS	67	Carballa et al. (2004)
	20	Brown et al. (2006)
MTP	32-66	Clara et al. (2005)
MTP	30-92	Gros et al. (2010)
MTP	60	Gobel et al. (2007)
MTP	17.8-100	Karthikeyan and Meyer (2006)

STS=septic treatment system; WET= wetland; ATS= activated sludge; MTP=municipal treatment plant.

SMX in sludge and wastewater effluent can lead to subsequent contamination to receiving aquatic environment through various pathways. After direct discharge of wastewater effluent, SMX can be released to surface water bodies. Soil contamination could also be resulted from irrigation of reclaimed water, land application of sludge and use of livestock waste as fertilizer. SMX could then leach to subsurface and the underlying groundwater.

The occurrence of SMX in the environment has been frequently reported (table II-3). In a USGS survey of national wide samples, SMX was detected in 19 % of surface water samples with the highest concentration of 0.52 μg/L, and 23.4 % in groundwater samples with the highest concentration of 1.11 μg/L and 2.7 % in untreated drinking water samples with estimated concentration above reporting level of 0.023 μg/L (Kolpin et al. 2002; Barnes et al. 2008; Focazio et al. 2008). In addition, the concentration of SMX previously reported in the environment was often higher than that of other antibiotics (Kolpin et al. 2002; Luo et al. 2010).

Table II-3. Occurrence of SMX in water bodies reported previously

Concentrations, μg/L	Water body	Reference
~1	surface water	Halling-Sorensen et al. (1998)
0.3	surface water	Brown et al. (2006)
0.005-0.169	surface water in Spain	Gros et al. (2007)
≤0.48	surface water	Hirsch et al. (1999)
0.612-4.33	surface water	Phan Thi Phuong et al. (2011)
0.06-1.9	surface water	Kolpin et al. (2002)
0.05-0.37	surface water	Luo et al. (2010)
~1-2	surface water	Lindsey et al. (2001)
0.033	surface water	Lopez-Serna et al. (2012)
0.00063-0.0022	surface water	Standley et al. (2008)
1.11	groundwater	Barnes et al. (2008)
0.22	groundwater	Lindsey et al. (2001)
≤0.47	groundwater	Hirsch et al. (1999)
0.0093-0.0576	groundwater	Zimmerman (2005)
0.038	groundwater	Loos et al. (2010)

Table II-3. Continued

0.15	groundwater	Verstraeten et al. (2005)
0.458	groundwater	Van Stempvoort et al. (2013)
0.5	downstream of WWTP	Haggard et al. (2006)
0.13-0.27	downstream of WWTP	Zimmerman (2005)
0.0017-0.036	downstream of WWTP	Kim et al. (2007)

2.3 Risks of SMX in the subsurface

The negative effects of SMX exposure at such low concentrations are still not clear. People suspect that SMX in nature could lead to two potential risks:

i). toxicity to aquatic organisms and to humans

ii). Induction of antibiotic resistance to bacteria

Direct evidence on the toxicity of environmental SMX contaminant to humans has not been reported. Although high resistance frequency was found in *Escherichia coli* isolated from human samples, the resistance is mainly due to the administration of SMX drug (Hoge et al. 1998; Enne et al. 2001; Bean et al. 2005). SMX concentrations in the environment are not believed to pose a risk to humans (Schwab et al. 2005). The effects of SMX on primary rainbow trout hepatocytes was tested and SMX was found to be able to inhibit the basal 7-ethoxyresorufin O-deethylase (EROD) activity at half maximal effective concentration (EC_{50}) EROD of 108 μM (Laville et al. 2004), which was still higher than the concentrations reported in the environment.

SMX resistance of bacteria was reported in effluent of wastewater treatment plants byReinthaler et al. (2003). These authors investigated E. coli strains in the influent, effluent and sludge of three wastewater treatment plants. The highest resistant rate was found to be 10 % in the effluent and 13 % in the sludge, which was then used in agriculture. SMX resistance of bacteria in water-sediment systems was examined and higher resistance frequencies were observed in sediment (28-43.7 %) than those in water(4-22.4 %) (Xu et al. 2011). However, the SMX dose in this study was 1mg/L and the SMX concentration detected in nature was much lower, below 10 μg/L (table II-3).

In addition to promoting a buildup of bacterial resistance, SMX was reported to be able to have effects on various biogeochemical processes in the environment (Roose-Amsaleg and Laverman 2016). It could have chronic inhibition effects on chemical oxygen demand removal (Schmidt et al. 2012), methanogenesis (Conkle and White 2012), denitrification(Conkle and White 2012; Yan et al. 2013) and nitrification (Schmidt et al. 2012). Acute inhibition effect was also reported on methanogenesis and nitrification in enrichment culture (Fountoulakis 2004). However, these reported effects were all at concentrations much higher than typical environmental values.

A hazard quotient method was recommended by the European Medicines Evaluation Agency (EMEA) for environmental risk assessment. In this approach, a hazard quotient is calculated in two ways, with either:

$$HQ = \frac{PEC}{PNEC} \tag{2.1}$$

Or

$$HQ = \frac{MEC}{PNEC} \tag{2.2}$$

where PEC is the predicted effect concentration, PNEC is the predicted no-effect concentration, MEC is the maximum environmental concentration. A typical value of HQ < 1 indicates that the compound can be considered as environmentally safe. HQ values of SMX were published in two comprehensive reviews and the values vary from 0.0097 to 59.30 (Garcia-Galan et al. 2009; Baran et al. 2011). Therefore, potential negative impact of SMX in the environment could not be ruled out.

Moreover, Segura et al. (2009) studied articles published in peer-reviewed journals since 1984 and summarized data in a density histogram. They found that the SMX concentrations reported in natural water and wastewater water had overlaps with the reported EC_{50}, even though the overlap was small, which suggested the possibility that SMX in natural water and in wastewater may impact the bacteria.

2.4 Removal of SMX in the subsurface

Once SMX is released into the environment, it may undergo different elimination processes, including photodegradation, biodegradation and adsorption (Kummerer 2009).

SMX is light sensitive and is subject to direct photolysis (direct adsorption of sunlight) and indirect photolysis (reaction with transient reactive species formed in natural waters) (Trovo et al. 2009). However, when SMX is in subsurface, photodegradation is limited due to low light exposure (Kummerer 2009).

Therefore, biodegradation and adsorption are usually considered as the two major removal processes and are of interest of this work. However, to a lesser or greater extent, the influence of biodegradation, compared to adsorption in terms of SMX removal in the subsurface was inconsistent in literature, and dependent on the specific samples. For instance, Lin and Gan (2011) found the biodegradation was an major removal process and sorption was negligible in soils sampled at arid regions. Srinivasan and Sarmah (2014) reported that sorption was as important for the dissipation of SMX in pasture soils. Martinez-Hernandez et al. (2016) investigated the removal kinetics of SMX in soils sampled at unsaturated zone of groundwater body with synthetic reclaimed water. They found that the sorption played a key role within the first 2 hours of contact with soil and gave way to biodegradation afterwards.

The current knowledge of biodegradation and adsorption processes is discussed in detail in the following sections.

2.4.1 Biodegradation of SMX in the subsurface

2.4.1.1 Efficiency and kinetics of biodegradation of SMX in the subsurface

Aerobic degradation of SMX was mostly reported in surface water and was not as important in the subsurface because of the low oxygen content. Studies of aerobic degradation of SMX was mostly in batch experiment with river water or synthesized water at enhanced concentrations of SMX. The aerobic degradation at low SMX concentration in wastewater was rarely reported.

First-order model was most used to describe the kinetics of SMX dissipation, which is defined by equation 2.3:

$$\frac{dC}{dt} = -k_1 C \quad (2.3)$$

where C [ML^{-3}] represents the concentration in water of a compound at time t [T] and k_1 [T^{-1}] is the first-order constant. In practice, the degradation half-life ($t_{1/2}$) was often used and is defined as the time needed to reduce the compound concentration by a factor of 2. It can be calculated using equation 2.4:

$$t_{1/2} = \frac{\ln(2)}{k_1} \quad (2.4)$$

In regards to the extent and rate of SMX degradation, opposing results have been published (table II-4). For instance, Xu et al. (2011) observed a 90 % removal of SMX after 36 days in a river sediment/water system, but at a higher SMX concentration, with values ranging from 1-20 mg/L. It agreed with the results reported by Radke et al. (2009), which had a similar half-life of about 17 days. Martinez-Hernandez et al. (2016) studied the degradation using synthesized reclaimed water and soils sampled from the unsaturated zone of a groundwater body. A slower SMX degradation was observed and the half-life could be prolong to 120 days. However, Grossberger et al. (2014) studied SMX degradation in agriculture soil and found SMX was persistent after 90 days.

Table II-4. Degradation of SMX in the soil/water system reported in literature. Entries in parentheses are values in sediment, and entries outside of parentheses are values in water.

SMX concentrate-eon	Description	Redox conditions	Kinetics		Reference
			k_1, d^{-1}	$t_{1/2}$, d	
35 µg/l, 3.76 mg/l	Persist after 28 days in the effluent of sewage treatment plant	aerobic	-	-	Alexy et al. (2004)
3.8 µg/ml	persist after 40 days in water only	aerobic	-	-	Al-Ahmad et al. (1999)

Table II-4. Continued.

1-20 mg/l	90 % after 36 days in river sediment/ river water	aerobic	0.041-0.042 (0.045-0.049)	16.62-17.11 (14.15-15.40)	Xu et al. (2011)
50 mg/l		aerobic	0.045(0.012)	15.27(57.79)	
100 mg/l		aerobic	0.017(0.008)	40.53(86.64)	
20 μg/l	~70 % after around 28 days in river sediment/river water	aerobic	0.040	17.2	Radke et al. (2009)
	water only	aerobic	0.003	273	
40 μg/kg soil	>90 % after 84 days in soil/synthesized solution with 0.01M $CaCl_2$	aerobic	0.0609-0.0766	9-11.4	Lin and Gan (2011)
		anaerobic	0.0379-0.0452	15.3-18.3	
50-5000 ng/g soil	persist after 90 days in agricultural soil	aerobic	-	-	Grossberger et al. (2014)
0.5 mg/kg soil	> 90 % after 36 days in pasture soil	aerobic	0.05-0.16	4.31-14.15	Srinivasan and Sarmah (2014)
100 μg/l	soil in groundwater /synthesized solution	aerobic	0.01-0.02*	30.74-120.33	Martinez-Hernandez et al. (2016)
100 μg/l	lake water	aerobic	0.0606	11.4	Zhang et al. (2013)

Table II-4. Continued.

10 mg/kg soil	lake sediment	aerobic	0.064-0.0659	10.5-10.8	
		anaerobic	0.0415-0.0725	9.6-16.7	
1 mg/l	53±16 % after 86 days in artificial water/sediment	denitrifying	-	-	Nodler et al. (2012)
1 μg/l	25±5 % after 10 days	denitrifying	-	-	Barbieri et al. (2012)
1 mg/l	47±20 % after 87 days		-	-	
0.1-20 μg/l	>60 % after 144h (pH 8.5); ~100 % after 144h (pH 5.6) in Soil/artificial water	denitrifying	-	-	Brienza et al. (2017)
25 uM	>95 % in <1 day in artificial water/soil	iron reducing	-	-	Mohatt et al. (2011)
	>95 % in <5 days	sulfate reducing	-	-	
	Similar to sterile soil control	nitrate reducing			
	>95 % in two weeks	aerobic	-	-	

* unit is h^{-1}.

2.4.1.2 Factors influencing the SMX degradation.

The contradicting results of SMX degradation are believed to arise, because the removal rates are dependent on various environmental variables such as microbial adaptation, seasonal temperature, available nutrients, initial SMX concentrations, *in situ* redox conditions, and soil

characteristics (Larcher and Yargeau 2012; Muller et al. 2013; Rodriguez-Escales and Sanchez-Vila 2016). Laboratory experiments have been completed to explore the effect under controlled conditions.

SMX degradation has also been found to be different for different matrices. Comparing published data in table II-4, a higher degradation rate was observed in batch experiments when soil was not saturated with a synthesized solution (Lin and Gan 2011; Srinivasan and Sarmah 2014). In a water-sediment system, Xu et al. (2011) monitored the SMX dissipation in water and sediment, and observed a lower degradation rate in water. The SMX removal was limited in waters without soil (Al-Ahmad et al. 1999; Radke et al. 2009). These findings suggested that the microorganisms in the sediment were responsible for the major degradation of SMX. A greater number of viable bacterial and resistant isolates have also been discovered in a sediment study (Xu et al. 2011).

Removal rates of SMX were studied under different redox conditions. Given the variation of soil and water samples, comparing results between different research projects may have little meaning. The few studies that explored the removal rates under different redox states within the same set of samples ended up with opposing results. Mohatt et al. (2011) observed the removal rates of SMX followed the trend, with higher to lower listed in order as: iron-reducing > sulfate reducing > aerobic >> nitrate reducing conditions. The degradation under nitrate reducing condition was close to that in that sterile soil control. However, Lin and Gan (2011) reported an elevated degradation rate under aerobic conditions ($t_{1/2}$ = 9-11.4 days) than anaerobic conditions ($t_{1/2}$ = 15.3-18.3 days), which were both faster than the sterile control ($t_{1/2}$ = 58.7 days). The results disagreed with the field data, which indicated that SMX was more effectively degraded under strictly anaerobic (Schmidt et al. 2004) and anoxic (Grunheid et al. 2005; Heberer et al. 2008) conditions, than under aerobic ones. An opposing trend was observed by Zhang et al. (2013) with lake sediments and the degradation under aerobic condition ($t_{1/2}$ = 10.6 days) was slower than that under anaerobic conditions ($t_{1/2}$ = 9.5 days).

The effects of initial concentrations of SMX were also studied. The effects of initial concentration on SMX degradation were insignificant for a number of observations when the initial concentrations were low (< 20 mg/L). When SMX concentrations were high, the

microbial activity could be inhibited and thus could slow the degradation (Xu et al. 2011; Zhang et al. 2013; Srinivasan and Sarmah 2014).

Soil properties may play an important role in SMX degradation through different ways. Organic matter content of soil has been considered to be the main nutrient source for bacterial metabolism. Correlation between soil organic matter and microbial activity was observed (Jia et al. 2005; Yang et al. 2009). Lower SMX degradation was observed in soils with lower organic matter content (Zhang et al. 2013). Different SMX dissipation rates were reported for soils collected at different depths and at adjacent locations for the same depth (Srinivasan and Sarmah 2014). Despite the factors of organic matter, depth and location, the variation in the microbial culture was one of the main reasons behind the miscellaneous degradation results.

Nutrient accessibility and abundance was another aspect that has been studied to understand the degradation of SMX. Most of the studies were conducted under aerobic conditions. To the knowledge of the author, no reports studying nutrient amendment under anaerobic conditions in water/soil systems were published. The addition of external carbon sources has been shown to lead to the acceleration of SMX degradation. In a water/sediment test, addition of 40 mmol of methanol reduced the SMX half-life from 17.2 days to 10.9 days (Radke et al. 2009). Xu et al. (2011) also observed the elevated degradation rate with increasing concentrations of humic acid in both water and sediment. The degradation rates were 67.8 %, 74.6 % to 86.8 % after 35 days in water with 0, 5 and 30 mg/l humic acid, respectively. The degradation rates in sediment were 78.6 %, 82.9 %, 90.1 % after 35 days, with 0, 5, 30 mg/l humic acid, respectively. Similar effects were also observed in wastewater without sediment (Alexy et al. 2004). The SMX degradation increased from 4 % to 38 % with the addition of 13 % acetate. However, SMX could also serve as a nitrogen and sulfur source to bacterial growth. Enhanced SMX degradation was observed through co-metabolism by ammonia oxidizing bacteria (Kassotaki et al. 2016). However, nitrogen and sulfur amendments in water soil system were not reported, to the knowledge of the author.

In summary, the intrinsic properties of the subsurface could influence the SMX biodegradation by varying the bacterial culture and bacterial activity. All of these variables are site dependent and temporal. High soil organic content and external carbon source could facilitate SMX

degradation by fostering microbial growth. Soil may play a more important role to SMX degradation compared to the aqueous phase. However, a high initial SMX concentration could inhibit the microbial activity to decrease the degradation rates. Contradicting results were reported for the degradation under different redox conditions. To note that most of the studies were conducted under aerobic conditions and the effects under anoxic conditions were rarely studied. In addition, studies on the effects of other nutrient, like external nitrogen and external sulfur, are lacking.

2.4.1.3 Metabolites and proposed mechanisms of biodegradation of SMX in the subsurface

The SMX degradation under different redox conditions results in different metabolites. Most of the detected metabolites of SMX degradation were observed in the activated sludge or in pure bacterial culture. The detection of these SMX transformations soil/water systems were rare (Radke et al. 2009; Xu et al. 2011; Martinez-Hernandez et al. 2016).

SMX transformation under aerobic conditions

The most frequent metabolite detected under aerobic conditions was 3-mino-5-methylisoxazole (Eibes et al. 2011; Muller et al. 2013; Reis et al. 2014; Rodriguez-Escales and Sanchez-Vila 2016). Gao et al. (2010) proposed that SMX was transformed into 3-mino-5-methylisoxazole and 4-aminobenzolsufonate through irreversible cleavage of S-N bond in the sulfonamide group (figure II-3). The byproduct, 4-aminobenzolsufonate, could be further degraded under aerobic condition leading to the complete mineralization of SMX.

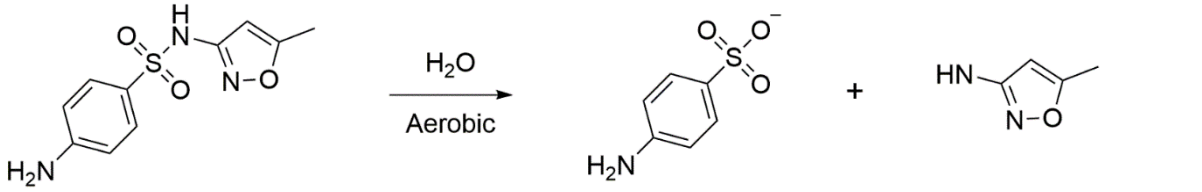

Figure II-3. Schematic of transformation of SMX to 3-mino-5-methylisoxazole under aerobic conditions.

Another metabolite that had been detected in the degradation in water-soil system was N4-acetyl-SMX, which was also the major metabolite in human bodies (Radke et al. 2009; Xu et al. 2011; Martinez-Hernandez et al. 2016). However, a only 1% transformation was reported by Xu et al. (2011). In addition, N4-acetyl-SMX could retransform back into the parent SMX in the presence of certain enzyme, which was reported to exist in soil/water system and activated sludge.(Gobel et al. 2005; Radke et al. 2009).

The degradation of SMX under aerobic conditions was proposed to be heterotrophic bacteria assimilating SMX-C. Alvarino 2016 studied the SMX degradation by heterotrophic and autotrophic nitrifying bacteria using ^{14}C-labeled SMX. The concentration of SMX was observed to decrease by over 94% in the heterotrophic aerobic condition while it remained constant in the autotrophic aerobic condition. Biotransformation of SMX started immediately with an external carbon source as a primary substrate and enhanced SMX degradation was observed with the degradation of external carbon sources (Radke et al. 2009; Gauthier et al. 2010; Muller et al. 2013; Alvarino et al. 2016). The effect of ammonium as primary substrate was not significant and biotransformation was not observed until 100h of operation (Alvarino et al. 2016).

SMX transformation under denitrifying condition

To be precise, the transformation of SMX under anoxic conditions was proposed to be microbial mediated abiotic process (Barbieri et al. 2012; Nodler et al. 2012; Brienza et al. 2017). The metabolites 4-nitro-SMX, 4-nitroso-SMX and desamino-SMX were detected under denitrifying conditions in laboratory experiments and as well as in field. The proposed mechanism was shown in figure II-4.

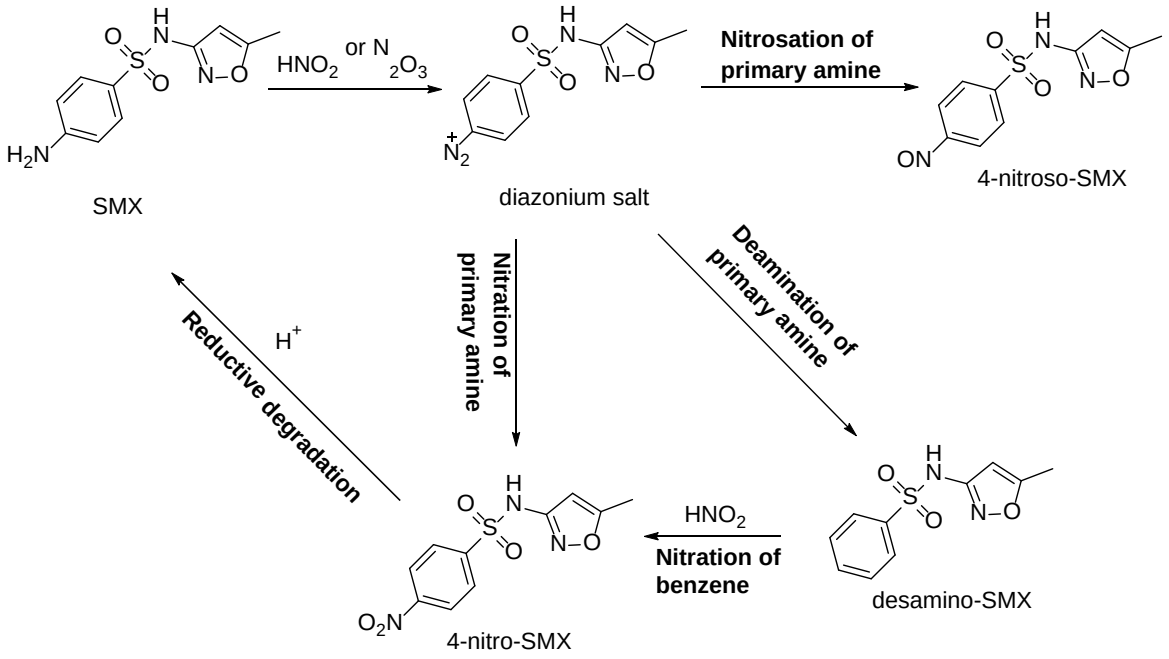

Figure II-4. Transformation of SMX to 4-nitro-SMX, 4-nitroso-SMX, and desamino-SMX under denitrifying condition.

Under a nitrate reducing condition, diazonium salt was formed from reaction of primary amine of SMX with nitrous acid (HONO) or nitric oxide (N_2O_3). HONO was the main source of N_2O_3 and both of them were the intermediate products of denitrification. In addition, the inhibition of denitrification by SMX could lead to the accumulation of N_2O_3 in the system (Brienza et al. 2017). The highly reactive diazonium salt could react with nitrous acid to form 4-nitro-SMX, with the NO· radical to form 4-nitroso-SMX or directly form desamino-SMX through deamination. Desamino-SMX could undergo further nitration of the benzene ring to form 4-nitro-SMX. Nitration of SMX was irreversible under anoxic conditions (Brienza et al. 2017). However, 4-nitro-SMX was not stable and could regenerate the parent compound, SMX, when nitrite and nitrate were depleted (Nodler et al. 2012). The retransformation of 4-nitro-SMX to SMX was confirmed in the absence of denitrification, which could be mediated abiotically or biotically (Nodler et al. 2012). However, 4-nitroso-SMX was relative persistent under anoxic conditions and was classified as SMX reactive metabolite with higher toxicity than SMX.

In summary, degradation of SMX followed co-metabolic pathway, driven by the presence of nitrous acid or nitric oxide, which was the intermediate products of the denitrification metabolism. Nevertheless, SMX did not participate directly in the denitrifying metabolism.

SMX transformation under iron-reducing condition

The transformation of SMX under iron-reducing condition was only reported by (Mohatt et al. 2011) in the soil/water system. The degradation of SMX occurred as co-metabolism, initiated by the degradation of organic carbon, which produced iron (II) by biological reduction. Single electron transfer between iron (II) and SMX leads to cleavage of N-O bond of the isoxazole ring in SMX forming radical anion compound (A). Under different conditions, compound (A) could be converted into four different products via three different pathways as illustrated in figure II-5.

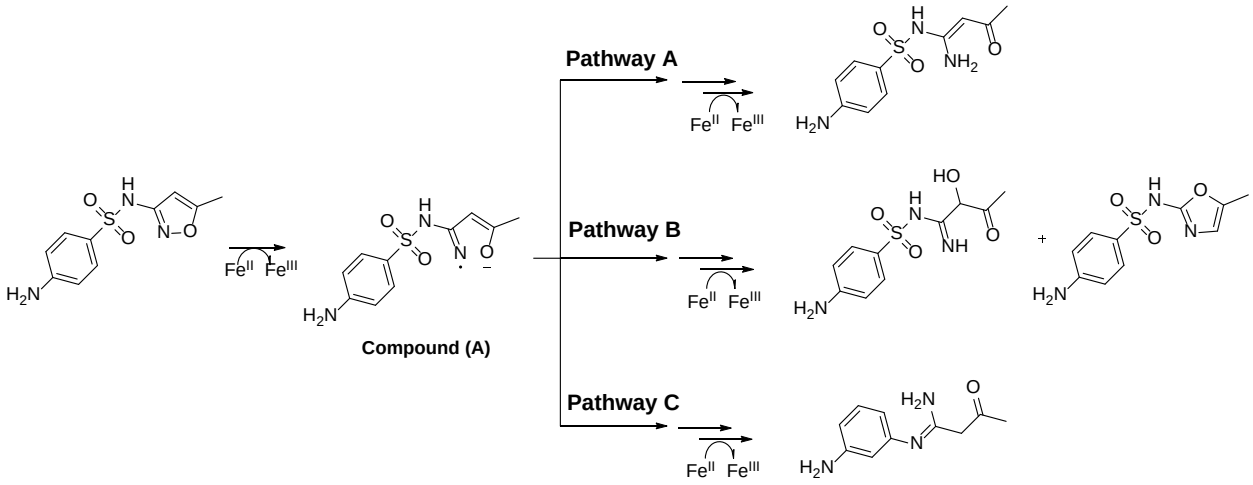

Figure II-5. Transformation of SMX under iron-reducing condition.

To summarize, the transformation of SMX followed different pathways depending on the redox condition of the system. The transformation under aerobic conditions was biological degradation, which could produce 3-mino-5-methylisoxazole or N4-acetyl-SMX through irreversible reaction. Under reducing conditions, the transformations of SMX were abiotic and facilitated by co-metabolism. During denitrifying conditions, the metabolites were formed through substitution of primary amine, whereas during iron reducing conditions, the isoxazole ring was irreversibly broken.

2.4.2 Adsorption of SMX in the subsurface

Once SMX is introduced to the environment, its physicochemical nature makes it especially persistent and mobile in subsurface. A low distribution coefficient K_d (which is discussed in detail in section 1.2.4.4) for SMX adsorption to soil or sediment has been reported (table II-5).

Table II-5. Adsorption of SMX onto different soil/sediment materials reported by literatures

Adsorbent	f_{OC} (%)	pH	Freundlich Model		K_d (L/kg) at		Reference
			K_F, $mg^{1-n}L^n/kg$	n	$0.01C_S$	$0.1C_S$	
soil	0.37	6.8	0.28	0.66	0.18	0.08	Drillia et al. (2005b)
soil	7.1	4.3	23.9	0.94	33.5	29.2	Yu et al., 2009
soil	6.3	2.9	20.0	1.01	17.7	18.1	
soil	2.3	5.8	0.67	0.93	1.63	1.39	Stein et al., 2008
sediment	0.74	6.6	0.1	0.93	0.29	0.25	
sediment	4.36	6.5	0.89	0.85	5.82	4.12	Zhang et al. (2010)
sediment	8.23	7	0.0297	0.44	13	4	
sediment	0.88	7			89		Xu et al., 2009

Mechanisms of sorption for SMX include hydrophobic partitioning, hydrogen bonding, electrostatic interaction, π-π interaction, complexation (cation bridging or surface complexation), etc. (Tan et al. 2015).

Since the pK_{a1} of SMX is far below the pH range of soil and the aqueous phase in the environment, the dominant speciation is the neutral or negatively charged compound while the positively charged fraction is negligible (figure II-6). The adsorption of SMX^- anion and neutral SMX is governed by different mechanisms.

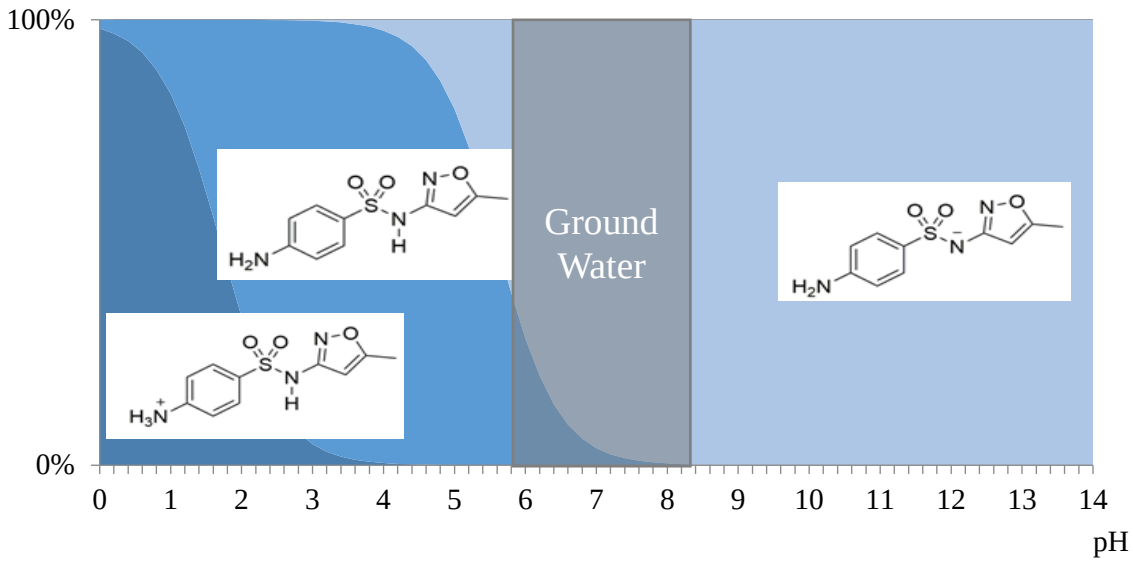

Figure II-6. Distribution of the three SMX conjugates at different pH ranges.

Sorption of neutral SMX is dominated by hydrophobic partitioning and surface complexation, thus is influenced by the properties of soil. SMX has a relative low log K_{OC} of 2.06 to 3.47 (Carballa et al. 2008). The low organic carbon fraction f_{OC} and low fraction of neutral SMX with an increase in pH could lead to a reduction in sorption. Batch reactions revealed that f_{OC} played an important role in controlling the overall adsorption of SMX (table II-5) (Zhang et al. 2010). Higher K_d values are noted with soils with higher f_{OC} under varying pHs. Studies on more detailed soil composition revealed humic acid, aromatic condensation, lignin decomposition products and functional groups like phenolic and carboxylic groups, N-heterocyclic structures play important roles in the sorption of neutral SMX through surface complexation, but weaker adsorption to mineral soil colloids (Thiele-Bruhn et al. 2004).

The adsorption of SMX^- anion is largely dependent on its electrostatic interaction to negatively charge soil particles (Mackay and Seremet 2008). At high pH, the SMX^- anion is highly mobile due to the repulsive interaction with soil particle. Further pH increases do not have much influence (Chen et al. 2011). At low concentration of aqueous SMX, changes in ionic strength have little effect on SMX mobility (Gao and Pedersen 2005; Chen et al. 2011; Lian et al. 2014; Morel et al. 2014). It means that SMX binds to specific sites but not to cation or anion exchange sites.

However, the repulsive force can be attenuated by the presence of cations in aqueous phase. Positively charged ions can mediate the negative charge of the soil surface and thus weaken electrostatic interaction between negative SMX and soil. In addition, SMX can chelate many cations present in water, such as Cu^{2+}, Mn^{2+}, Ni^{2+}, etc. The adsorbed cations on soil surface can increase sorption sites by forming soil-metal-SMX bridges (Morel et al. 2014). SMX adsorption was found to increase by a factor of 6 times in the presence of Cu^{2+}. Ca^{2+} can also affect the adsorption behavior (Lian et al. 2014). At low Ca^{2+} concentrations, the adsorption of SMX was enhanced by Ca^{2+} bridging or Ca^{2+}/SMX^{-} paring. At high Ca^{2+} concentrations, SMX adsorption decreased with binding sites hindered by the hydration shell of adsorbed Ca^{2+}.

2.4.2.1 Biochar and its application in soil amendments

Upon realizing the limited affinity of soil for SMX adsorption, it would be advantageous to consider adsorptive materials could be used to improve the adsorptive removal of SMX in subsurface. Materials to promote adsorption are often available at a relatively low cost. They are often simple to design and operate, invulnerable to biological toxicity and efficient for removing organic contaminants (Ahmaruzzaman 2008; Homem and Santos 2011; Ahmad et al. 2014). Many adsorptive materials have been studied, including activated carbon (AC), ion exchangeable materials, natural clay materials, silica nanospheres, metallic oxide particles and et al. (Tiwari and Paul 2009; Ahmed et al. 2015).

Among the adsorptive materials, biochar (BC) is a green and economic material that is suitable for adsorption treatment in both water and soil. BC is defined as “a solid material obtained from the thermochemical conversion of biomass in an oxygen-limited environment” (IBI, 2012). BC features include a porous structure, high surface area, hydrophobicity and great degree of aromaticity, making it a good sorbent. Studies show that BC is capable of reducing the concentration of organic and inorganic contaminants in both water and soil media (Cao et al. 2009; Spokas et al. 2009; Beesley et al. 2010; Ahmad et al. 2014). Specifically, for SMX remediation, batch experiments have shown that BC has a high partition coefficient Kd and addition of BC can significantly increase overall K_d value of soil (Ji et al. 2011; Yao et al. 2012; Zheng et al. 2013; Srinivasan and Sarmah 2015). Results from a vadose soil column

experiment showed that addition of bamboo and sugarcane bagasse BC to sandy soil increased the SMX removal from 60 % to 85 % and 98 % at a low loading rate of 2 % (Yao et al. 2012).

Added benefits have also been reported for soil application of BC. It has been demonstrated that BC application in soil can improve the soil fertility, increase carbon sequestration and reduce greenhouse gas emissions (Lehmann et al. 2008; Sohi et al. 2010; Woolf et al. 2010; Taghizadeh-Toosi et al. 2011). Compared to other sorbents like AC, BC is cost effective. Its production technique is inexpensive and can produce bioenergy during the pyrolysis. It is usually produced from agricultural biomass and solid waste, whose cost is almost negligible. It also does not require high temperature and costly post-treatment reagents like AC (McCarl et al. 2009; Ahmed et al. 2015).

Despite all the benefits of BC as a sorbent for antibiotic remediation, the adsorption efficiency of BC is affected by a number of factors, including production parameters, chemistry of the contaminant and properties of water and soil media (Gell et al. 2011). Most of the reported sorption studies have been conducted under conditions different from real-world situations, using artificial solutions in deionized water and SMX concentrations in mg/L, which are higher than detected (Ji et al. 2011; Yao et al. 2012; Zheng et al. 2013). Also, BC's application to SMX remediation in soil is rare (Srinivasan and Sarmah 2015). Therefore, a systematic study on BC remediation of SMX in water and soil media under conditions that are close to actual situations is needed to provide insight into the influential interactions that could be overlooked and to assess the actual efficiency that BC could deliver in both water and soil media in the real world.

2.4.2.2 Adsorption kinetics

Adsorption kinetics are an important aspect to characteristics in investigations of adsorption mechanisms, The kinetics show the uptake rate of solute from bulk solution to adsorbent's surface, which can be utilized to calculate residence time and scale of treatment system, such as fixed bed and flow-through systems.

Adsorption kinetic models have been developed to simulate the changes of solute over time. Generally, the kinetic models can be categorized into two groups: adsorption reaction models

and adsorption diffusion models. Adsorption reaction models are developed from chemical reaction kinetics between solute and adsorbent active site, examples of which include Pseudo-first-order, Pseudo-second-order and Elovich models. However, adsorption diffusion models are formulated from three consecutive steps:

1) Film diffusion - Diffusion of solute from bulk solution across the thin film surrounding the adsorbent surface;
2) Intra-particle diffusion - Diffusion in the liquid within pores and along pore walls;
3) Interaction of solute and active site of adsorbent.

A first order model can be expressed as:

$$\frac{dq_t}{dt} = k_1 q_t \tag{2.5}$$

Where k_1 [T^{-1}] is first-order rate constant, q_t [ML^{-3}] is the concentration of a compound adsorbed on the adsorbent at time t [T].

Expression for a second order model is presented as:

$$\frac{dq_t}{dt} = k_2 {q_t}^2 \tag{2.6}$$

where k_2 [T^{-1}] is the rate constant of second-order reaction.

A pseudo-first order model was first presented by Lagergren in 1898. It can be presented as follows:

$$\frac{dq_t}{dt} = k_{p1}(q_e - q_t) \tag{2.7}$$

where k_{p1} [T^{-1}] is the rate constant of pseudo-first-order model and q_e [ML^{-3}] is the adsorbate concentration on the adsorbents at equilibrium. This kind of reaction is greatly influenced by q_t and q_e, which means that the reaction rate is directly proportional to the number of active sites on the adsorbent's surface, q_e-q_t. This model has been applied in the adsorption of organic solute to adsorbents (Lagergren 1898; Hameed 2008; Tan et al. 2008)

A pseudo-second order model was established by Ho in 1995 to describe the adsorption of divalent metals onto peat (Ho and McKay 1998). The function is presented as follows:

$$\frac{dq_t}{dt} = k_{p2}(q_e - q_t)^2 \tag{2.8}$$

where k_{p2} [M^{-1} L^3 T^{-1}] is the rate constant of pseudo-second-order model. It is based on the assumption that the rate-limiting step may be a chemical sorption involving valent forces through sharing or exchange of electrons between adsorbent and adsorbate (Taty-Costodes et al. 2003). It describes that the adsorption rate is related to the active site available, $q_e - q_t$.

The Elovich model was originally used to describe chemisorption of gas, assuming a multilayer sorption with different activation energy on each layer (Alberti et al. 2012). The function of Elovich model can be expressed as:

$$\frac{dq_t}{dt} = \alpha e^{-\beta q_t} \tag{2.9}$$

Where α [$ML^{-3}T^{-1}$] is the initial adsorption rate and β [$M^{-1}L^3$], is the sorption constant. It covers a big range of slow adsorption (Cheung et al. 2000). Now it is widely used to explain the adsorption of aqueous contaminant, assuming strong heterogeneity of sorbent surface (Ahmad et al. 2013).

The Weber-Morris model describes the intraparticle diffusion, and internal diffusion determines the adsorption in many liquid systems. The general representation is as follows:

$$q_t = c + k_{int} t^{1/2} \tag{2.10}$$

Where k_{int} [$ML^{-3}T^{-1/2}$] is the rate constant and intercept c [ML^{-3}] is related to the mass transfer across the boundary layer. The ½ exponent was an estimated value for Fickian diffusion and plate geometry. k_{int} can be obtained by plotting q_t verses $t^{1/2}$ and is related to the intraparticle diffusion coefficient D, as shown in equation 2.11.

$$k_{int} = 6\frac{q_0}{R}\sqrt{\frac{D}{\pi}} \tag{2.11}$$

The mathematical expression of the models are summarized in table (II-6).

Table II-6. Summary of kinetic models applied in this study for SMX adsorption on adsorbents

Model	Mathematical expression	Plot	Parameters
First order	$lnq_t = lnq_0 - k_1 t$	lnq_t vs t	k_1 = slope
Second order	$1/q_t = 1/q_0 - k_2 t$	$1/q_t$ vs t	k_2 = slope
Pseudo-first order	$ln(q_e - q_t) = lnq_e - k_{p1} t$	$ln(q_e - q_t)$ vs t	k_{p1} = slope $q_e = e^{intercept}$
Pseudo-second order	$\frac{t}{q_t} = \frac{1}{k_{p2} q_e^2} + \frac{1}{q_e} t$	t/q_t vs t	$k_{p2} = slope^2 / intercept$ q_e= 1/slope
Elovich	$q_t = \frac{1}{\beta} ln(\alpha\beta) + \left(\frac{1}{\beta}\right) ln\ t$	q_t vs $ln\ t$	$\alpha = \text{slope} \cdot e^{\frac{intercept}{slope}}$ β = 1/slope
Weber-Morris	$q_t = c + k_{int} t^{1/2}$	q_t vs $t^{0.5}$	k_{int} = slope c = intercept

2.4.2.3 Adsorptive isotherms

An adsorption isotherm is the equilibrium relationship between the substance in the aqueous phase and the adsorbed amount at a constant temperature and pH (Limousin et al. 2007). It is a mathematical correlation of the adsorbed amount and the remaining concentration in solution, and describes how the adsorbate interact with the adsorbents (Foo and Hameed 2010). The physicochemical parameters and the underlying thermodynamic assumptions provide insights to the surface properties, adsorption mechanism and the affinity of the adsorbents (Bulut et al. 2008). Therefore, adsorption isotherms are crucial for operational design and applicability of adsorbent systems.

The adsorption isotherm models used in this work include the Linear, Freundlich and Langmuir model.

A Langmuir isotherm model is an empirical model that is originally developed to describe gas-solid-phase adsorption onto activated carbon (Langmuir 1917). The mathematical expression can be represented as:

$$q_e = \frac{Q_0 b C_e}{1+bC_e} \tag{2.12}$$

Where b [L^3M^{-1}] refers to Langmuir isotherm constant, Ce [ML^{-3}] is the equilibrium concentration in solution, q_e is the adsorbed amount in the adsorbent at equilibrium, and Q_0 is denoted to maximum monolayer coverage capacities. The linear form can be written as:

$$\frac{1}{q_e} = \frac{1}{Q_0} + \frac{1}{bQ_0C_e} \tag{2.13}$$

The underlying assumption include 1) monolayer adsorption; 2) identical and equivalent adsorption sites; 3) no lateral interaction and steric hindrance between adsorbed molecules; 4) adsorption only occurs at definite sites (Vijayaraghavan et al. 2006). Therefore, Langmuir adsorption is a homogeneous process to both adsorbate molecule and adsorbent site, meaning that each adsorbate molecule has same enthalpy and sorption activation energy (Kundu and Gupta 2006).

The Freundlich isotherm model is also an empirical model, which is historically developed for adsorption of animal charcoal (Ahmaruzzaman 2008). The non-linear expression is exhibited as:

$$q_e = K_F C_e^N \tag{2.14}$$

Where K_F is denoted as Freundlich isotherm constant [$L^{3N}M^{-N}$], and N is the non-linear coefficient. The adsorbed amount is a summation of adsorption on all sites, with the stronger binding sites occupied first, and adsorption energy decreases exponentially until the completion. Its non-linear form is termed as:

$$lnq_e = lnK_F + NlnC_e \tag{2.15}$$

Freundlich isotherm model can be used to describe multilayer adsorption on heterogeneous surface with non-uniform distribution of adsorption energy and affinity (Adamson and Gast 1997). An exponent value, N, above one is an indicative of cooperative adsorption while a value below one implies chemosorption. The Freundlich isotherm model is now applied widely in systems of organic compounds on activated carbon and biochar.

2.4.2.4 Adsorptive mechanisms and influential properties

Adsorption mechanisms between organic compounds and biochars are summarized in a review article by (Tan et al. 2015). Interactions involved in the adsorptive removal of SMX by biochar include electrostatic effect, precipitation, pore filling, hydrogen bond, partitioning to non-carbonized fractions and ect. (figure II-7). The physicochemical properties of SMX and biochar materials play major role in the adsorption process.

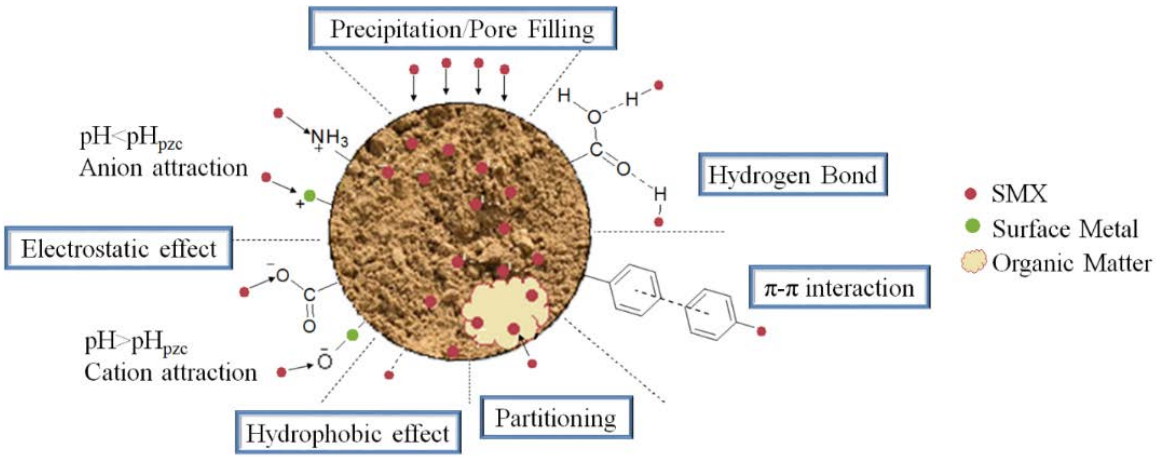

Figure II-7. Interactions for SMX adsorbing onto soil/biochar particles. Modified from Tan et al. (2015).

Biochar is heterogeneous material, consisting of carbonized fractions and non-carbonized fractions, which interact with SMX differently. Surface functional groups of the non-carbonized fraction could enhance SMX adsorption through interactions like hydrogen bonding and π-π interactions. Lian et al. (2014) observed higher sorption capacity of SMX on biochars produced at lower temperature, which was enriched with oxyl groups and could bind SMX by negative charge-assisted H-bond [(-)CAHB]. C=O groups of the biochars may also play an important role in enhancing SMX sorption on biochar. Srinivasan and Sarmah (2015) showed higher SMX sorption affinity of biochars enriched in C=O groups. However, contradictory results were reported by Xie et al. (2014). Identical SMX affinity was observed in two biochars that were different in surface oxygen-functionalities. A high degree of aromaticity of carbonized fractions could facilitate sulfonamides sorption to biochar due to the formation of π-π electron donor-acceptor interactions between SMX and the graphitized carbon surface (Ji et al. 2011; Xie et al. 2014; Srinivasan and Sarmah 2015) . High surface

areas are often observed with the high removal capacities for organic compound onto biochars due to the major adsorptive mechanism of pore filling (Wu et al. 2013; Srinivasan and Sarmah 2015).

Table II-7. Effect of pyrolysis temperature on biochar properties. Source: Zhang et al. (2015).

Biochar properties	Changes with increasing pyrolysis temperature from 300 ˚C to 900 ˚C
Carbon content	Decreased
Fixed carbon content	Decreased from 300 ˚C to 500 ˚C and then Increased
Waster-soluble nutrients content	Decreased from 300 ˚C to 500 ˚C
pH	Increased from 300 ˚C to 700 ˚C and then decreased
Total nutrient content	Increased
Total heavy metals content	Increased
Surface area	Increased
Graphitization	Decreased for 300 ˚C to 800 ˚C, then increased
Aromatization degree	Increased

The physical properties of biochar are dependent on the feedstock and pyrolysis temperature. Different feedstocks could result in the variation of exchangeable cations, surface area, and surface functional groups. The effect of pyrolysis temperature takes place via the differential elimination of organic components based on the thermo-stability. An increase of pyrolysis temperature could lead to an increase in surface area, aromatization degree, total nutrient content and total heavy metals content (Zheng et al. 2013; Srinivasan and Sarmah 2015; Zhang et al. 2015). Zhang et al. (2015) studied structural and characteristic changes of biochars produced at different temperatures (table II-7). Their findings provided knowledge on the effect of pyrolysis temperature on material properties, and could provide guidance on the design of biochar.

2.5 Summary

This chapter provided an overview of the occurrence of SMX in the subsurface, and the current knowledge on the degradation and adsorption studies on SMX.

Degradation rates of SMX were summarized with different matrices under various conditions. The influential factors for SMX degradation in subsurface were discussed and proposed degradation mechanisms were presented. Research gaps were found in current studies on SMX degradation in the subsurface. First, contradictions exist for degradation under different redox conditions. Second, studies on the effects of accessible nutrients are limited with external organic carbon, while studies on the effects of external nitrogen and external sulfate is lacking. Third, studies on nutrients effects were mostly conducted aerobic condition but rarely under anoxic conditions. Our studies presented in chapter 3 explored the matrix effect and nutrient effect, including external organic carbon, nitrogen and sulfur, on SMX degradation under aerobic and anoxic conditions, which could provide information that helps filling the gaps.

The literature review on SMX adsorption summarized the adsorption rates of SMX on soils and pointed out that biochar has promising future in the application in SMX remediation in subsurface. Models typically used for describing SMX adsorption kinetics and isotherms were introduced. These models were used for sorption data analysis in chapter 4. Proposed adsorption mechanisms and influential factors were summarized. However, the sorption studies have been conducted under simplified conditions, using deionized water as aqueous phase and high SMX concentrations in mg/L. In addition, BC's application to SMX remediation in soil is rare (Srinivasan and Sarmah 2015). To address these issues, Chapter 4 presented a systematic study on BC remediation of SMX at low concentrations in µg/L with real septic effluents to provide insight into the influential interactions that could be overlooked and to assess the actual efficiency that BC could deliver in both wastewater and soil media in the real world.

References

Adamson, A. W. and Gast, A. P. (1997). Physical Chemistry of Surfaces. 6th ed. New York, Wiley Interscience

Ahmad, M., Lee, S. S., Oh, S. E., Mohan, D., Moon, D. H., Lee, Y. H. and Ok, Y. S. (2013). "Modeling adsorption kinetics of trichloroethylene onto biochars derived from soybean stover and peanut shell wastes." *Environmental Science and Pollution Research* 20(12), 8364-8373.

Ahmad, M., Rajapaksha, A. U., Lim, J. E., Zhang, M., Bolan, N., Mohan, D., Vithanage, M., Lee, S. S. and Ok, Y. S. (2014). "Biochar as a sorbent for contaminant management in soil and water: A review." *Chemosphere* 99, 19-33.

Ahmaruzzaman, M. (2008). "Adsorption of phenolic compounds on low-cost adsorbents: A review." *Advances in Colloid and Interface Science* 143(1-2), 48-67.

Ahmed, M. B., Zhou, J. L., Ngo, H. H. and Guo, W. S. (2015). "Adsorptive removal of antibiotics from water and wastewater: Progress and challenges." *Science of the Total Environment* 532, 112-126.

Al-Ahmad, A., Daschner, F. D. and Kummerer, K. (1999). "Biodegradability of cefotiam, ciprofloxacin, meropenem, penicillin G, and sulfamethoxazole and inhibition of waste water bacteria." *Archives of Environmental Contamination and Toxicology* 37(2), 158-163.

Alberti, G., Amendola, V., Pesavento, M. and Biesuz, R. (2012). "Beyond the synthesis of novel solid phases: Review on modelling of sorption phenomena." *Coordination Chemistry Reviews* 256(1-2), 28-45.

Alexy, R., Kumpel, T. and Kummerer, K. (2004). "Assessment of degradation of 18 antibiotics in the Closed Bottle Test." *Chemosphere* 57(6), 505-512.

Alvarino, T., Nastold, P., Suarez, S., Omil, F., Corvini, P. F. X. and Bouju, H. (2016). "Role of biotransformation, sorption and mineralization of C-14-labelled sulfamethoxazole under different redox conditions." *Science of the Total Environment* 542, 706-715.

Baran, W., Adamek, E., Ziemianska, J. and Sobczak, A. (2011). "Effects of the presence of sulfonamides in the environment and their influence on human health." *Journal of Hazardous Materials* 196, 1-15.

Barbieri, M., Carrera, J., Ayora, C., Sanchez-Vila, X., Licha, T., Nodler, K., Osorio, V., Perez, S., Kock-Schulmeyer, M., de Alda, M. L. and Barcelo, D. (2012). "Formation of diclofenac and sulfamethoxazole reversible transformation products in aquifer material under denitrifying conditions: Batch experiments." *Science of the Total Environment* 426, 256-263.

Barnes, K. K., Kolpin, D. W., Furlong, E. T., Zaugg, S. D., Meyer, M. T. and Barber, L. B. (2008). "A national reconnaissance of pharmaceuticals and other organic wastewater contaminants in the United States - I) Groundwater." *Science of the Total Environment* 402(2-3), 192-200.

Bean, D. C., Livermore, D. M., Papa, I. and Hall, L. M. C. (2005). "Resistance among Escherichia coli to sulphonamides and other antimicrobials now little used in man." *Journal of Antimicrobial Chemotherapy* 56(5), 962-964.

Beesley, L., Moreno-Jimenez, E. and Gomez-Eyles, J. L. (2010). "Effects of biochar and greenwaste compost amendments on mobility, bioavailability and toxicity of inorganic and organic contaminants in a multi-element polluted soil." *Environmental Pollution* 158(6), 2282-2287.

Boreen, A. L., Arnold, W. A. and McNeill, K. (2004). "Photochemical fate of sulfa drugs in the aquatic environment: Sulfa drugs containing five-membered heterocyclic groups." *Environmental Science & Technology* 38(14), 3933-3940.

Brienza, M., Duwig, C., Perez, S. and Chiron, S. (2017). "4-nitroso-sulfamethoxazole generation in soil under denitrifying conditions: Field observations versus laboratory results." *Journal of Hazardous Materials* 334, 185-192.

Brown, K. D., Kulis, J., Thomson, B., Chapman, T. H. and Mawhinney, D. B. (2006). "Occurrence of antibiotics in hospital, residential, and dairy, effluent, municipal wastewater, and the Rio Grande in New Mexico." *Science of the Total Environment* 366(2-3), 772-783.

Bulut, E., Ozacar, M. and Sengil, I. A. (2008). "Adsorption of malachite green onto bentonite: Equilibrium and kinetic studies and process design." *Microporous and Mesoporous Materials* 115(3), 234-246.

Cao, X. D., Ma, L. N., Gao, B. and Harris, W. (2009). "Dairy-Manure Derived Biochar Effectively Sorbs Lead and Atrazine." *Environmental Science & Technology* 43(9), 3285-3291.

Carballa, M., Fink, G., Omil, F., Lema, J. M. and Ternes, T. (2008). "Determination of the solid-water distribution coefficient (K-d) for pharmaceuticals, estrogens and musk fragrances in digested sludge." *Water Research* 42(1-2), 287-295.

Carballa, M., Omil, F., Lema, J. M., Llompart, M., Garcia-Jares, C., Rodriguez, I., Gomez, M. and Ternes, T. (2004). "Behavior of pharmaceuticals, cosmetics and hormones in a sewage treatment plant." *Water Research* 38(12), 2918-2926.

Castiglioni, S., Bagnati, R., Fanelli, R., Pomati, F., Calamari, D. and Zuccato, E. (2006). "Removal of pharmaceuticals in sewage treatment plants in Italy." *Environmental Science & Technology* 40(1), 357-363.

Chen, H., Gao, B., Li, H. and Ma, L. Q. (2011). "Effects of pH and ionic strength on sulfamethoxazole and ciprofloxacin transport in saturated porous media." *Journal of Contaminant Hydrology* 126(1-2), 29-36.

Cheung, C. W., Porter, J. F. and McKay, G. (2000). "Elovich equation and modified second-order equation for sorption of cadmium ions onto bone char." *Journal of Chemical Technology and Biotechnology* 75(11), 963-970.

Clara, M., Strenn, B., Gans, O., Martinez, E., Kreuzinger, N. and Kroiss, H. (2005). "Removal of selected pharmaceuticals, fragrances and endocrine disrupting compounds in a membrane bioreactor and conventional wastewater treatment plants." *Water Research* 39(19), 4797-4807.

Conkle, J. L. and White, J. R. (2012). "An initial screening of antibiotic effects on microbial respiration in wetland soils." *Journal of Environmental Science and Health Part a-Toxic/Hazardous Substances & Environmental Engineering* 47(10), 1381-1390.

Crasto, A. (2016). Pharmaceutical Manufacturing Encyclopedia, 3rd Edition. New Drug Approvals

Drillia, P., Dokianakis, S. N., Fountoulakis, M. S., Kornaros, M., Stamatelatou, K. and Lyberatos, G. (2005a). "On the occasional biodegradation of pharmaceuticals in the activated sludge process: The example of the antibiotic sulfamethoxazole." *Journal of Hazardous Materials* 122(3), 259-265.

Drillia, P., Stamatelatou, K. and Lyberatos, G. (2005b). "Fate and mobility of pharmaceuticals in solid matrices." *Chemosphere* 60(8), 1034-1044.

Du, B., Price, A. E., Scott, W. C., Kristofco, L. A., Ramirez, A. J., Chambliss, C. K., Yelderman, J. C. and Brooks, B. W. (2014). "Comparison of contaminants of emerging concern removal, discharge, and water quality hazards among centralized and on-site wastewater treatment system effluents receiving common wastewater influent." *Science of the Total Environment* 466, 976-984.

Eibes, G., Debernardi, G., Feijoo, G., Moreira, M. T. and Lema, J. M. (2011). "Oxidation of pharmaceutically active compounds by a ligninolytic fungal peroxidase." *Biodegradation* 22(3), 539-550.

Enne, V. I., Livermore, D. M., Stephens, P. and Hall, L. M. C. (2001). "Persistence of sulphonamide resistance in Escherichia coli in the UK despite national prescribing restriction." *Lancet* 357(9265), 1325-1328.

Focazio, M. J., Kolpin, D. W., Barnes, K. K., Furlong, E. T., Meyer, M. T., Zaugg, S. D., Barber, L. B. and Thurman, M. E. (2008). "A national reconnaissance for pharmaceuticals and other organic wastewater contaminants in the United States - II) Untreated drinking water sources." *Science of the Total Environment* 402(2-3), 201-216.

Foo, K. Y. and Hameed, B. H. (2010). "Insights into the modeling of adsorption isotherm systems." *Chemical Engineering Journal* 156(1), 2-10.

Fountoulakis, M. (2004). "Toxic effect of pharmaceuticals on methanogenesis." *Water science and technology* 50(5), 335.

Gao, J. A. and Pedersen, J. A. (2005). "Adsorption of sulfonamide antimicrobial agents to clay minerals." *Environmental Science & Technology* 39(24), 9509-9516.

Gao, J. F., Ellis, L. B. M. and Wackett, L. P. (2010). "The University of Minnesota Biocatalysis/Biodegradation Database: improving public access." *Nucleic Acids Research* 38, D488-D491.

Garcia-Galan, M. J., Diaz-Cruz, M. S. and Barcelo, D. (2009). "Combining chemical analysis and ecotoxicity to determine environmental exposure and to assess risk from sulfonamides." *Trac-Trends in Analytical Chemistry* 28(6), 804-819.

Gauthier, H., Yargeau, V. and Cooper, D. G. (2010). "Biodegradation of pharmaceuticals by Rhodococcus rhodochrous and Aspergillus niger by co-metabolism." *Science of the Total Environment* 408(7), 1701-1706.

Gell, K., van Groenigen, J. W. and Cayuela, M. L. (2011). "Residues of bioenergy production chains as soil amendments: Immediate and temporal phytotoxicity." *Journal of Hazardous Materials* 186(2-3), 2017-2025.

Gobel, A., McArdell, C. S., Joss, A., Siegrist, H. and Giger, W. (2007). "Fate of sulfonamides, macrolides, and trimethoprim in different wastewater treatment technologies." *Science of the Total Environment* 372(2-3), 361-371.

Gobel, A., Thomsen, A., Mcardell, C. S., Joss, A. and Giger, W. (2005). "Occurrence and sorption behavior of sulfonamides, macrolides, and trimethoprim in activated sludge treatment." *Environmental Science & Technology* 39(11), 3981-3989.

Gros, M., Petrovic, M. and Barcelo, D. (2007). "Wastewater treatment plants as a pathway for aquatic contamination by pharmaceuticals in the ebro river basin (northeast spain)." *Environmental Toxicology and Chemistry* 26(8), 1553-1562.

Gros, M., Petrovic, M., Ginebreda, A. and Barcelo, D. (2010). "Removal of pharmaceuticals during wastewater treatment and environmental risk assessment using hazard indexes." *Environment International* 36(1), 15-26.

Grossberger, A., Hadar, Y., Borch, T. and Chefetz, B. (2014). "Biodegradability of pharmaceutical compounds in agricultural soils irrigated with treated wastewater." *Environmental Pollution* 185, 168-177.

Grunheid, S., Amy, G. and Jekel, M. (2005). "Removal of bulk dissolved organic carbon (DOC) and trace organic compounds by bank filtration and artificial recharge." *Water Research* 39(14), 3219-3228.

Haggard, B. E., Galloway, J. M., Green, W. R. and Meyer, M. T. (2006). "Pharmaceuticals and other organic chemicals in selected north-central and northwestern Arkansas streams." *Journal of Environmental Quality* 35(4), 1078-1087.

Halling-Sorensen, B., Nielsen, S. N., Lanzky, P. F., Ingerslev, F., Lutzhoft, H. C. H. and Jorgensen, S. E. (1998). "Occurrence, fate and effects of pharmaceutical substances in the environment - A review." *Chemosphere* 36(2), 357-394.

Hameed, B. H. (2008). "Equilibrium and kinetic studies of methyl violet sorption by agricultural waste." *Journal of Hazardous Materials* 154(1-3), 204-212.

Hansch, C., Leo, A. and Hoekman, D., Eds. (1995). Exploring QSAR: Hydrophobic, electronic, and steric constants. ACS Professional Reference Book. Washington, DC, American Chemical Society.

Heberer, T., Massmann, G., Fanck, B., Taute, T. and Duennbier, U. (2008). "Behaviour and redox sensitivity of antimicrobial residues during bank filtration." *Chemosphere* 73(4), 451-460.

Hirsch, R., Ternes, T., Haberer, K. and Kratz, K. L. (1999). "Occurrence of antibiotics in the aquatic environment." *Science of the Total Environment* 225(1-2), 109-118.

Ho, Y. S. and McKay, G. (1998). "Sorption of dye from aqueous solution by peat." *Chemical Engineering Journal* 70(2), 115-124.

Hoge, C. W., Gambel, J. M., Srijan, A., Pitarangsi, C. and Echeverria, P. (1998). "Trends in antibiotic resistance among diarrheal pathogens isolated in Thailand over 15 years." *Clinical Infectious Diseases* 26(2), 341-345.

Holtge, S. and Kreuzig, R. (2007). "Laboratory testing of sulfamethoxazole and its metabolite acetyl-sulfamethoxazole in soil." *Clean-Soil Air Water* 35(1), 104-110.

Homem, V. and Santos, L. (2011). "Degradation and removal methods of antibiotics from aqueous matrices - A review." *Journal of Environmental Management* 92(10), 2304-2347.

Ji, L. L., Wan, Y. Q., Zheng, S. R. and Zhu, D. Q. (2011). "Adsorption of Tetracycline and Sulfamethoxazole on Crop Residue-Derived Ashes: Implication for the Relative Importance of Black Carbon to Soil Sorption." *Environmental Science & Technology* 45(13), 5580-5586.

Jia, G. M., Cao, J., Wang, C. Y. and Wang, G. (2005). "Microbial biomass and nutrients in soil at the different stages of secondary forest succession in Ziwulin, northwest China." *Forest Ecology and Management* 217(1), 117-125.

Karthikeyan, K. G. and Meyer, M. T. (2006). "Occurrence of antibiotics in wastewater treatment facilities in Wisconsin, USA." *Science of the Total Environment* 361(1-3), 196-207.

Kassotaki, E., Buttiglieri, G., Ferrando-Climent, L., Rodriguez-Roda, I. and Pijuan, M. (2016). "Enhanced sulfamethoxazole degradation through ammonia oxidizing bacteria co-metabolism and fate of transformation products." *Water Research* 94, 111-119.

Kim, S. D., Cho, J., Kim, I. S., Vanderford, B. J. and Snyder, S. A. (2007). "Occurrence and removal of pharmaceuticals and endocrine disruptors in South Korean surface, drinking, and waste waters." *Water Research* 41(5), 1013-1021.

Kolpin, D. W., Furlong, E. T., Meyer, M. T., Thurman, E. M., Zaugg, S. D., Barber, L. B. and Buxton, H. T. (2002). "Pharmaceuticals, hormones, and other organic wastewater contaminants in US streams, 1999-2000: A national reconnaissance." *Environmental Science & Technology* 36(6), 1202-1211.

Kummerer, K. (2009). "Antibiotics in the aquatic environment - A review - Part I." *Chemosphere* 75(4), 417-434.

Kundu, S. and Gupta, A. K. (2006). "Arsenic adsorption onto iron oxide-coated cement (IOCC): Regression analysis of equilibrium data with several isotherm models and their optimization." *Chemical Engineering Journal* 122(1-2), 93-106.

Lagergren, S. (1898). "Zur theorie der sogenannten adsorption gelöster stoffe." *Kungliga Svenska Vetenskapsakademiens. Handlingar* 24(4), 1-39.

Langmuir, I. (1917). "THE CONSTITUTION AND FUNDAMENTAL PROPERTIES OF SOLIDS AND LIQUIDS. II. LIQUIDS.1." *Journal of the American Chemical Society* 39(9), 1848-1906.

Larcher, S. and Yargeau, V. (2012). "Biodegradation of sulfamethoxazole: current knowledge and perspectives." *Applied Microbiology and Biotechnology* 96(2), 309-318.

Laville, N., Ait-Aissa, S., Gomez, E., Casellas, C. and Porcher, J. M. (2004). "Effects of human pharmaceuticals on cytotoxicity, EROD activity and ROS production in fish hepatocytes." *Toxicology* 196(1-2), 41-55.

Lee, C. O. H., K.J.; Thomson, B.M. (2009). "State of Knowledge of Pharmaceutical, Personal Care Product, and Endocrine Disrupting Compound Removal during Municipal Wastewater Treatment." Report to New Mexico Environment Department. http://www.unm.edu/~howe/UNM%20Howe%20PPCP%20Final%20Report.pdf [Accessed January 20, 2018]

Lehmann, J., Skjemstad, J., Sohi, S., Carter, J., Barson, M., Falloon, P., Coleman, K., Woodbury, P. and Krull, E. (2008). "Australian climate-carbon cycle feedback reduced by soil black carbon." *Nature Geoscience* 1(12), 832-835.

Lian, F., Sun, B. B., Song, Z. G., Zhu, L. Y., Qi, X. H. and Xing, B. S. (2014). "Physicochemical properties of herb-residue biochar and its sorption to ionizable antibiotic sulfamethoxazole." *Chemical Engineering Journal* 248, 128-134.

Limousin, G., Gaudet, J. P., Charlet, L., Szenknect, S., Barthes, V. and Krimissa, M. (2007). "Sorption isotherms: A review on physical bases, modeling and measurement." *Applied Geochemistry* 22(2), 249-275.

Lin, K. D. and Gan, J. (2011). "Sorption and degradation of wastewater-associated non-steroidal anti-inflammatory drugs and antibiotics in soils." *Chemosphere* 83(3), 240-246.

Lindsey, M. E., Meyer, M. and Thurman, E. M. (2001). "Analysis of trace levels of sulfonamide and tetracycline antimicrobials, in groundwater and surface water using solid-phase extraction and liquid chromatography/mass spectrometry." *Analytical Chemistry* 73(19), 4640-4646.

Loos, R., Locoro, G., Comero, S., Contini, S., Schwesig, D., Werres, F., Balsaa, P., Gans, O., Weiss, S., Blaha, L., Bolchi, M. and Gawlik, B. M. (2010). "Pan-European survey on the occurrence of selected polar organic persistent pollutants in ground water." *Water Research* 44(14), 4115-4126.

Lopez-Serna, R., Petrovic, M. and Barcelo, D. (2012). "Occurrence and distribution of multi-class pharmaceuticals and their active metabolites and transformation products in the Ebro River basin (NE Spain)." *Science of the Total Environment* 440, 280-289.

Luo, Y., Mao, D. Q., Rysz, M., Zhou, D. X., Zhang, H. J., Xu, L. and Alvarez, P. J. J. (2010). "Trends in Antibiotic Resistance Genes Occurrence in the Haihe River, China." *Environmental Science & Technology* 44(19), 7220-7225.

Mackay, A. A. and Seremet, D. E. (2008). "Probe Compounds to Quantify Cation Exchange and Complexation Interactions of Ciprofloxacin with Soils." *Environmental Science & Technology* 42(22), 8270-8276.

Martinez-Hernandez, V., Meffe, R., Lopez, S. H. and de Bustamante, I. (2016). "The role of sorption and biodegradation in the removal of acetaminophen, carbamazepine, caffeine, naproxen and sulfamethoxazole during soil contact: A kinetics study." *Science of the Total Environment* 559, 232-241.

McCarl, B. A., Peacoke, C., Chrisman, R., Kung, C.-C. and Sands, R. A. (2009). "Economics of biochar production, utilization and greenhouse gas offsets". In: J. Lehmann and S. Joseph

(eds). *Biochar for Environmental Management-Science and Technology*. London, Washington D.C., Earthscan**:** 341-358.

Michael, I., Rizzo, L., McArdell, C. S., Manaia, C. M., Merlin, C., Schwartz, T., Dagot, C. and Fatta-Kassinos, D. (2013). "Urban wastewater treatment plants as hotspots for the release of antibiotics in the environment: A review." *Water Research* 47(3), 957-995.

Mohatt, J. L., Hu, L. H., Finneran, K. T. and Strathmann, T. J. (2011). "Microbially Mediated Abiotic Transformation of the Antimicrobial Agent Sulfamethoxazole under Iron-Reducing Soil Conditions." *Environmental Science & Technology* 45(11), 4793-4801.

Morel, M. C., Spadini, L., Brimo, K. and Martins, J. M. F. (2014). "Speciation study in the sulfamethoxazole-copper-pH-soil system: Implications for retention prediction." *Science of the Total Environment* 481, 266-273.

Muller, E., Schussler, W., Horn, H. and Lemmer, H. (2013). "Aerobic biodegradation of the sulfonamide antibiotic sulfamethoxazole by activated sludge applied as co-substrate and sole carbon and nitrogen source." *Chemosphere* 92(8), 969-978.

Nodler, K., Licha, T., Barbieri, M. and Perez, S. (2012). "Evidence for the microbially mediated abiotic formation of reversible and non-reversible sulfamethoxazole transformation products during denitrification." *Water Research* 46(7), 2131-2139.

Peng, X. Z., Wang, Z. D., Kuang, W. X., Tan, J. H. and Li, K. (2006). "A preliminary study on the occurrence and behavior of sulfonamides, ofloxacin and chloramphenicol antimicrobials in wastewaters of two sewage treatment plants in Guangzhou, China." *Science of the Total Environment* 371(1-3), 314-322.

Phan Thi Phuong, H., Managaki, S., Nakada, N., Takada, H., Shimizu, A., Duong Hong, A., Pham Hung, V. and Suzuki, S. (2011). "Antibiotic contamination and occurrence of antibiotic-resistant bacteria in aquatic environments of northern Vietnam." *Science of the Total Environment* 409(15), 2894-2901.

Radke, M., Lauwigi, C., Heinkele, G., Muerdter, T. E. and Letzel, M. (2009). "Fate of the Antibiotic Sulfamethoxazole and Its Two Major Human Metabolites in a Water Sediment Test." *Environmental Science & Technology* 43(9), 3135-3141.

Reinthaler, F. F., Posch, J., Feierl, G., Wust, G., Haas, D., Ruckenbauer, G., Mascher, F. and Marth, E. (2003). "Antibiotic resistance of E-coli in sewage and sludge." *Water Research* 37(8), 1685-1690.

Reis, P. J. M., Reis, A. C., Ricken, B., Kolvenbach, B. A., Manaia, C. M., Corvini, P. F. X. and Nunes, O. C. (2014). "Biodegradation of sulfamethoxazole and other sulfonamides by Achromobacter denitrificans PR1." *Journal of Hazardous Materials* 280, 741-749.

Rodriguez-Escales, P. and Sanchez-Vila, X. (2016). "Fate of sulfamethoxazole in groundwater: Conceptualizing and modeling metabolite formation under different redox conditions." *Water Research* 105, 540-550.

Roose-Amsaleg, C. and Laverman, A. M. (2016). "Do antibiotics have environmental side-effects? Impact of synthetic antibiotics on biogeochemical processes." *Environmental Science and Pollution Research* 23(5), 4000-4012.

Schmidt, C. K., Lange, F. T. and Brauch, H.-J. (2004). Assessing the impact of different redox conditions and residence times on the fate of organic micropollutants during riverbank filtration. 4th International Conference on Pharmaceuticals and Endocrine Disrupting Chemicals in Water.

Schmidt, S., Winter, J. and Gallert, C. (2012). "Long-Term Effects of Antibiotics on the Elimination of Chemical Oxygen Demand, Nitrification, and Viable Bacteria in Laboratory-Scale Wastewater Treatment Plants." *Archives of Environmental Contamination and Toxicology* 63(3), 354-364.

Schwab, B. W., Hayes, E. P., Fiori, J. M., Mastrocco, F. J., Roden, N. M., Cragin, D., Meyerhoff, R. D., D'Aco, V. J. and Anderson, P. D. (2005). "Human pharmaceuticals in US surface waters: A human health risk assessment." *Regulatory Toxicology and Pharmacology* 42(3), 296-312.

Segura, P. A., Francois, M., Gagnon, C. and Sauve, S. (2009). "Review of the Occurrence of Anti-infectives in Contaminated Wastewaters and Natural and Drinking Waters." *Environmental Health Perspectives* 117(5), 675-684.

Sohi, S. P., Krull, E., Lopez-Capel, E. and Bol, R. (2010). "A Review of Biochar and Its Use and Function in Soil." *Advances in Agronomy, Vol 105* 105, 47-82.

Spokas, K. A., Koskinen, W. C., Baker, J. M. and Reicosky, D. C. (2009). "Impacts of woodchip biochar additions on greenhouse gas production and sorption/degradation of two herbicides in a Minnesota soil." *Chemosphere* 77(4), 574-581.

Srinivasan, P. and Sarmah, A. K. (2014). "Dissipation of sulfamethoxazole in pasture soils as affected by soil and environmental factors." *Science of the Total Environment* 479, 284-291.

Srinivasan, P. and Sarmah, A. K. (2015). "Characterisation of agricultural waste-derived biochars and their sorption potential for sulfamethoxazole in pasture soil: A spectroscopic investigation." *Science of the Total Environment* 502, 471-480.

Srinivasan, P., Sarmah, A. K., Manley-Harris, M. and Wilkins, A. L. (2010). Sorption of sulfamethoxazole, sulfachloropyridazine and sulfamethazine onto six New Zealand dairy

farm soils 19th World Congress of Soil Science, Soil Solutions for a Changing World Brisbane, Australia.

Standley, L. J., Rudel, R. A., Swartz, C. H., Attfield, K. R., Christian, J., Erickson, M. and Brody, J. G. (2008). "wastewater-contaminated groudwater as a source of endogenous hormones and pharmaceuticals to surface water ecosystems." *Environmental Toxicology and Chemistry* 27(12), 2457-2468.

Taghizadeh-Toosi, A., Clough, T. J., Condron, L. M., Sherlock, R. R., Anderson, C. R. and Craigie, R. A. (2011). "Biochar Incorporation into Pasture Soil Suppresses in situ Nitrous Oxide Emissions from Ruminant Urine Patches." *Journal of Environmental Quality* 40(2), 468-476.

Tan, I. A. W., Ahmad, A. L. and Hameed, B. H. (2008). "Adsorption of basic dye on high-surface-area activated carbon prepared from coconut husk: Equilibrium, kinetic and thermodynamic studies." *Journal of Hazardous Materials* 154(1-3), 337-346.

Tan, X. F., Liu, Y. G., Zeng, G. M., Wang, X., Hu, X. J., Gu, Y. L. and Yang, Z. Z. (2015). "Application of biochar for the removal of pollutants from aqueous solutions." *Chemosphere* 125, 70-85.

Taty-Costodes, V. C., Fauduet, H., Porte, C. and Delacroix, A. (2003). "Removal of Cd(II) and Pb(II) ions, from aqueous solutions, by adsorption onto sawdust of Pinus sylvestris." *Journal of Hazardous Materials* 105(1-3), 121-142.

Thiele-Bruhn, S., Seibicke, T., Schulten, H. R. and Leinweber, P. (2004). "Sorption of sulfonamide pharmaceutical antibiotics on whole soils and particle-size fractions." *Journal of Environmental Quality* 33(4), 1331-1342.

Tiwari, S. K. and Paul, B. K. (2009). "Application of Nickel Nanoparticles in Diffusion Bonding of Stainless Steel Surfaces." *Msec 2008: Proceedings of the Asme International Manufacturing Science and Engineering Conference 2008, Vol 2*, 441-446.

Trovo, A. G., Nogueira, R. F. P., Aguera, A., Sirtori, C. and Fernandez-Alba, A. R. (2009). "Photodegradation of sulfamethoxazole in various aqueous media: Persistence, toxicity and photoproducts assessment." *Chemosphere* 77(10), 1292-1298.

Van Stempvoort, D. R., Roy, J. W., Grabuski, J., Brown, S. J., Bickerton, G. and Sverko, E. (2013). "An artificial sweetener and pharmaceutical compounds as co-tracers of urban wastewater in groundwater." *Science of the Total Environment* 461, 348-359.

Verstraeten, I. M., Fetterman, G. S., Meyer, M. T., Bullen, T. and Sebree, S. K. (2005). "Use of tracers and isotopes to evaluate vulnerability of water in domestic wells to septic waste." *Ground Water Monitoring and Remediation* 25(2), 107-117.

Vijayaraghavan, K., Padmesh, T. V. N., Palanivelu, K. and Velan, M. (2006). "Biosorption of nickel(II) ions onto Sargassum wightii: Application of two-parameter and three-parameter isotherm models." *Journal of Hazardous Materials* 133(1-3), 304-308.

Woolf, D., Amonette, J. E., Street-Perrott, F. A., Lehmann, J. and Joseph, S. (2010). "Sustainable biochar to mitigate global climate change." *Nature Communications* 1.

Wu, M., Pan, B., Zhang, D., Xiao, D., Li, H., Wang, C. and Ning, P. (2013). "The sorption of organic contaminants on biochars derived from sediments with high organic carbon content." *Chemosphere* 90(2), 782-788.

Xie, M. X., Chen, W., Xu, Z. Y., Zheng, S. R. and Zhu, D. Q. (2014). "Adsorption of sulfonamides to demineralized pine wood biochars prepared under different thermochemical conditions." *Environmental Pollution* 186, 187-194.

Xu, B., Mao, D., Luo, Y. and Xu, L. (2011). "Sulfamethoxazole biodegradation and biotransformation in the water-sediment system of a natural river." *Bioresource Technology* 102(14), 7069-7076.

Xu, W. H., Zhang, G., Li, X. D., Zou, S. C., Li, P., Hu, Z. H. and Li, J. (2007). "Occurrence and elimination of antibiotics at four sewage treatment plants in the Pearl River Delta (PRD), South China." *Water Research* 41(19), 4526-4534.

Yalkowsky, S. H. H., Yan (2003). Handbook of Aqueous Solubility Data: An Extensive Compilation of Aqueous Solubility Data for Organic Compounds Boca Raton, FL, CRC Press LLC.658

Yan, C., Dinh, Q. T., Chevreuil, M., Garnier, J., Roose-Amsaleg, C., Labadie, P. and Laverman, A. M. (2013). "The effect of environmental and therapeutic concentrations of antibiotics on nitrate reduction rates in river sediment." *Water Research* 47(11), 3654-3662.

Yang, J. F., Ying, G. G., Zhou, L. J., Liu, S. and Zhao, J. L. (2009). "Dissipation of oxytetracycline in soils under different redox conditions." *Environmental Pollution* 157(10), 2704-2709.

Yao, Y., Gao, B., Chen, H., Jiang, L. J., Inyang, M., Zimmerman, A. R., Cao, X. D., Yang, L. Y., Xue, Y. W. and Li, H. (2012). "Adsorption of sulfamethoxazole on biochar and its impact on reclaimed water irrigation." *Journal of Hazardous Materials* 209, 408-413.

Zhang, J., Lu, F., Zhang, H., Shao, L., Chen, D. and He, P. (2015). "Multiscale visualization of the structural and characteristic changes of sewage sludge biochar oriented towards potential agronomic and environmental implication." *Scientific Reports* 5.

Zhang, X., Pan, B., Yang, K., Zhang, D. and Hou, J. (2010). "Adsorption of sulfamethoxazole on different types of carbon nanotubes in comparison to other natural adsorbents." *Journal of Environmental Science and Health Part a-Toxic/Hazardous Substances & Environmental Engineering* 45(12), 1625-1634.

Zhang, Y., Xu, J., Zhong, Z. X., Guo, C. S., Li, L., He, Y., Fan, W. H. and Chen, Y. C. (2013). "Degradation of sulfonamides antibiotics in lake water and sediment." *Environmental Science and Pollution Research* 20(4), 2372-2380.

Zheng, H., Wang, Z. Y., Zhao, J., Herbert, S. and Xing, B. S. (2013). "Sorption of antibiotic sulfamethoxazole varies with biochars produced at different temperatures." *Environmental Pollution* 181, 60-67.

Zimmerman, M. J. (2005). "Occurrence of Organic Wastewater Contaminants, Pharmaceuticals, and Personal Care Products in Selected Water Supplies, Cape Cod, Massachusetts, June 2004." Open-File Report 2005-1206. http://pubs.er.usgs.gov/publication/ofr20051206 [Accessed Nov. 01, 2017]

Chapter III. Biodegradation of sulfamethoxazole in subsurface: a closed bottle simulation using soil/wastewater system

3.1 Introduction

Antibiotics are frequently used to treat bacterial infection and promote animal growth since their first introduction. These antibiotics are not completely removed in conventional wastewater treatment systems and can be released to the environment through effluent discharges or land application of sludge (Hirsch et al. 1999). The antibiotics in the environment pose threats to humans and ecosystems by promoting the development of bacterial resistance, altering existing bacterial culture, along with a number of impacts (Boxall et al. 2012; WHO 2014). The WHO (1998) identified the emergence of antimicrobial resistance as one of the serious concerns of health policies in the future.

Sulfamethoxazole (SMX) is one of the most widely used antibiotics (Garcia-Galan et al. 2009). Significant amounts of these antibiotics are excreted from human or animal bodies in unchanged form SMX or in its human transformation products N4-acetyl-SMX or N-SMX-glucuronide due to partial metabolism (Vanderven et al. 1995; Hirsch et al. 1999). The occurrence of SMX in the environment has been reported in many countries, at concentrations in the magnitude of ng/L to µg/L (Kolpin et al. 2002; Focazio et al. 2008). Studies on the elimination of SMX in natural systems revealed the persistency and mobility of SMX in subsurface, where photochemical degradation is limited (Alexy et al. 2004; Barber et al. 2009; Henzler et al. 2014). The intrinsic properties of SMX, including hydrophilicity, poor chelating ability and water solubility, makes its adsorptive removal limited to soil or sediment. Biodegradation is thus considered as an important elimination mechanism for SMX in the subsurface.

Laboratory experiments have been completed to explore the biodegradation of SMX in the system of soil and water. Factors such as nutrient composition, system redox condition, accompanying matrix and bacterial flora have been found to play important roles in SMX degradation, which might be the reason for the discrepancies of reported degradation results. Nutrient effects on SMX degradation have been studied by adding external organic carbons,

which led to the elevation of SMX degradation rate in soil/water or sediment/water systems (Radke et al. 2009; Xu et al. 2011). In addition, soil was suspected to contribute to the major degradation of SMX (Al-Ahmad et al. 1999; Xu et al. 2011). However, studies on SMX degradation in subsurface were still not completed because several important pieces are still missing. First, study of nutrient effects were mainly conducted under aerobic conditions (Radke et al. 2009; Xu et al. 2011). The influence of nutrients on the system was not well understood under anoxic conditions. Second, most of the laboratory experiments were completed in artificial wastewater or river water, but rarely in septic effluent, which is an important entering route concerns to a population of 1.3 billion (1 out of 4.3 people in the world are using septic system) (Mohatt et al. 2011; Barbieri et al. 2012; Martinez-Hernandez et al. 2016; WHO 2017). Third, SMX has the potential to serve as a nitrogen and sulfur source and studies in sludge systems and pure bacterial cultures have shown that the external nitrogen could improve SMX degradation (Swindoll et al. 1988; Drillia et al. 2005; Muller et al. 2013; Alvarino et al. 2016; Kassotaki et al. 2016). However, studies on the external nitrogen and sulfur have not been reported for soil/water systems.

To fill the gaps of the research on SMX degradation in the subsurface, our study used closed bottle experiments to explore the nutrient effect under both aerobic and anoxic conditions in a soil/water system. Instead of using synthetic water or river water, septic effluent was collected and used as the aqueous phase. Moreover, SMX degradation was compared with three matrices: soil, wastewater, and soil combined with wastewater to understand the contribution of every matrix to SMX removal. Nutrient changes were also examined in all experiments to understand the process from the nutrient perspective. The hypothesis of the nutrient effect was that SMX could be consumed by bacteria as C, N or S sources based on its molecular structure. After addition of a nutrient (C, N, or S),

- Enhanced degradation would suggest this nutrient is the limiting metabolism of SMX;
- Inhibited degradation would indicate the nutrient is a preferred competitor of SMX for bacterial utilization;
- No change in degradation would imply SMX doesn't serve as a source of this nutrient.

3.2 Materials and methods

3.2.1 Materials

Sulfamethoxazole (analytical standard) was purchased from Sigma-Aldrich (St. Louis, MO, USA). Sodium sulfate anhydrous (Na_2SO_4), sodium acetate trihydrate ($NaAc{\cdot}3H_2O$) and ammonium chloride (NH_4Cl) were obtained from Fisher Scientific (USA). Wastewater used in this study was the effluent collected from a septic tank at Massachusetts Alternative Septic System Test Center (MASSTC). The wastewater sample was filtered through Whatman grade 4 filter paper and stored at 4°C before use. Soil was also sampled from MASSTC, and its properties were characterized (appendix A). It was air dried and stored at room temperature in a capped container. All treatments were carried out with the same batch of wastewater and soil.

3.2.2 Characterizations

Basic properties of wastewater that were characterized include pH, total ammonia, total phosphorus (TP), dissolved organic carbon (DOC) and dissolved anions.

pH was measured with a pH meter (Fisher Scientific Accumet® AB150). Total ammonia was determined using Nesslerization method at colorimetric quantification at 425 nm (HACH DR3900). TP was measure using standard method 4500-PC at a wavelength of 400 nm (APHA 2005). Detailed procedures for TP and total ammonia can be find in appendix B.

After filtering the samples through 0.45 µm filters, DOC samples were acidified to pH ≈ 1 with 6 N hydrochloride acid and then bubbled for 3 min with CO_2-free air to purge inorganic carbon. DOC was measured by high temperature catalytic oxidation (HTCO) using a Shimadzu TOC 5000 analyzer following the same protocol as Sohrin and Semper´ e (2005). Three to five 66 µL replicates of each sample were injected into the 680 °C column. The coefficient of variation of the DOC replicates was always smaller than 2 %. Quantification was performed using a four-point calibration curve with standards of 0 ppm, 2 ppm, 5 ppm and 8 ppm prepared by diluting potassium hydrogen phthalate in DI water.

Aqueous anions were analyzed using Ion Chromatography (DIONEX ICS-2100) with Dionex IonPac^{TM} AS15 2 × 250 mm Column. The column temperature was maintained at 30 °C at a

flowrate of 0.25 ml/min. The injection volume was 100 μL with loop mode. Cell temperature was set at 35 °C and KOH eluent of 38 mM was generated online.

The properties of wastewater was summarized in table III-1.

Table III-1. Properties of septic effluent sampled from MASSTC

Property	Value
pH	6.97
Total ammonium, ppm	37.2
DO, mg/L	0.24
DOC, ppm	45.8
Dissolved anion, ppm	
Chloride	39.75
Nitrate	0.379
Nitrite	0.791
Phosphate	12.84
Sulfate	6.36

3.2.3 Degradation experiments

The degradation experiments were based on a simplified OECD 308 test scheme (2002) reported by Xu et al. (2011). Seventy grams of soil and 150 ml wastewater were introduced into 250ml glass amber bottles with septum caps. The water to soil volume ratio was 3.5 : 1 and soil layer was 2 cm in depth. Prior spiking in SMX, the wastewater-soil system was acclimated for a week. 0.75 ml of SMX stock solution were added to a target concentration of 1000 ppb. The bottles were then well mixed to reach a homogenous condition. The system was then kept at a controlled lab temperature of 22 °C. Blank batch experiments were also conducted without SMX addition. A control experiment was performed by adding SMX to wastewater only. Samples were first collected after 2 hours settling to test the initial properties of the system. Subsequent samples were collected for 18 days at days 3, 5, 9, and 18. One-half ml of samples were collected after gently swirling the solution, followed by 1 hour of settling. Analytical characterization was conducted for each sample with dilutions by a factor of 10. To investigate the influence of nutrients, Na_2SO_4, $NaAc{\cdot}3H_2O$ and NH_4Cl were spiked into DI

water, respectively, to obtain a nutrient content simulating that of a wastewater system. Two replicates were run for each condition. A T test with 95% confidence interval was performed for statistical analysis.

For anoxic degradation, an air free environment was created by purging N_2 gas into a sealed system for 3 hours. The anoxic condition was then maintained by positive N_2 pressure. After each sampling time, the system was sealed by applying a layer of vacuum grease on any punctured spot and then purged with N_2 gas for another hour. For aerobic degradation, two needles were inserted through septum cap into the headspace to facilitate air exchange (Radke et al. 2009). The system was purged with air after each sampling.

Inhibition experiments were also conducted to evaluate the contribution of sorption to the total SMX removal. The microbial activity was inhibited by the adding 1% w/v NaN_3 solution to the wastewater to achieve a resulting concentration of 200 ppm. The SMX removal determined in inhibited samples was considered to be due to SMX sorption. The difference between the inhibited samples and not inhibited samples were attributed to biodegradation.

3.2.4 LC-MS analysis

The remaining concentration of SMX was quantified by liquid chromatography–mass spectrometry (Agilent Techonologies 5130 Qradupole) equipped with Epic C18 MSO 2.3 µ 150 Å 5 cm × 2.1 mm column, UV detector at 277 nm and targeting at m/z of 254. HPLC water with 0.1 % formic acid (A) and 95 % acetonitrile with 5 % water and 0.1 % formic acid (B) were used as mobile phases. The column was maintained at 30 °C at a flow rate of 0.3 ml/min and the inject volume was 75 µL. The limitation of detection (LOD) was 4.01 µg/L and the limit of quantification was 13.0 µg/L.

3.3 Results and discussions

Changes of system pH values are presented in the section 3.3.1. Results for the matrices effect and nutrient effect on SMX biodegradation under aerobic and anoxic conditions are presented and discussed in this section.

3.3.1 pH changes

System pH is crucial to the biodegradation of SMX. It not only affects the process of degradation, the pH change over time is also an apparent reflection of the effects of the relative degradation processes. Aqueous pH controls the availability and transformation of nutrients by affecting the extent of protonation, precipitation and mineralization. $NH_4^+ \Leftrightarrow NH_3$, $H_2CO_3 \Leftrightarrow HCO_3^- \Leftrightarrow CO_3^{2-}$ and $CH_3COOH \Leftrightarrow CH_3COO^-$ are the main conjugate acid-base pairs that control system pH (Sommer and Husted 1995; Moller and Muller 2012). Reduction of sulfate increases solution pH by consuming H^+ ions. Removal of the sulfate reduction product H_2S and carbonate protonation product CO_2 was considered to be one of the main mechanisms to increase pH (Sommer and Husted 1995). However, evaporation of NH_3 reduces the solution pH. The pH value is also influenced by the precipitation of cations (e.g. Ca^{2+}, Mg^{2+}, Fe^{2+}) with weak acidic anions (e.g. CO_3^{2-}, PO_4^{3-}), which usually includes the release of H^+ ions (Le Corre et al. 2009; Hjorth et al. 2010). Degradation of organic matter affects solution pH in two different ways. The incomplete degradation of organic carbon decreases solution pH through formation of organic acid. On the other hand, degradation of protein-rich organics converts organic nitrogen into inorganic ammonium, which causes pH to increase (Moller and Muller 2012). Thus, the apparent pH change during anoxic degradation is the summation of the effects of all the influential reactions.

Other than the influence on the nutrients, pH also determines the biodegradation of SMX by preferential growth and activity of microorganism under different pH values (Siddique et al. 2002; Kim et al. 2013; Shah 2014).

The pH values for the systems in this study can be described as weak alkaline under aerobic and anoxic conditions, within a range of 7.2 to 8.3 (figure III-1). Under this pH, the dominant transformation of SMX is the negatively charged form. Nutrients studied in this research mainly existed in the forms of NH_4^+ (pK_a = 10), NO_3^- (pK_a = -1.4), SO_4^{2-} (pK_a = -3, 2) and CH_3COO^- (pK_a = 4.76).

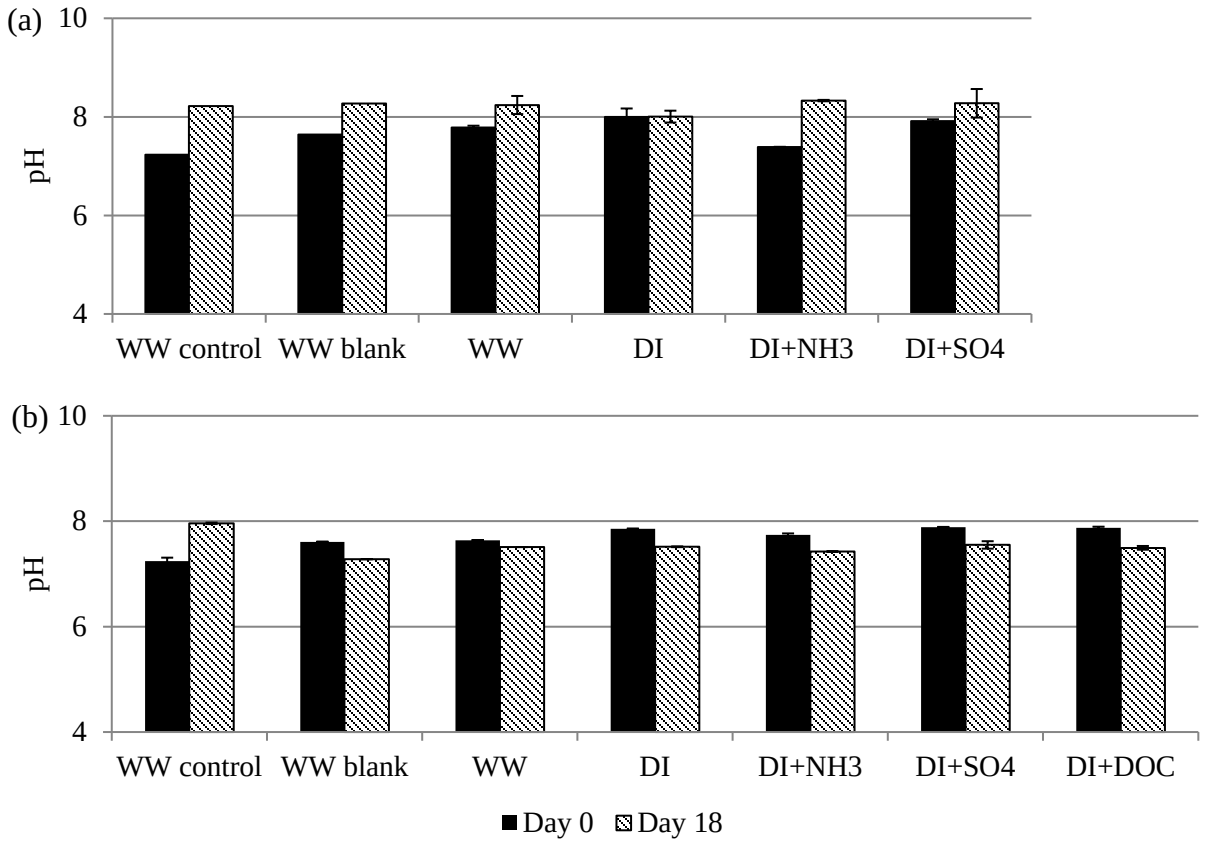

Figure III-1. pH changes in different systems. WW stands for wastewater and DI stands for Deionized water, NH3 stands for ammonia, SO4 stands for sulfate and DOC stands for dissolved organic carbon. (a) anoxic condition (b) aerobic condition.

Under the anoxic condition, pH of the system remained constant in the DI sample where no wastewater was present. When spiked with nutrients, the pH increased by 0.4 to 1 unit, to a pH about 8.2 after 18 days of contact time. The pH increase under anoxic degradation was previously reported and 0.5 to 2 units of increase was observed (Webb and Hawkes 1985; Pain et al. 1990; Kirchmann and Witter 1992; Chantigny et al. 2009; Moller and Muller 2012). Similar changes also occurred in the batches of wastewater control and wastewater, which contains similar amount of ammonium and sulfate as spiked DI samples. These results indicated the increase of pH might be linked to the aqueous nutrient content. However, the increase in pH will not affect the dominance of SMX, NH_4^+, NO_3^-, SO_4^{2-} and CH_3COO^- because of the big difference between their pKa's and aqueous pH value.

Under aerobic conditions, pH decreased and a pH value of 7.5 was achieved for all batches with different nutrient contents, except for the case of the wastewater control experiment. The lower end pH in the aeration condition is likely due to the slow dissolution of CO_2, which has three potential sources - air, respiration of bacteria, and mineral products of aerobic degradation process. For the application of similar analyze, the pH change would not change the major transformation of SMX, NH_4^+, NO_3^-, SO_4^{2-} and CH_3COO^- .

Therefore, aqueous pH of the systems increased in samples under anoxic conditions and decreased under aerobic conditions. The pH change would not affect the dominant transformation of the compounds of this study, which were SMX^-, NO_3^-, SO_4^{2-}, NH_4^+ and CH_3COO^-.

3.3.2 Effect of nutrient amendments on SMX degradation

Nitrogen, sulfur and DOC are important nutrients for bacterial growth, and are also crucial indices reflecting water quality. Based on the molecular structure, SMX could potentially be utilized by bacteria as nitrogen, sulfur or carbon source to support bacteria growth. The study of the influence of accessible nutrients could shed some light on the mechanism of SMX degradation. Nutrient amendments could affect SMX degradation by inhibiting SMX consumption as a competitor or enhancing SMX removal via facilitating relative bacterial growth.

The dissolved nitrogen compounds studied in this research were in the forms of ammonium and nitrate, which are not only the products of the nitrogen transformation, but also known as easy-degradable nitrogen sources. Sulfate, a common sulfur source enriched in soil and wastewater, was selected as an amendment to study its influence on SMX degradation. Sodium acetate was used as the external carbon source and DOC was analyzed as the indicator of the concentration of the available carbon source in the aqueous phase. The influence of external nutrients was investigated under both aerobic and anoxic conditions. After 7 days acclimation, the concentrated nutrient amendment solution, along with the SMX stock solution, was added into soil/DI water system. Concentrations of dissolved SMX were monitored at each time interval and then compared with those having no nutrient addition.

3.3.2.1 Aerobic conditions

SMX removal exhibited similar trends for all nutrient amendment samples and DI controls. The SMX concentration started to decrease immediately after the addition of SMX, suggesting no acclimation period was required for microorganisms in the soil system of this study. During the 18 days of the experiment, the SMX concentration kept decreasing and about 80 % of SMX remained at the end (figure III-2). Changes in SMX concentrations in samples of DI + SO4 and DI + NH3 were close to that in the DI control, suggesting no significant effect of the sulfate and ammonium amendment to SMX degradation. However, SMX degradation was enhanced by the acetate amendment. The SMX removal increased from 20 % in unspiked samples to 31 % in spiked samples.

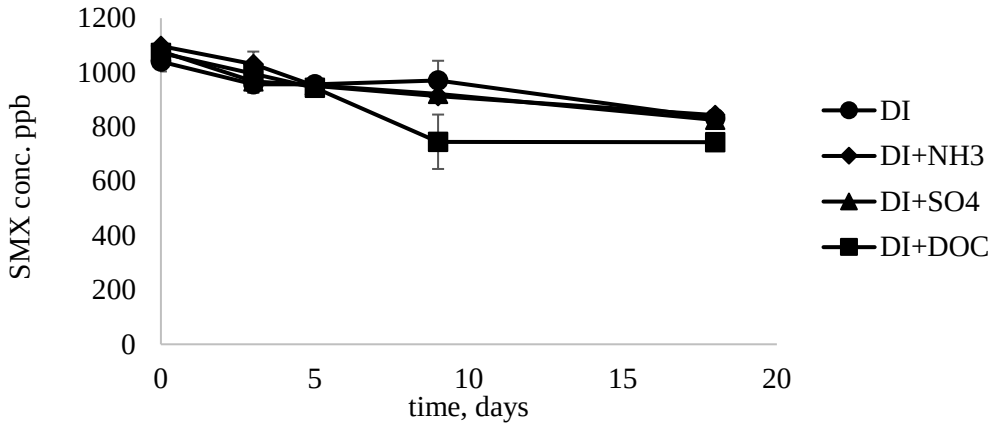

Figure III-2. Influence of ammonium, sulfate and acetate amendment on the degradation of SMX under aerobic condition.

The results of ammonium and nitrate changes indicated that nitrogen was used by the bacteria in the system and the degradation was fostered by the ammonium amendment (figure III-3). Under the aerobic condition in the DI + NH3 samples, the ammonium concentration decreased by 9.44 ppm, while the nitrate concentration increased by 15.1 ppm. A greater nitrate increase was observed in relation to the expected value associated with nitrification of the consumed ammonia, which indicated that nitrification of organic nitrogen occurred in the system. The nitrification of organic nitrogen was also implied by the results of DI samples under aerobic condition, but at a smaller magnitude. These results suggested that nitrogen utilized in this bacteria culture under aerobic conditions include ammonium and organic nitrogen.

The fact that SMX degradation was not enhanced after the ammonium amendment, even though ammonium was used as a nitrogen source, suggests that microorganism growth related with ammonium usage was probably indicative of non-degraders rather than those utilizing SMX (Drillia et al. 2005; Alvarino et al. 2016). Nitrification might not be the primary pathway for SMX degradation. The apparent irrelevance of ammonium amendment to the degradation of organic compounds under the aerobic condition was also published by other researchers in the study of SMX degradation in sludge. (Swindoll et al. 1988; Drillia et al. 2005; Alvarino et al. 2016). No impact on SMX degradation by the ammonium addition was reported, even in a microorganism culture that has been adapted and enrich with SMX degraders. However, the influence of nitrogen on the aerobic mineralization of the organic contaminant varied with soil samples, nitrogen concentration and the nature of organic contaminant (Swindoll et al. 1988). Both no influence and enhanced mineralization were reported for the same organic contaminant using soil samples collected in close proximity (Swindoll et al. 1988)

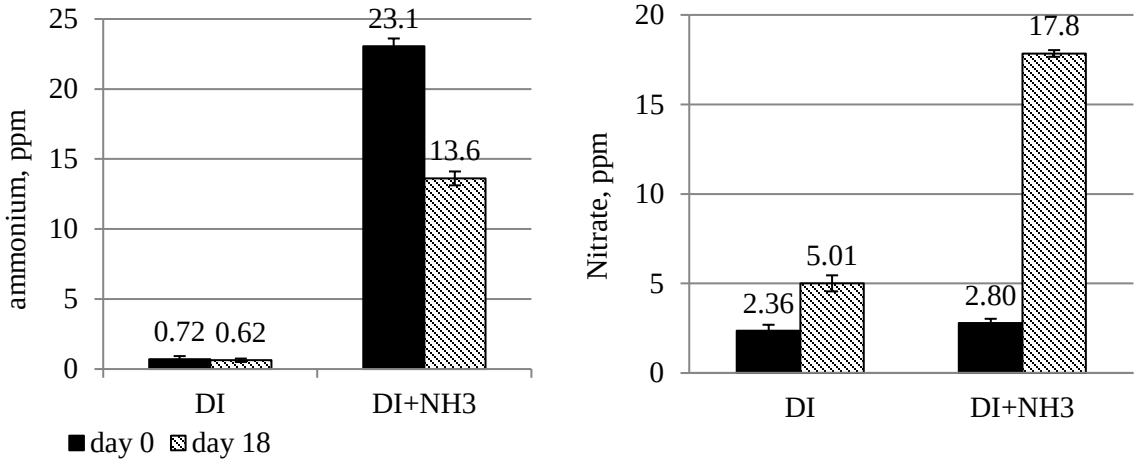

Figure III-3. Change of ammonium and nitrate in ammonium amendment samples under aerobic condition.

However, sulfate was not consumed by the bacteria given that the concentrations did not change significantly under aerobic conditions after 18 days (figure III-4). Sulfate was not subject to reduction under aerobic conditions because of the abundance of the more thermodynamically favorable terminal electron acceptor, O_2 ($E_H° = +0.81$ V for $O_{2(g)}/H_2O$ and -0.22 V for SO_4^{2-}/HS^-) (Schwarzenbach 2003). The slight increase in DI sample was probably

resulted from degradation of sulfur-containing organic matter or from the dissociation on soil (Moller and Muller 2012).

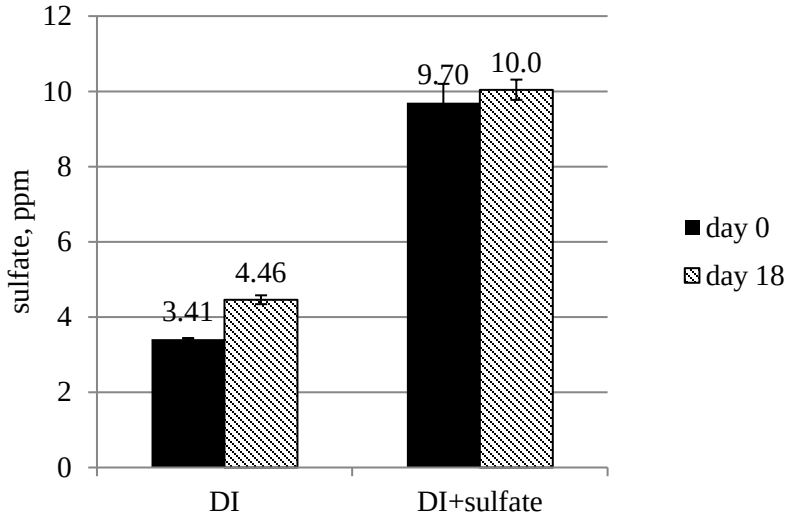

Figure III-4. Change of sulfate in sulfate amendment samples under aerobic conditions.

The DOC concentration decreased to 68 % in DI + acetate samples, and only slightly increased in the DI controls (figure II-5). A plausible explanation is that the external carbon source fostered the bacterial growth, which led to higher DOC consumption. This result also suggested that the enhanced removal of SMX was probably coupled with increased elimination of DOC. A similar effect of the DOC amendment was also observed in laboratory experiment with the soil/water systems with the external carbon source of methanol (Radke et al. 2009). This is a common phenomenon that has been frequently reported for SMX degradation in sludge/water systems where an enriched microbial culture was present and various carbon sources have been added, including glucose humic acid, acetate and isolated biopolymer fraction of DOC (Alexy et al. 2004; Drillia et al. 2005; Baumgarten et al. 2011; Xu et al. 2011; Alvarino et al. 2016). The parallel behavior of SMX and DOC suggested that the degradation of SMX might heterotrophic and DOC supported SMX degradation by establishing and maintaining sufficient bacterial activity (Alvarino et al. 2016).

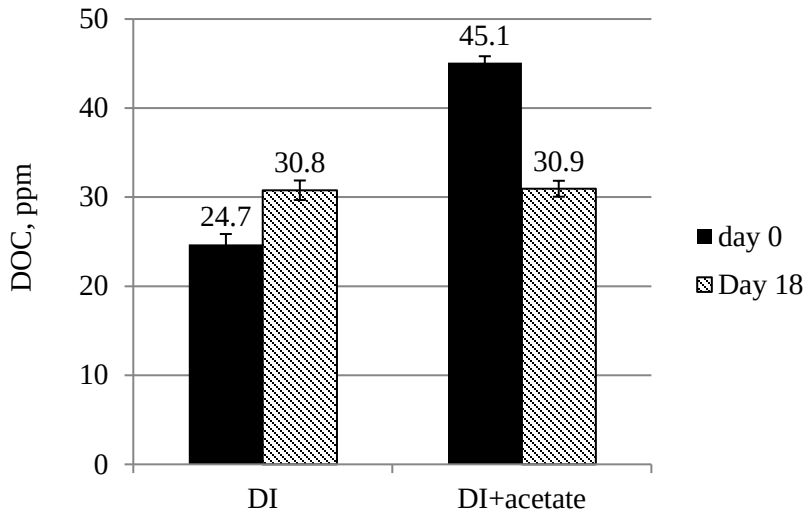

Figure III-5. Change of DOC in acetate amendment samples under aerobic condition.

To summarize, SMX degradation could be a heterotrophic process, serving as a carbon source for the bacterial flora in this system and was co-metabolized with easily degradable carbon of acetate. Nitrogen consumption was also needed in the system and nitrification of ammonium was observed. However, nitrifying bacteria might be non-degraders for SMX because SMX degradation was not effected by ammonium amendment. Sulfate was not involved in the degradation under the aerobic condition and the addition of which had no influence on SMX degradation.

3.3.2.2 Anoxic conditions

Changes of SMX concentration under anoxic conditions showed no acclimation period for the ammonium and sulfate amendment (figure III-6). The SMX concentrations kept decreasing from day 0 and the decreasing trend didn't stop until after 18 days. There were some variations in SMX concentrations between the nutrient amendment samples and DI controls during the degradation experiment, but no significant difference were observed for their final removal percentages, which were all about 75 %.

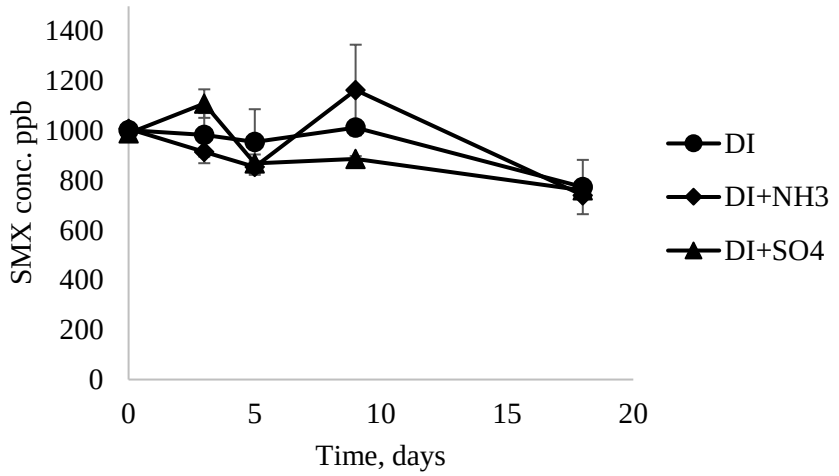

Figure III-6. Influence of ammonium and sulfate amendment on the degradation of SMX under anoxic condition.

Comparing the concentrations at day 0 and day 18 shows that a significant amount of ammonium was removed and nitrate was almost depleted, indicating that both ammonium and nitrate were used as nitrogen sources, most probably via denitrification (figure III-7a, b).

Under anoxic conditions, sulfate was subject to biodegradation by bacteria, such as sulfate-reducing bacteria (Moller and Muller 2012). Sulfate-reducing bacteria are organisms that exist under anoxic conditions and reduce sulfate into forms of S^0 and S^{2-} during respiration. However, in this work, sulfate concentrations did not change significantly for both DI and DI + SO4 samples under anoxic conditions after 18 days (figure III-7c). It was most likely that the system was not at the redox state appropriate for sulfate-reduction, and sulfate was likely not a thermodynamically favorable electron acceptor as compared to nitrate ($E_H° = -0.22$ V for SO_4^{2-}/HS^- and +0.74 V for $NO_3^-/N_{2(g)}$). Therefore, the system developed in this study could potentially be nitrate reducing but not sulfate reducing.

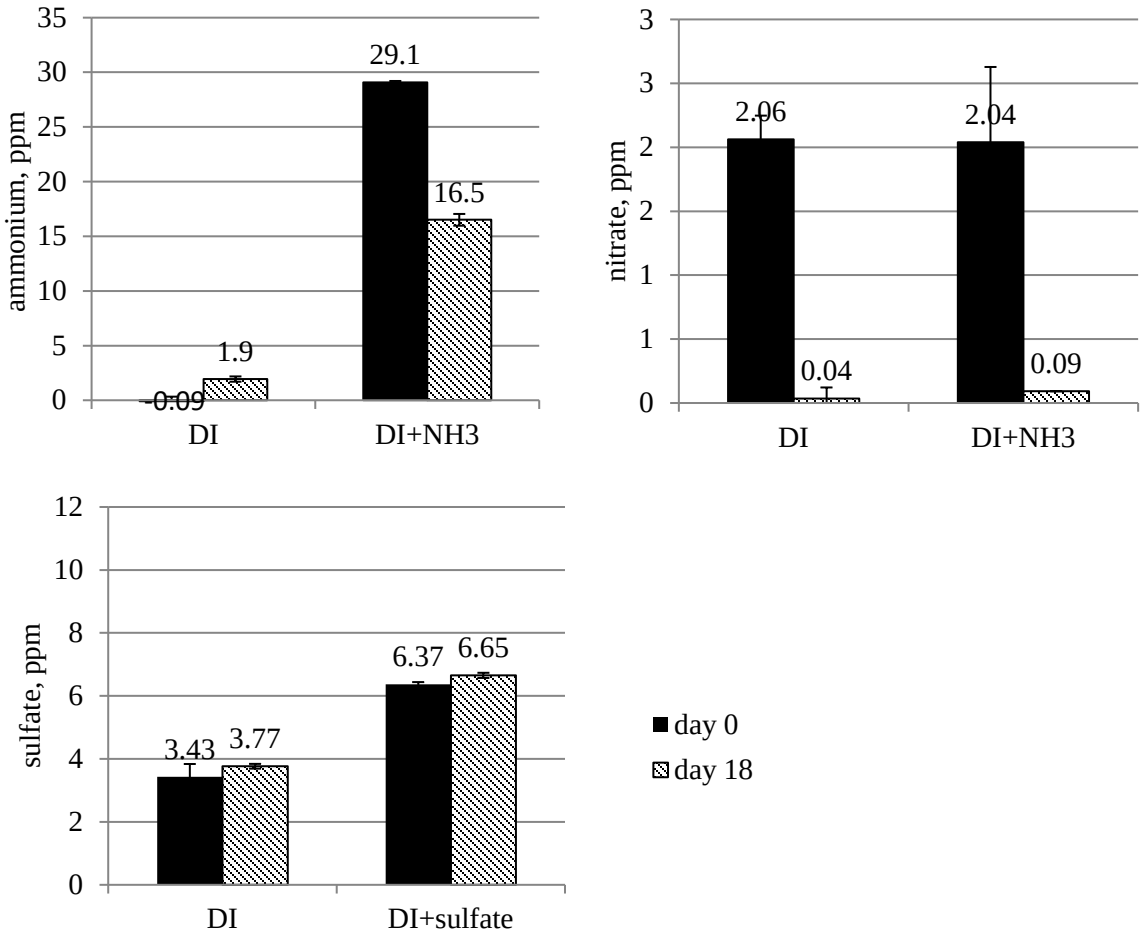

Figure III-7. Change of nutrients in corresponding nutrient amendment samples under anoxic condition.

Degradation of SMX under nitrate reducing conditions was also reported by Mohatt et al. (2011) in a system of soil and artificially formulated water. Slow degradation of SMX, close to the sterile control, was observed with < 30 % dissipation rate after 20 days, which agrees with our result. SMX degradation was also observed under a nitrate reducing condition in studies with sludge via a proposed co-metabolism mechanism driven by nitrous oxide, producing 4-nitro-SMX and 4-nitroso-SMX (Nodler et al. 2012; Brienza et al. 2017). A low degradation rate of 25 % after 10 days was reported, which was close to the result of this study. The low apparent removal percentage was attributed to the retransformation of 4-nitro-SMX into SMX when nitrate was depleted (Nodler et al. 2012). As nitrate depletion was also observed in this study, retransformation of 4-nitro-SMX was also expected.

Therefore, it could be a plausible pathway for the SMX in our nitrate reducing system to undergo nitration of the primary amine to produce 4-nitrous-SMX and 4-nitro-SMX, and the latter could then retransform into SMX. However, analysis limitation kept us from confirming the pathway by monitoring the byproducts of 4-nitro-SMX and 4-nitrous-SMX.

3.3.3 Degradation of SMX in different matrices

SMX degradation could be different in a different entry matrix. Wastewater, soil and combination of them could vary various properties such as bacterial flora and nutrient composition, which may play an important role in SMX degradation. Three entry matrices, wastewater, soil, and wastewater + soil were studied under aerobic and anoxic conditions, and SMX concentration was monitored over time for 18 days. Results are shown in figure III-9 and figure III-11.

To evaluate the contribution of soil sorption to the SMX removal during the experiment, inhibition experiments were conducted using 200 ppm of NaN_3 to inhibit the bioactivities in the systems. The results were presented in figure III-8.

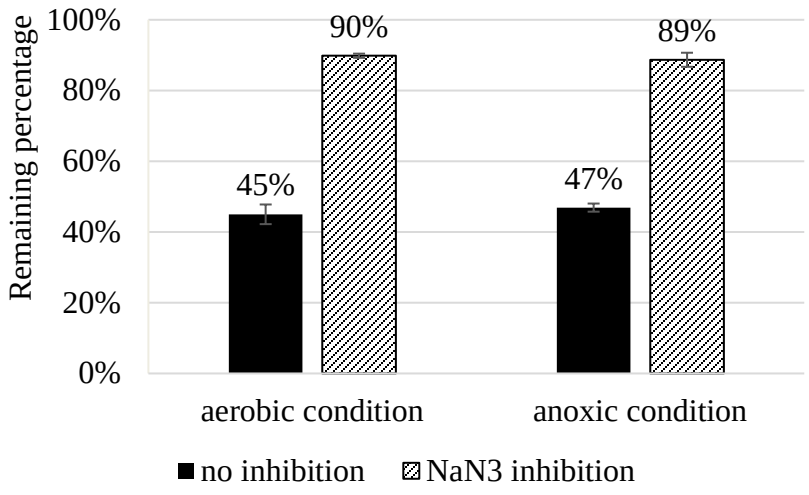

Figure III-8. Inhibition experiment of SMX for aerobic and anoxic conditions. The system was treated for 18 days in soil and wastewater systems.

The SMX removal in inhibited samples was mainly resulted from adsorption to soil. The removal difference between the inhibited and no-inhibited samples could be attributed to

biodegradation. Results showed that 45 % of SMX was removed after 18 days under aerobic condition, in which 10 % was resulted from sorption and the rest 35 % was from biodegradation. No significant difference was observed for the anoxic condition. Under the anoxic condition, 10 % was removed by sorption and 33 % was removed by biodegradation.

3.3.3.1 Aerobic condition

The SMX concentration started to decrease immediately after addition of SMX, showing no acclimation period. The removal of SMX in the three matrices followed the trend of WW + soil > soil only > WW only, where WW+Soil had the highest removal and WW had the lowest removal. SMX was persistent in WW only. Similar results have been reported by others (Al-Ahmad et al. 1999; Radke et al. 2009; Xu et al. 2011). Compared to wastewater, a higher removal percentage was obtained in soil. Xu et al. (2011) found that higher vial bacterial numbers existed in soil, compared to those that would exist in water, and suggested that soil might be the major contributor to SMX degradation. The highest removal was achieved in WW + soil and 55 % of initial concentration was removed after day 18, which implied that the interaction between soil and water was important (Xu et al. 2011).

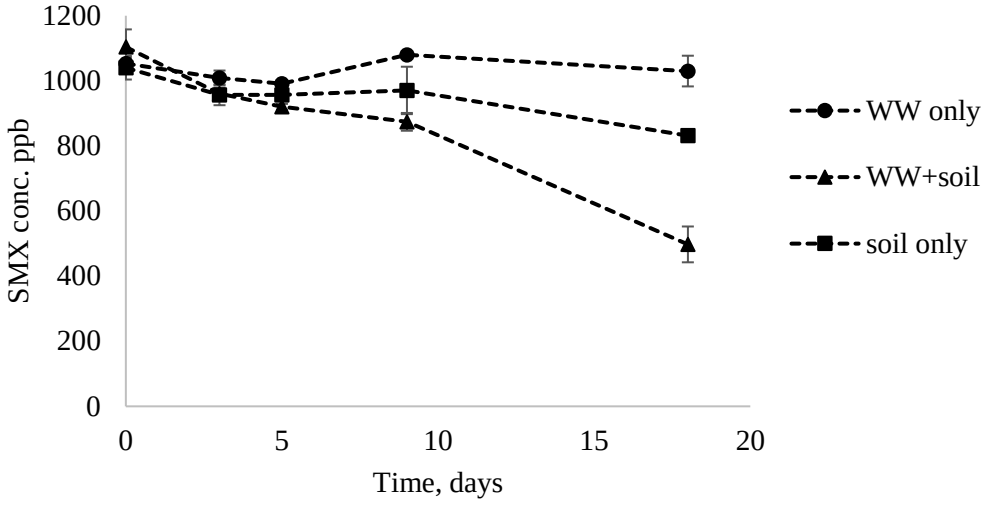

Figure III-9. Degradation of SMX in different matrices under aerobic condition.

The importance of soil in the SMX degradation has been noted, but is not well understood (Xu et al. 2011). The nutrient content in the three matrices was analyzed at the beginning and at the

end of the experiment to study the effects of soil on the dissolved nutrients. Results are presented in figure III-10.

With consideration to the initial concentrations in WW only, the soil-only sample was low in ammonium but high in nitrate. The concentration of sulfate and DOC was at the same order of magnitude in the WW only and soil only cases. This observation indicates that soil was not the main source for ammonium but was the main source of nitrate, and that both wastewater and soil were the suppliers of aqueous sulfate and DOC. However, when wastewater was added to soil, the nutrient composition of the WW + soil sample was closer to the WW only case than the soil only case. The results suggested that wastewater played an important role in the nutrient properties in aqueous phase, although the soil contributed to the majority of the SMX dissipation.

Unlike the result with the soil/DI water system (samples of soil only, DI and DI + nutrients), the ammonium concentration for the WW and WW + soil cases increased by 11.1 % and 11.4 % respectively after 18 days of experiment. However, the ammonium increase was not expected under the aerobic condition due to nitrification processes. Nitrification was evident in the soil only sample, in which the nitrate concentration increased significantly by 2.6 ppm. A nitrate increase was also observed in the WW and WW + soil case, but only in a small amount (by 0.03 ppm in the WW + soil sample and insignificantly in the WW only). Therefore, nitrification could be occurring in the WW and WW + soil cases but at low extent. The increase in ammonium concentration could be the result of the mineralization of protein enriched wastewater (Moller and Muller 2012).

In general, sulfate concentrations did not change significantly in the three matrices. As noted in section 3.3.2.1, a slight increase was observed for the soil only sample, which probably resulted from degradation of sulfur-containing organic matter or from the dissociation on soil (Moller and Muller 2012).

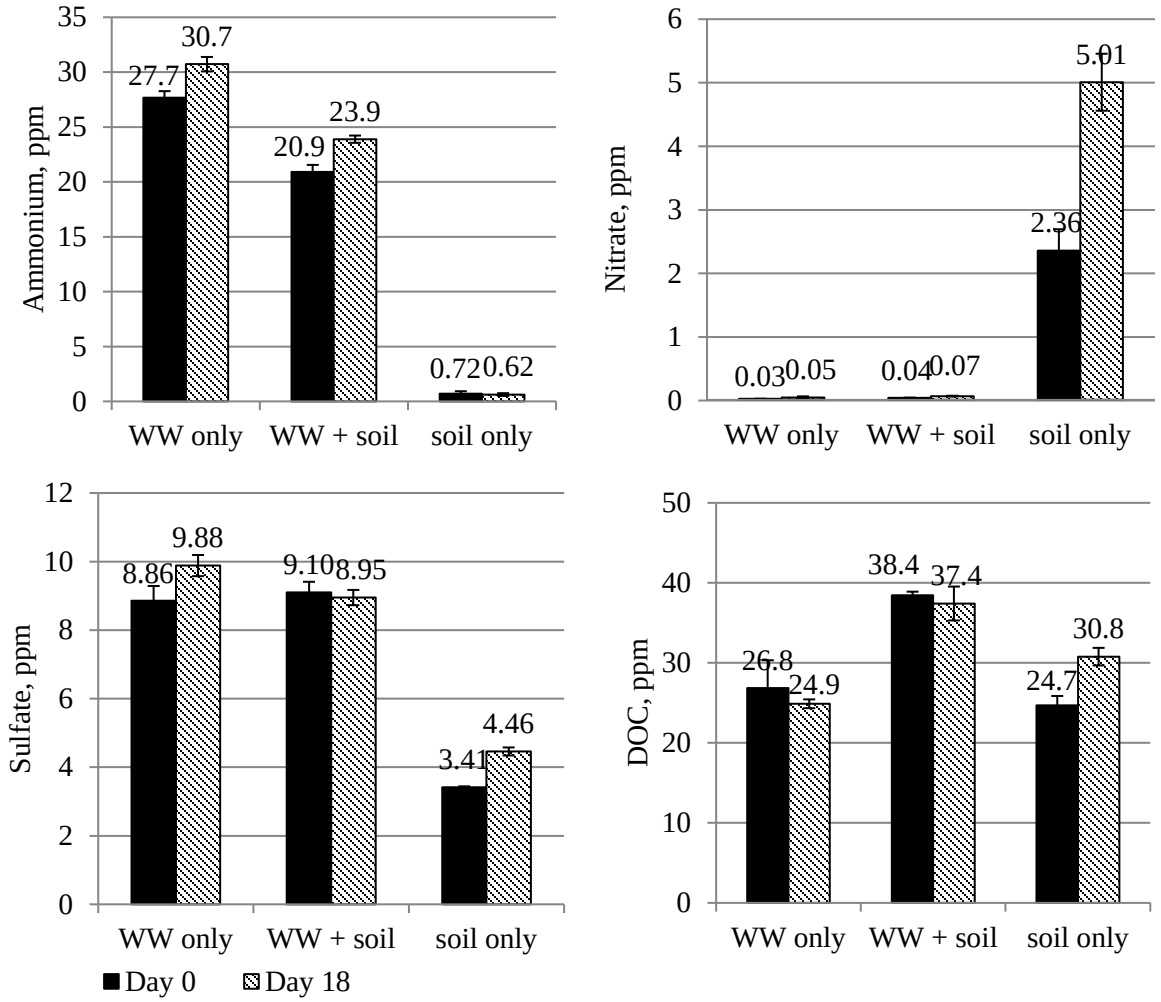

Figure III-10. Change of nutrients in different matrices under aerobic condition.

Compared to the WW only and soil only samples, the WW + soil contained the highest DOC content. Considering the positive correlation between DOC and SMX dissipation (as found in section 3.3.2.1), the highest DOC of WW +Soil could be a plausible explanation for its highest SMX removal rate. DOC didn't change significantly after 18 days of aerobic degradation in samples with wastewater (samples of WW only and WW + soil), while it increased by 24.6 % in the sample of soil only. One explanation could be that the enhanced bioactivity in the wastewater consumed extra DOC, but it would be unlikely for the amount of DOC consumed by the bacteria to be the same as the desorbed DOC for both the WW only and WW + soil samples. Another explanation could be that the presence of wastewater inhibited the desorption of DOC from soil.

In summary, the SMX dissipation rate under aerobic conditions varied in different matrices of wastewater, soil and wastewater/soil. It was persistent when only wastewater was present. Soil was the contributor to SMX removal, and the combination with wastewater further elevated the removal. From the perspective of aqueous nutrients, soil was mainly providing nitrate, sulfate and DOC. As discussed in section 3.3.2.1, DOC could facilitate the SMX degradation while ammonium and sulfate did not show significant influence. Thus, we suspect that the highest dissipation of WW + soil sample was due to its highest DOC.

3.3.3.2 Anoxic conditions

SMX dissipation under anoxic conditions follows different trends in different matrices (figure III-11). First, different lag phases were observed for SMX reduction, with the shortest lag phase of 3 days in the WW + soil samples and 9 days in the soil only samples. SMX was persistent in the WW only samples. The SMX removal rate after completion of the18-day experiment followed the trend of WW + Soil > soil only > WW only. The highest SMX reduction was obtained with WW + soil samples, in which 46.9 % of initial concentration remained at the end of the experiment, while 77.2 % remained at the end of the soil only experiment. As for the cases under aerobic conditions, soil also played important role in SMX degradation under anoxic conditions and it was found that the interaction between soil and wastewater could facilitate the removal.

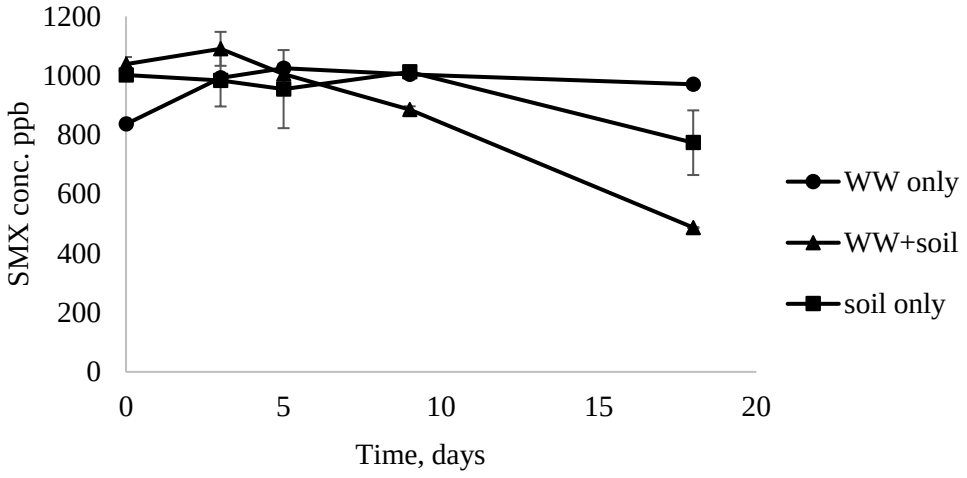

Figure III-11. Degradation of SMX in different matrices under anoxic condition.

The study on system nutrients in the aqueous phase was also completed under anoxic conditions to shed light on the role of different matrices on SMX degradation from the perspective of nutrient consumption and redox state. Results are presented in figure III-12.

As for the results observed under the aerobic condition, the concentration of ammonium was high in the WW only sample, but ammonium was almost absent in the aqueous phase of the soil only sample. However, the nitrate concentration in soil only sample was higher than that in WW only sample by an order of magnitude. Thus, wastewater was the main source of ammonium in the system while soil was the main source of nitrate. Sulfate and DOC were provided by both wastewater and soil, given that comparable initial amounts were presented in WW only and soil only samples.

The change in ammonium under anoxic conditions was not as significant as that under aerobic conditions. Nitrate was almost depleted in the soil only sample at the end of the experiment, probably due to denitrification, suggesting a nitrate-reducing condition of the system. Nitrate concentrations started low in the WW only and the WW + Soil samples, and didn't change significantly during the experiment, which was similar to the results under the aerobic conditions. Therefore, we believe that nitrate-reducing condition was established in the soil only sample but it was not as evident in WW only and WW + soil samples.

Note that sulfate concentrations didn't change significantly in the soil only and WW only samples. However, the interaction between wastewater and soil led to the significant reduction in sulfate concentration, indicating a sulfate-reducing condition. Therefore, given the findings from nitrate changes, the redox state of the soil only samples was nitrate-reducing and the redox state of WW + soil samples was sulfate-reducing. The redox state of the WW only samples could also be nitrate-reducing but it was not obvious from the data.

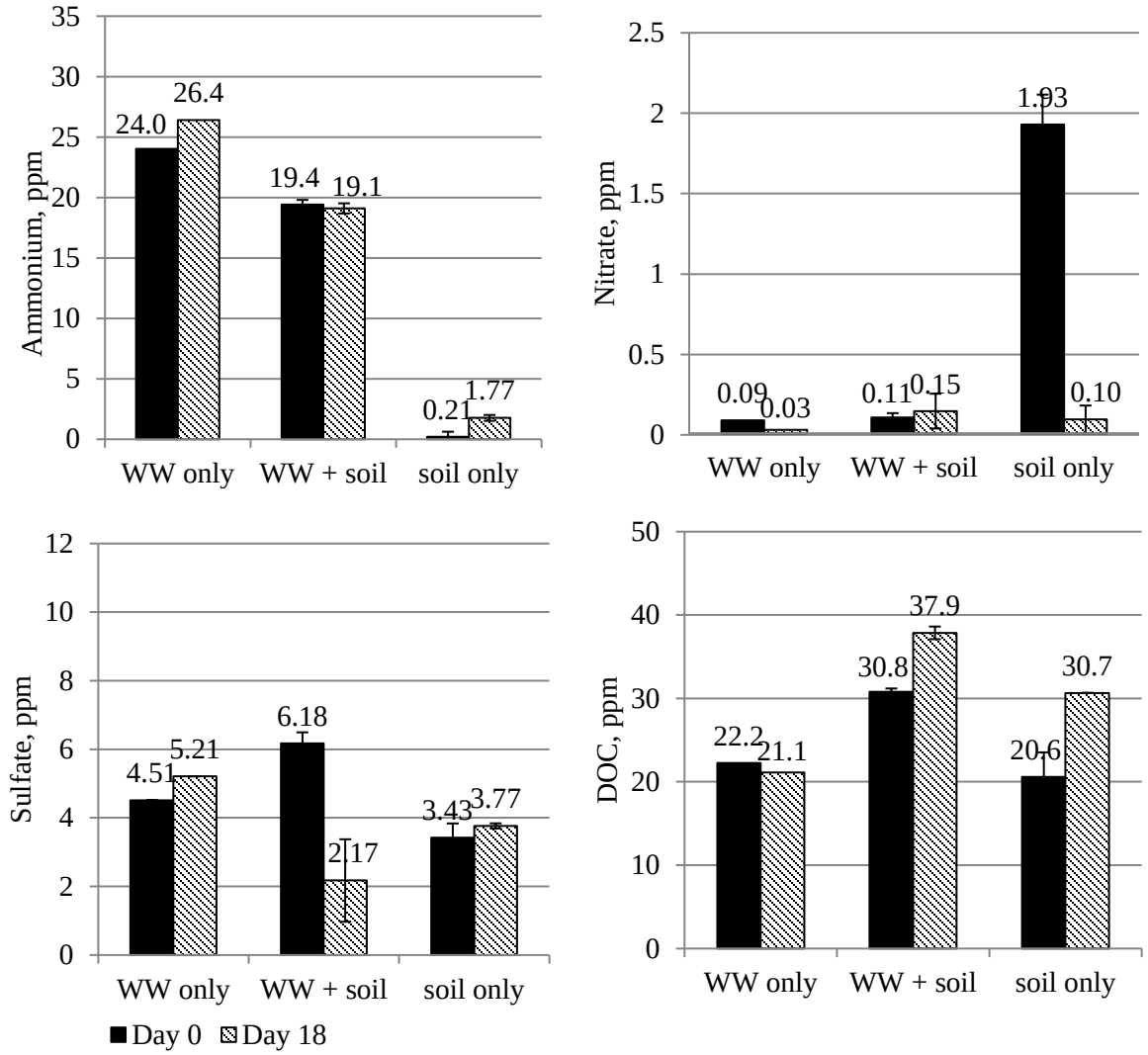

Figure III-12. Change of nutrients in different matrices under aerobic condition.

As discussed in section 3.3.2.2, an ammonium and sulfate enriched environment didn't benefit the SMX degradation. Therefore, the difference in SMX reduction in the three matrices may not have resulted from the variation in nutrient composition of ammonium and sulfate. Considering the discoveries of the system redox condition and SMX degradation rate, we found that the SMX removal rate was higher under sulfate-reducing conditions than the rate under nitrate-reducing conditions, which agrees with the findings reported by Mohatt et al. (2011). However, Nodler et al. (2012) observed the presence of SMX reduction coupled with nitrate removal, and proposed that nitrate may support SMX degradation by increasing denitrifying microbial activity. It indicated that higher SMX removals may be expected in soil only samples where the nitrate amount was highest among the three matrices, which was not

consistent with the observations in these experiments. Nodler noted that a high initial ratio of nitrate to SMX was important to promote the coupling effect. However, the nitrate to SMX ratio of our study was less than that reported by Nodler et al. (2012) by two orders of magnitude, and was close to that used by Mohatt et al. (2011). This difference could explain the limited amount of SMX reduction observed for nitrate-reducing conditions of Mohatt's study and of our study.

To summarize, the SMX dissipation varied with different matrices under anoxic conditions. Soil played an important role in the SMX degradation, through altering the redox condition of the systems. The interaction between soil and wastewater further enhanced the overall removal with shorter lag phase, probably due to the establishment of sulfate-reducing condition.

In comparison with wastewater, the soil matrix was found to be a major contributor to SMX dissipation under both aerobic and anoxic conditions. Nevertheless, the interaction between soil and wastewater could facilitate the removal of SMX under both conditions, but via different mechanisms. High DOC content could be the crucial factor for enhancing SMX degradation under aerobic conditions, while the creation of sulfate-reducing state could be the main reason under anoxic condition.

3.4 Conclusions

Occurrence of SMX has been widely reported in the environment. The biodegradation of SMX in the subsurface could vary significantly with in-situ properties. The objectives of the study described in this chapter were to assess nutrient effect and matric effect on the biodegradation of SMX in real soil/wastewater systems for aerobic and anoxic conditions.

Under aerobic conditions, SMX degradation was enhanced by DOC addition but not effected by ammonia and sulfate addition. SMX degradation was likely to be heterotrophic and could be co-metabolized with DOC. However, nitrifying bacteria may be non-degraders for SMX. Under nitrate reducing conditions, SMX degradation was not influenced by the addition of ammonium and sulfate. Nutrient analysis indicated the development of nitrate reducing condition in the systems. SMX degradation could undergo nitration of the primary amine.

The biodegradation of SMX also varied in different matrices under both aerobic and anoxic conditions. The highest degradation was achieved in WW + Soil systems and SMX was persistent in the wastewater only condition. Soil was the main contributor for SMX dissipation by providing DOC for aerobic condition and creating a stronger reducing condition (sulfate-reducing condition) for anoxic experiments.

The findings of this work could add to our understanding of biological removal of SMX by subsurface bacteria and reveal ways to improve SMX remediation by enhancing the biodegradation.

In the future, biodegradation experiments could be conducted for a longer period of time and more degradation data could be obtained for the kinetic analysis. The role of soil in the biodegradation could be studied in detail with the variation in soil/solution ratios and characterization of the system. Determination of metabolites and microorganism studies could be conducted in the future to help understand the mechanisms of SMX biodegradation.

References

Al-Ahmad, A., Daschner, F. D. and Kummerer, K. (1999). "Biodegradability of cefotiam, ciprofloxacin, meropenem, penicillin G, and sulfamethoxazole and inhibition of waste water bacteria." *Archives of Environmental Contamination and Toxicology* 37(2), 158-163.

Alexy, R., Kumpel, T. and Kummerer, K. (2004). "Assessment of degradation of 18 antibiotics in the Closed Bottle Test." *Chemosphere* 57(6), 505-512.

Alvarino, T., Nastold, P., Suarez, S., Omil, F., Corvini, P. F. X. and Bouju, H. (2016). "Role of biotransformation, sorption and mineralization of C-14-labelled sulfamethoxazole under different redox conditions." *Science of the Total Environment* 542, 706-715.

Barber, L. B., Keefe, S. H., Leblanc, D. R., Bradley, P. M., Chapelle, F. H., Meyer, M. T., Loftin, K. A., Kolpin, D. W. and Rubio, F. (2009). "Fate of Sulfamethoxazole, 4-Nonylphenol, and 17 beta-Estradiol in Groundwater Contaminated by Wastewater Treatment Plant Effluent." *Environmental Science & Technology* 43(13), 4843-4850.

Barbieri, M., Carrera, J., Ayora, C., Sanchez-Vila, X., Licha, T., Nodler, K., Osorio, V., Perez, S., Kock-Schulmeyer, M., de Alda, M. L. and Barcelo, D. (2012). "Formation of diclofenac and sulfamethoxazole reversible transformation products in aquifer material under denitrifying conditions: Batch experiments." *Science of the Total Environment* 426, 256-263.

Baumgarten, B., Jaehrig, J., Reemtsma, T. and Jekel, M. (2011). "Long term laboratory column experiments to simulate bank filtration: Factors controlling removal of sulfamethoxazole." *Water Research* 45(1), 211-220.

Boxall, A. B. A., Rudd, M. A., Brooks, B. W., Caldwell, D. J., Choi, K., Hickmann, S., Innes, E., Ostapyk, K., Staveley, J. P., Verslycke, T., Ankley, G. T., Beazley, K. F., Belanger, S. E., Berninger, J. P., Carriquiriborde, P., Coors, A., DeLeo, P. C., Dyer, S. D., Ericson, J. F., Gagne, F., Giesy, J. P., Gouin, T., Hallstrom, L., Karlsson, M. V., Larsson, D. G. J., Lazorchak, J. M., Mastrocco, F., McLaughlin, A., McMaster, M. E., Meyerhoff, R. D., Moore, R., Parrott, J. L., Snape, J. R., Murray-Smith, R., Servos, M. R., Sibley, P. K., Straub, J. O., Szabo, N. D., Topp, E., Tetreault, G. R., Trudeau, V. L. and Van Der Kraak, G. (2012). "Pharmaceuticals and Personal Care Products in the Environment: What Are the Big Questions?" *Environmental Health Perspectives* 120(9), 1221-1229.

Brienza, M., Duwig, C., Perez, S. and Chiron, S. (2017). "4-nitroso-sulfamethoxazole generation in soil under denitrifying conditions: Field observations versus laboratory results." *Journal of Hazardous Materials* 334, 185-192.

Chantigny, M. H., MacDonald, J. D., Beaupre, C., Rochette, P., Angers, D. A., Masse, D. and Parent, L. E. (2009). "Ammonia volatilization following surface application of raw and treated liquid swine manure." *Nutrient Cycling in Agroecosystems* 85(3), 275-286.

Drillia, P., Dokianakis, S. N., Fountoulakis, M. S., Kornaros, M., Stamatelatou, K. and Lyberatos, G. (2005). "On the occasional biodegradation of pharmaceuticals in the activated sludge process: The example of the antibiotic sulfamethoxazole." *Journal of Hazardous Materials* 122(3), 259-265.

Focazio, M. J., Kolpin, D. W., Barnes, K. K., Furlong, E. T., Meyer, M. T., Zaugg, S. D., Barber, L. B. and Thurman, M. E. (2008). "A national reconnaissance for pharmaceuticals and other organic wastewater contaminants in the United States - II) Untreated drinking water sources." *Science of the Total Environment* 402(2-3), 201-216.

Garcia-Galan, M. J., Diaz-Cruz, M. S. and Barcelo, D. (2009). "Combining chemical analysis and ecotoxicity to determine environmental exposure and to assess risk from sulfonamides." *Trac-Trends in Analytical Chemistry* 28(6), 804-819.

Henzler, A. F., Greskowiak, J. and Massmann, G. (2014). "Modeling the fate of organic micropollutants during river bank filtration (Berlin, Germany)." *Journal of Contaminant Hydrology* 156, 78-92.

Hirsch, R., Ternes, T., Haberer, K. and Kratz, K. L. (1999). "Occurrence of antibiotics in the aquatic environment." *Science of the Total Environment* 225(1-2), 109-118.

Hjorth, M., Christensen, K. V., Christensen, M. L. and Sommer, S. G. (2010). "Solid-liquid separation of animal slurry in theory and practice. A review." *Agronomy for Sustainable Development* 30(1), 153-180.

Kassotaki, E., Buttiglieri, G., Ferrando-Climent, L., Rodriguez-Roda, I. and Pijuan, M. (2016). "Enhanced sulfamethoxazole degradation through ammonia oxidizing bacteria co-metabolism and fate of transformation products." *Water Research* 94, 111-119.

Kim, J., Cho, K. J., Han, G., Lee, C. and Hwang, S. (2013). "Effects of temperature and pH on the biokinetic properties of thiocyanate biodegradation under autotrophic conditions." *Water Research* 47(1), 251-258.

Kirchmann, H. and Witter, E. (1992). "Composition of Fresh, Aerobic and Anaerobic Farm Animal Dungs." *Bioresource Technology* 40(2), 137-142.

Kolpin, D. W., Furlong, E. T., Meyer, M. T., Thurman, E. M., Zaugg, S. D., Barber, L. B. and Buxton, H. T. (2002). "Pharmaceuticals, hormones, and other organic wastewater contaminants in US streams, 1999-2000: A national reconnaissance." *Environmental Science & Technology* 36(6), 1202-1211.

Le Corre, K. S., Valsami-Jones, E., Hobbs, P. and Parsons, S. A. (2009). "Phosphorus Recovery from Wastewater by Struvite Crystallization: A Review." *Critical Reviews in Environmental Science and Technology* 39(6), 433-477.

Martinez-Hernandez, V., Meffe, R., Lopez, S. H. and de Bustamante, I. (2016). "The role of sorption and biodegradation in the removal of acetaminophen, carbamazepine, caffeine, naproxen and sulfamethoxazole during soil contact: A kinetics study." *Science of the Total Environment* 559, 232-241.

Mohatt, J. L., Hu, L. H., Finneran, K. T. and Strathmann, T. J. (2011). "Microbially Mediated Abiotic Transformation of the Antimicrobial Agent Sulfamethoxazole under Iron-Reducing Soil Conditions." *Environmental Science & Technology* 45(11), 4793-4801.

Moller, K. and Muller, T. (2012). "Effects of anaerobic digestion on digestate nutrient availability and crop growth: A review." *Engineering in Life Sciences* 12(3), 242-257.

Muller, E., Schussler, W., Horn, H. and Lemmer, H. (2013). "Aerobic biodegradation of the sulfonamide antibiotic sulfamethoxazole by activated sludge applied as co-substrate and sole carbon and nitrogen source." *Chemosphere* 92(8), 969-978.

Nodler, K., Licha, T., Barbieri, M. and Perez, S. (2012). "Evidence for the microbially mediated abiotic formation of reversible and non-reversible sulfamethoxazole transformation products during denitrification." *Water Research* 46(7), 2131-2139.

Pain, B. F., Misselbrook, T. H., Clarkson, C. R. and Rees, Y. J. (1990). "Odor and Ammonia Emissions Following the Spreading of Anaerobically-Digested Pig Slurry on Grassland." *Biological Wastes* 34(3), 259-267.

Radke, M., Lauwigi, C., Heinkele, G., Muerdter, T. E. and Letzel, M. (2009). "Fate of the Antibiotic Sulfamethoxazole and Its Two Major Human Metabolites in a Water Sediment Test." *Environmental Science & Technology* 43(9), 3135-3141.

Schwarzenbach, R. P. G., Philip. M.; Imboden, Dieter. M. (2003). Environmental Organic Chemistry. Hoboken, NJ, Wiley Interscience.

Shah, M. (2014). "Efficacy of Rhodococcus rhodochrous in Microbial Degradation of Toludine Dye." *Journal of Petroleum and Environmental Biotechnology* 5(4), 187.

Siddique, T., Okeke, B. C., Arshad, M. and Frankenberger, W. T. (2002). "Temperature and pH effects on biodegradation of hexachlorocyclohexane isomers in water and a soil slurry." *Journal of Agricultural and Food Chemistry* 50(18), 5070-5076.

Sommer, S. G. and Husted, S. (1995). "A Simple-Model of Ph in Slurry." *Journal of Agricultural Science* 124, 447-453.

Swindoll, C. M., Aelion, C. M. and Pfaender, F. K. (1988). "Influence of Inorganic and Organic Nutrients on Aerobic Biodegradation and on the Adaptation Response of Subsurface Microbial Communities." *Applied and Environmental Microbiology* 54(1), 212-217.

Vanderven, A. J. A. M., Vree, T. B., Kolmer, E. W. J. V., Koopmans, P. P. and Vandermeer, J. W. M. (1995). "Urinary Recovery and Kinetics of Sulfamethoxazole and Its Metabolites in Hiv-Seropositive Patients and Healthy-Volunteers after a Single Oral Dose of Sulfamethoxazole." *British Journal of Clinical Pharmacology* 39(6), 621-625.

Webb, A. R. and Hawkes, F. R. (1985). "Laboratory Scale Anaerobic-Digestion of Poultry Litter - Gas Yield Loading Rate Relationships." *Agricultural Wastes* 13(1), 31-49.

WHO (1998). "Antimicrobial Resistance" Geneva: World Health Organization (WHO). Available: http://www.who.int/mediacentre/factsheets/fs194/en/ [Accessed Nov. 1, 2017]

WHO (2014). "Antimicrobial resistance: global report on surveillance" Geneva: World Health Organization (WHO). Available: http://www.who.int/antimicrobial-resistance/publications/surveillancereport/en/ [Accessed 10 October 2017]

WHO (2017). "Progress on Drinking Water, Sanitation and Hygiene: 2017 Update and SDG Baselines" Geneva: World Health Organization (WHO) and the United Nations Children's Fund (UNICEF). Available: http://www.who.int/mediacentre/news/releases/2017/launch-version-report-jmp-water-sanitation-hygiene.pdf [Accessed Nov. 1, 2017]

Xu, B., Mao, D., Luo, Y. and Xu, L. (2011). "Sulfamethoxazole biodegradation and biotransformation in the water-sediment system of a natural river." *Bioresource Technology* 102(14), 7069-7076.

Chapter IV. Application of biochar for SMX adsorption in the subsurface: adsorption effectiveness and influential factors

4.1 Introduction

With an increasing demand since their introduction in late 1930s, antibiotics are widely used to treat disease in humans and promote animal growth in livestock (Gelband et al. 2015). However, the metabolism of antibiotics in human bodies and animals is incomplete (Hirsch et al. 1999; Boxall and Sinclair 2001; Boxall et al. 2002). Therefore, significant amounts of antibiotics and their metabolites are excreted and end up in the environment. Because these antibiotics are not treated effectively in current wastewater treatment systems, the high antibiotics usage poses threats to the environment through direct or secondary exposure (Ternes 1998; Castiglioni et al. 2006; Gros et al. 2007; Du et al. 2014). Moreover, the occurrence of antibiotics and their metabolites has been detected worldwide in water and soil media (Heberer 2002; Kolpin et al. 2002; Barnes et al. 2008; Focazio et al. 2008). Therefore, it is important to develop a treatment method that has wide applicability to treat these constituents. An ideal approach would be suitable for application to both wastewater systems as well as in soil to remediate contamination related to on-site disposal systems and other discharges. In this study, sulfamethoxazole (SMX) was selected as model antibiotic compound because of its wide usage, ubiquitous occurrence and persistence in environment (Kolpin et al. 2002; Barnes et al. 2008; Focazio et al. 2008).

Adsorption is a widely used approach for the removal of contaminants from wastewater, because it is relatively low cost, simple to design and operate, invulnerable to biological toxicity and efficient for removing organic contaminants (Ahmaruzzaman 2008; Homem and Santos 2011; Ahmad et al. 2014). Adsorption is also an important process for natural attenuation of contaminants in the subsurface. However, limit adsorptive removal of SMX was reported in conventional treatment systems (Brown et al. 2006; Xu et al. 2007) and in the subsurface (Drillia et al. 2005; Yu et al. 2009).

In addition, among the adsorptive materials, biochar is of interest because of its adsorptive capacity, low capital input and sustainable nature. Studies show that biochar is capable of

reducing organic and inorganic contamination in both water and soil media (Beesley et al. 2010; Ahmad et al. 2014; Mohan et al. 2014). Besides its potential for water purification, biochar can also increase water retention, nutrient availability, microbial activity and crop yields when used for soil amendment. In addition, the production of biochar adds environmental benefits such as increasing carbon sequestion and reducing greenhouse gas emission.

Studies on the application of biochar in the SMX removal have been reported, but questions remain. First, the performance of biochar in actual wastewater is not well understood. Current studies on antibiotic removal using biochar are mostly conducted using artificial water, which is a simplified condition in deionized water. However, actual wastewater always contains various components, including organic carbon, nutrients, metal ions, etc., which can have inter-influence on biochar adsorption (Seol and Lee 2000; Thiele-Bruhn and Aust 2004; Wu et al. 2012; Zhang et al. 2014). Moreover, previously completed studies include SMX concentrations at levels in the mg/L range, which are higher than those detected in the environment (in ng/L or µg/L) (Ji et al. 2011; Yao et al. 2012; Zheng et al. 2013). Second, the effectiveness of biochar application to subsurface remediation is poorly understood. Use of biochar for SMX remediation in soil is rare (Srinivasan and Sarmah 2015). Third, the factors that determine the adsorption efficiency of biochar are not well known. The adsorption efficiencies of biochars could be affected by a variety of factors, including production parameters, chemistry of the contaminant and properties of water and soil media (Gell et al. 2011). Therefore, a systematic study on BC remediation of SMX in water and soil media under conditions that are close to the field conditions is needed to shed light on the influential interactions that could be overlooked and to assess the actual efficiency that BC could deliver in both water and soil media in the real world.

The goals of the present research were to:

(1) test the remediation ability of biochar in wastewater and soil for SMX and other constituents in wastewater;
(2) examine the characteristics of biochars prepared at different pyrolysis temperatures from different feedstocks to understand the effect of preparation conditions on biochar properties, and

(3) evaluate the SMX remediation performance of different biochars to elucidate the effective preparation conditions and interaction mechanisms of biochar and SMX. In addition, activated carbon was included for comparison.
This chapter summarizes the materials, methods, and results for these investigations.

4.2 Materials and methods

4.2.1 Materials

Commercial biochar (BC) used in this study was obtained from Biochar Now US, which was generated by pyrolysis at around 500 °C from wood-based feedstock. SMX (analytical standard) was purchased from Sigma Aldrich, Australia. Activated carbon, used for comparison, was obtained from Norit Americas Inc. (Marshall, TX, USA) labeled as Norit Hydrodarco 4000 M-1785. Wastewater used in all adsorption experiments was septic effluent collected from a septic tank at Massachusetts Alternative Septic System Test Center (MASSTC). The wastewater sample was stored at 4 °C and filtered through Whatman grade 4 filter paper before use. Soil samples were also collected from MASSTC and were stored at room temperature in capped containers. The characterization of the soil was presented in appendix A. The soil was passed through 2300 µm sieve before use. The wastewater was used for all the adsorption experiments. All the BC materials was crushed in pestle and passed through a 2300 µm sieve.

For biochar production, pine sawdust, bamboo sawdust, woodchips, and pine cones were used as feedstock given their availability and reported sorption affinities. To determine the pyrolysis temperature, raw materials were examined by thermal gravimetric analysis (TGA) and differential thermal gravimetric (DTG) to help understand the process during pyrolysis (appendix C). Two pyrolysis temperatures of 350 ˚C and 500 ˚C were selected. At 350 ˚C, cellulose of the feedstock started to degrade but was not completely eliminated, while at 500 ˚C cellulose were completely destroyed. Feedstock was heated within a muffle furnace (Thermolyne F6010) under limited air conditions created by capped porcelain. The materials were heated at a rate of 10 ˚C/min from room temperature to target temperature, pyrolyzed for 2 hours, and then cooled down to room temperature overnight in the furnace. The obtained biochars were gently crushed and passed through a 2300 µm sieve. After drying in a desiccator

for a week, the biochars were stored in sealed containers for later use. The prepared samples were labeled as B350 and B500 for bamboo sawdust, P350 and P500 for pine sawdust, C350 and C500 for pine cones, and W350 and W500 for woodchips.

4.2.2 Characterization of wastewater

Basic properties of wastewater were characterized. The pH was measured with a pH meter (Fisher Scientific Accumet® AB150). NH_3-N was determined using Nesslerization method with colorimetric quantification at 425nm (HACH DR3900). Total phosphors (TP) was measured using standard method 4500-PC at wavelength of 400nm (APHA 2005). Dissolved metals were analyzed with inductively coupled plasma mass spectrometry (ICP-MS) (PerkinElmer NexIONTM 350X). The basic properties of wastewater can be found in table IV-1. Dissolved organic carbon (DOC) was analyzed using total organic carbon analyzer (Shimadzu TOC 5000A) with filtered wastewater.

Table IV-1. Properties of wastewater sampled from MASSTC

pH	Alkalinity, mg/L as $CaCO_3$	DOC mg/L	NH_3-N, ppm	TP, ppm	Dissolved cations, ppm							
					Na	K	Mg	Ca	Fe	Mn	Cu	Zn
6.94	276	21	66	205	112	53	6.5	1.8	0.51	0.025	0.036	0.02

4.2.3 Characterization of biochars

A series of physicochemical properties of biochars were characterized. First, pH was measured at a biochar to deionized (DI) water ratio of 1:10 w/v after mixing for 10 min (Brown 1998). The sample was then filtered through a 0.45 μm filter and analyzed with ICP-MS for multi-elements. Total exchangeable cations were determined using the United States Environmental Protection Agency (USEPA) standard method 3050B of acid digestion, followed by ICP-MS quantification (Edgell 1989). The specific surface area (SSA) was determined by N_2 sorption at 77 K and Dubinn-Radushkevic (DR) method. The surface functional groups were characterized using Fourier transform infrared spectrometer (FTIR) (Bruker Optics FTIR Spectrometer Vetex 70). The graphite-like microstructure of the sorbents were also

characterized using Raman technique. Raman spectroscopy analysis was conducted with a visible Raman system (Horiba Scientific Xplora) with 1200 gratings at 532 nm laser.

4.2.4 Adsorption experiments

Preliminary studies were carried out to determine the appropriate solid to solution ratio for batch sorption studies, so that the remaining SMX concentration was above the detection limit (appendix D). Thirty ml of wastewater spiked with 200 ppb SMX was added to adsorbents in a 45 ml amber glass bottle. The samples were mixed using a rotary drum shaker at room temperature. For every time interval, triplicate samples were removed from shaker and centrifuged (Eppendorf centrifuge 5804) at 2350 rpm for 8 min. Supernatants were filtered through 0.45 μm before analysis. Inhibition experiments were also conducted to verify the insignificant contribution of biodegradation to the total SMX removal. The microbial activity was inhibited by the adding 1% w/v NaN_3 solution to the wastewater to achieve a resulting concentration of 200 ppm.

The pH and metal cations were monitored over time using a pH meter and ICP-MS. The remaining concentration of SMX was quantified by liquid chromatography–mass spectrometry (Agilent Techonologies 5130 Qradupole) equipped with Epic C18 MSO, 2.3 μ, 150 Å 5 cm × 2.1 mm column, UV detector at 277 nm and targeting at m/z of 254. Two solutions, water with 0.1% formic acid (FA) and 95 % acetonitrile with 5 % water and 0.1 % FA, were used as mobile phase at 0.3 ml/min gradient. The limitation of detection (LOD) was 4.01 μg/L and limit of quantification was 13.0 μg/L. The sorbed amount of SMX at time t, q_t [ppm], was estimated using a mass balance equation as follows:

$$q_t=(C_0-C_t)V/m \tag{4.1}$$

where C_0 is the initial concentration of SMX in wastewater [ppm], V is the volume of solution added [L], and m is biochar mass [kg].

The equilibrium time for sorption isotherms were determined by the results of kinetics, which was 48 hours for the biochars and 24 hours for activated carbon (appendix E). The desired amounts of SMX stock solution were spiked into wastewater to produce a series of concentrations of 50 ppb, 100 ppb, 200 ppb, 400 ppb, 800 ppb, and 1000 ppb. Same sample

preparation and analysis procedures were then performed for kinetics experiments to obtain the aqueous-phase concentration of SMX, which remained at the equilibrium C_e [ppm]. A mass balance equation was used to obtain the equilibrium concentration of sorbed SMX, q_e [ppm].

$$q_e=(C_0-C_e)V/m \quad (4.2)$$

4.2.5 Adsorption kinetics modeling

Kinetics data were analyzed using the 6 commonly used models (table IV-2).

Table IV-2. Summary of the adsorption kinetic models used in this study

Model	Physical expression	Mathematical expression	Parameters
First order	$\frac{dq_t}{dt} = k_1 q_t$	$\ln q_t = \ln q_0 - k_1 t$	k_1 = first-order rate constant
Second order	$\frac{dq_t}{dt} = k_2 {q_t}^2$	$\frac{1}{q_t} = \frac{1}{q_0} - k_2 t$	k_2 = second-order rate constant
Pseudo-first order	$\frac{dq_t}{dt} = k_{p1}(q_e - q_t)$	$\ln(q_e - q_t) = \ln q_e - k_{p1} t$	k_{p1} = rate constant of pseudo-first order q_e = solid adsorbed amount at equilibrium
Pseudo-second order	$\frac{dq_t}{dt} = k_{p2}(q_e - q_t)^2$	$\frac{t}{q_t} = \frac{1}{k_{p2} q_e^2} + \frac{1}{q_e} t$	k_{p2} = rate constant of pseudo-second order
Elovich	$\frac{dq_t}{dt} = \alpha e^{-\beta q_t}$	$q_t = 1/\beta \ln(\alpha\beta) + \frac{1}{\beta} t$	α = initial adsorption rate β = elovich sorption constant

A pseudo-first-order model was first suggested by Lagergren (1898). It defines an adsorption rate that is related to the active sites available. This model has been applied in the adsorption of organic solute to adsorbents (Lagergren 1898; Hameed 2008; Tan et al. 2008) A pseudo-

second order model was established by Ho in 1995 to describe the adsorption of bivalent metal onto peat (Ho and McKay 1998). It is based on the assumption that the rate-limiting step may be a chemical sorption involving valent bonds through the sharing or exchanging of electrons between the adsorbent and adsorbate. This kind of reaction is greatly influenced by the adsorbate amount adsorbed on the adsorbent's surface at time t (q_t), and adsorbate amount adsorbed at equilibrium (q_e). The reaction rate is directly proportional to the number of active sites on the adsorbent's surface (q_e-q_t).

The Elovich model was originally used to describe chemisorption of gas, assuming a multilayer sorption with different activation energies on each layer (Alberti et al. 2012). It covers a large range of slow adsorption (Cheung et al. 2000) and now it is widely used to explain the adsorption of aqueous contaminants, assuming strong heterogeneity of sorbent surfaces (Ahmad et al. 2013). When comparing different models, coefficient of determination (R^2) and residual sum of squares (RSS) were the two criteria considered.

4.2.6 Adsorption isotherms modeling

Linear, Freundlich and Langmuir models were used to fit the sorption data in this study.

$$\text{Linear model: } q_e = K_d C_e \tag{4.3}$$

$$\text{Freundlich model: } q_e = K_F C_e^N \tag{4.4}$$

$$\text{Langmuir model: } q_e = \frac{Q_0 b C_e}{1 + b C_e} \tag{4.5}$$

where q_e [ppm] and C_e [ppm] are adsorbed and remaining concentrations of solute at equilibrium, respectively; K_d is the distribution coefficient; K_F [ppm^{1-N}] and b [ppm^{-1}] are Freundlich and Langmuir sorption coefficients; N is the nonlinear coefficient and Q_0 [ppm] is the Langmuir sorption capacity.

4.2.7 Desorption experiment

Desorption was performed with BC after the adsorption experiment with 800 ppb of SMX in wastewater. After the adsorption experiment, the samples were filtered through Whatman

grade 4 filter paper under vacuum. The solids were dried in desiccator for 5 days. The dried solids were weighed into 45 ml amber glass bottles and the desired amounts of wastewater were added. A high solid: solution ratio of 1: 100 were used for desorption experiment considering the quantification limits of LC-MS. After continuous mixing for 3 days, the aqueous phase was filtered with a 0.45 µm filter and analyzed for SMX. The solutions used for desorption experiment were spiked with 1 % NaN_3 to a concentration of 200 ppm to inhibit biodegradation.

4.3 Results and discussions

This study was mainly focused on two topics. The first topic was the assessment of the applicability of biochar for adsorptive removal of SMX in wastewater and in soil/wastewater systems. To design biochars with improved adsorption efficiency, a second topic was included. This topic involved the investigation of the effect of the production conditions on SMX adsorption capabilities.

4.3.1 Commercial biochar and its application in adsorptive remediation.

The biochar and wastewater were characterized to provide fundamental information for understanding the interactions between adsorbates and adsorbents. The effects of biochar on the other constituents, including accessible nutrients, dissolved mineral cations and heavy metals in the aqueous phase, were also analyzed to assess the general effects of biochar application.

4.3.1.1 Characterization of biochar

Physicochemical properties

Basic properties of commercial biochar were characterized and presented in table IV-3. The pH of biochar was slightly alkaline, which is often observed in biochars produced from different feedstock at a similar temperature. It led to a pH of around 7.5 of wastewater after addition of biochar. At this pH, SMX is negatively charged (pK_{a1} = 1.7, pK_{a2} = 5.1), while ammonia is mainly protonated as NH_4^+ (pK_a = 9.4) (Khoo et al. 1977; Lucida et al. 2000). Under this condition, electrostatic interactions and ion exchange between charged

contaminants and charged sites of the solid were likely to have significant influence on contaminant sorption (Chen et al. 2011; Lian et al. 2014). Low exchangeable cations were detected in this biochar, which limited the extent of ion sorption. However, the presence of cations has been linked to the hydrophilic property of sorbents, which hinders the sorption of organic contaminants like SMX (Bornemann et al. 2007). Thus, the low exchangeable cation could be beneficial to SMX sorption.

Surface area is one of the main contributing factors to high sorption. The SSA of the biochar was 171 m^2/g, which was comparable to what was reported for biochars, but was lower than what was often observed with commercial activated carbon (~1000 m^2/g) (Zhang et al. 2010; Ahmad et al. 2014; Srinivasan and Sarmah 2015; Zhang et al. 2015).

Table IV-3. Physicochemical properties of biochars. G550: biochar produced from green waste at 550 °C; B600: biochar produced from bamboo at 600 °C; PW600: biochar produced from pepper wood at 600 °C; S600: biochar produced from sugarcane bagasse at 600 °C; H600: biochar produced from hickory wood at 600 °C; D600: biochar produced from Danshen at 600 °C

Biochar	pH	SSA* m^2/g	Exchangeable cations, ppm				Heavy metals, ppm				References
			Na	K	Mg	Ca	Fe	Mn	Cu	Zn	
BC	8.7	171	80#	451#	37#	1.6#	0.20#	1.41#	na#	na#	this study
			450	1.8E3	648	586	1.2E3	204	2.3	33	
G550	8.4	153	2.8E3	3.7E3	9.3E3	1.0E5					Srinivasan et al. 2015
B600	8.9	376		5.2E3	2.3E3	3.4E3					Yao et al. 2012

Table IV-3. Continued

PW600	9.7		2.6E3	2.5E3	24E3	
S600	7.7	388	1.5E3	2.1E3	9.1E3	
H600	9.4	401	2.4E3	1.3E3	8.2E3	
D600		51				Lian et al. 2014

*: SSA of other studies used BET method and SSA of this study was DR method.

#: exchangeable cations within DI water.

Sorption of heavy metals on biochars in contact with wastewater has also been reported in previous studies (Beesley et al. 2011; Ahmad et al. 2014; Mohan et al. 2014). In our wastewater sample, the concentrations of heavy metals were low. However, the biochar of this study was enriched with heavy metals, which were readily released to aqueous phase (table IV-3). The metal cations have been reported to be able to facilitate the sorption of SMX from wastewater possibly by forming a SMX-metal-sorbent bridge (Wu et al. 2012; Morel et al. 2014) or electrostatic interaction (Kahle and Stamm 2007). Thus, the high content of heavy metals in biochar could favor SMX removal.

Surface functional groups

Surface functional groups of the biochar were characterized by FT-IR (figure IV-1). From the absorption spectrum, some functional groups still could be seen after pyrolysis at 500 °C. The adsorption band observed at 1700 cm^{-1} was associated with aromatic carboxyl /carbonyl C=O bonds (Chun et al. 2004; Sitko et al. 2013). Another band appeared at 1580 cm^{-1}, which was previously assigned to two different functional groups, the vibration of C=C of non-oxidized graphitic domain (Sitko et al. 2013; Jindo et al. 2014) and anti-symmetric stretching of aromatic -COO- group (Chun et al. 2004; Cheng et al. 2008; Qiu et al. 2008; Yuan et al. 2011). The bands at 750-770 cm^{-1} were associated with the deviational vibration and symmetric

stretching of the carboxylate (-COO-) group (Cheng et al. 2008; Fu et al. 2009; Lammers et al. 2009; Yuan et al. 2011). Aliphatic -CH, $-CH_2$, $-CH_3$ adsorption was reported at 2855 cm^{-1} and 2925 cm^{-1} from vibration and at 2120 cm^{-1} from stretching (Sitko et al. 2013; Zhang et al. 2015), but no adsorption bands were observed at these wavenumbers in the spectrum. Since the adsorption of aliphatic C-H was usually weak, the "absence" of the characteristic peak was not solid evidence for the absence of aliphatic carbons. In addition, the adsorption band at 3200-3600 cm^{-1} was often observed in biochar, which was associated with free or associated -OH groups from structural hydroxyl groups, intercalated water or moisture (Ozcimen and Ersoy-Mericboyu 2010; Yuan et al. 2011). Absence of such an adsorption band in the spectrum indicated that the biochar was dry and had limited hydroxyl groups.

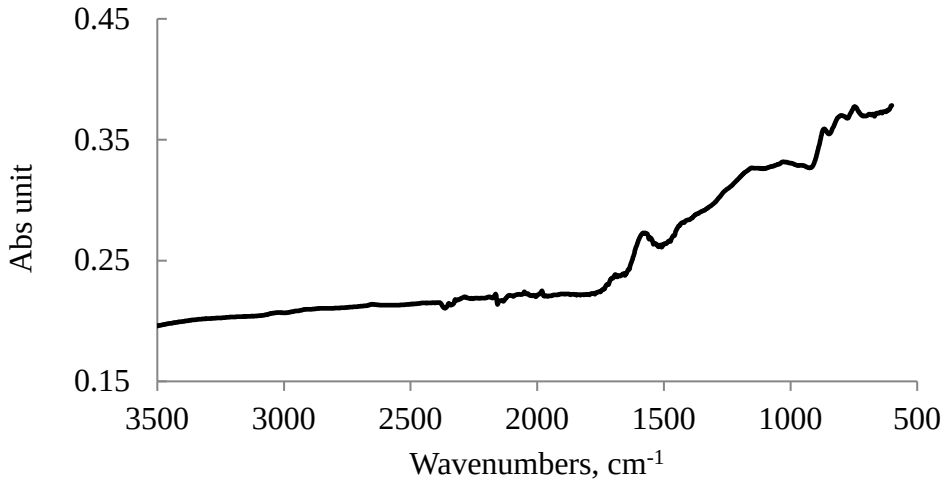

Figure IV-1. FT-IR spectrum of the commercial biochar.

Analysis of Raman spectrum

The carbon structure of the material was analyzed using a Raman spectrum (figure IV-2). The biochar consisted of non-graphitic carbon and nano-crystalline graphite, which were proposed to be small graphene-like sheets oriented randomly for non-graphitic carbon and in-layers for nano-crystalline graphite. These graphene-like sheets are hexagonal ring systems with oxygenated groups and defects within a carbon matrix (Smith et al. 2016). Two adsorption bands were exhibited in the spectrum of the biochar of this study, which were often reported in carbonaceous materials. The adsorption band at a Raman shift of 1592 cm^{-1} was commonly

assigned to the G-band for the nano-crystalline graphite. The band at 1344 cm^{-1} was assigned to the D-band for the disordered non-graphitic carbon attributing to in-plane vibrations of sp2 bonded carbon within structural defects (Ishimaru et al. 2007; Rhim et al. 2010b; Zhang et al. 2015). The overlap of the D band and the G band was due to the contribution of amorphous carbon in the region between 1400 and 1550 cm^{-1}, called the valley region "V". Graphite degree was calculated using the Gaussian function of the two bands (I_D/I_G). Rhim et al. (2010b) reported I_D/I_G in the range of 0-2.6 and Zhang et al. (2015) reported the values from 3.8-8.3. The variations were mainly from the purity and property of the materials, generated from different feedstock and pyrolysis temperatures. An increase of the graphite degree could have resulted from the condensation of the small aromatic ring systems into larger ones (Keiluweit et al. 2010). The value of I_D/I_G of the studied biochar, which was 0.72, indicated that it was enriched with condensed aromatic ring systems. The π electron in graphitic carbon was proposed to facilitate the sorption by forming π-π interaction with SMX and cation- π binding with metal ions (Wu et al. 2012).

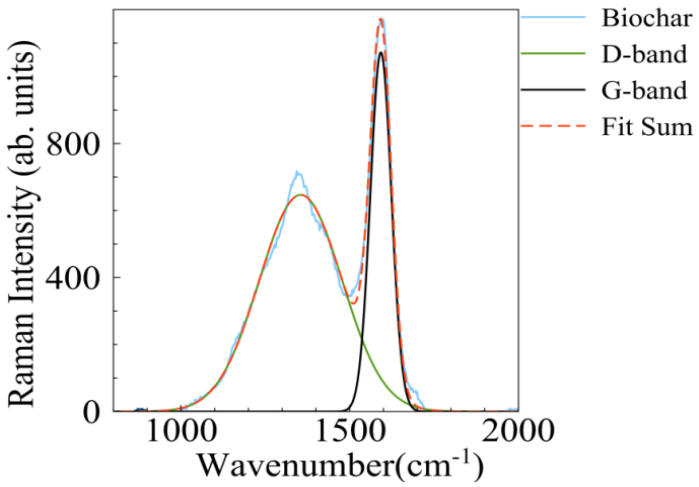

Figure IV-2. Raman spectrum of the commercial biochar, BC. D-band and G-band were fitted by Gaussian function.

4.3.1.2 Applicability of biochar in wastewater remediation

The overall performance of biochar in regards to the remediation of wastewater was determined using closed bottle experiments. The remaining percentages of nutrients, metal cations and SMX after mixing with biochar for 48h are presented in figure IV-3.The

concentrations of Ammonia N, total P, exchangeable cations (Na, Mg, K, Ca), and the heavy metal Zn were close to the original values in wastewater. Significant removals were observed in SMX, Fe and Cu, over half of which were adsorbed within the experiment's timespan. However, an increase of Mn was detected. Considering water exchangeability of Mn in biochar itself (table IV-3), the increased level of Mn probably resulted from Mn, leaching from the biochar through cation exchange during the mixing.

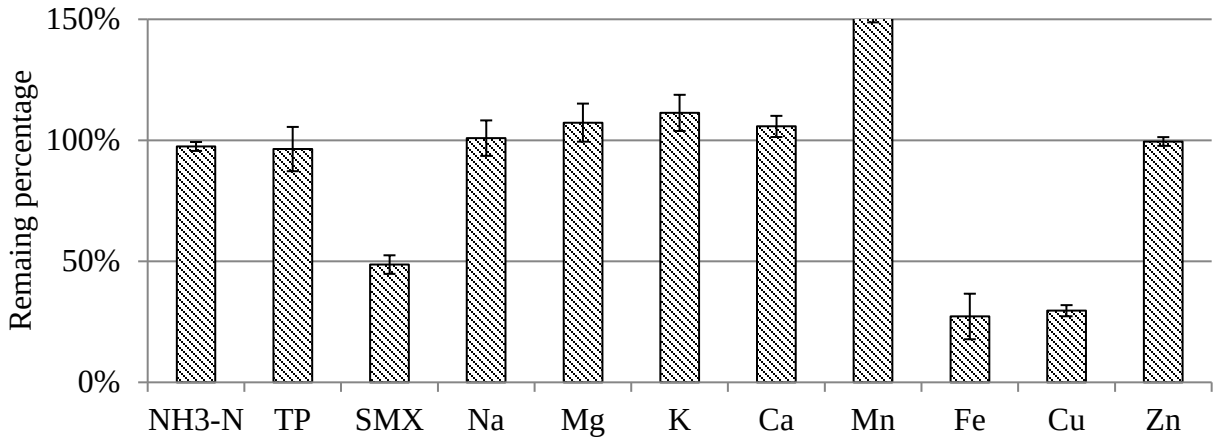

Figure IV-3. The percentage of nutrients, SMX and metal cations remained in wastewater after mixing with biochar for 48 hr. SMX was spiked to 200ppb, and others were measured at the original concentrations. Error bars represent sample standard deviation (n = 3).

To evaluate the contribution of biodegradation to the reduction of SMX, inhibition experiments were conducted with 200 ppm of NaN_3. The removal differences between inhibited samples and non-inhibited samples were attributed to biodegradation. The results in figure IV-4 showed that there were no significant differences in the SMX removal between inhibited and non-inhibited samples. Therefore, biodegradation was considered to be negligible during the short time period of sorption experiments and the SMX reductions were considered to be a result of the adsorption process.

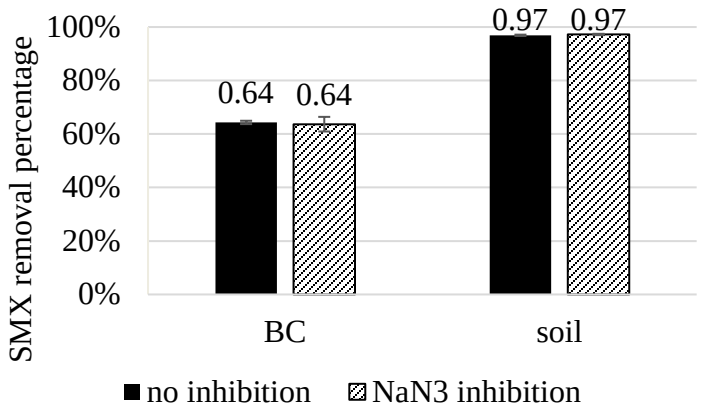

Figure IV-4. Inhibition experiment of SMX removal in BC and soil.

The concentrations of SMX, Fe and Cu in the aqueous phase over time were analyzed (figure IV-5). A two-stage adsorption pattern was observed for the three contaminants, probably because less adsorption sites were available, with more contaminants adsorbed. The adsorption of SMX was fast within the first 10 hours and then slowed down until equilibrium was reached after 48 hours. The adsorption of Cu and Fe was quick and the majority was removed within the 3 hours, which was also observed by Chen et al. (2011).

The adsorption kinetics of Fe, Cu and SMX were explored further to understand the nature of adsorption process between contaminants and biochar (figure IV-5). Concentrations of aqueous phase q_t were collected over time and a series of kinetic models were used to fit the data. The results are summarized in table IV-4. For the adsorption of SMX, both the Elovich and pseudo-second order model resulted in high R^2 values. However, the Elovich model showed lower RSS values with no apparent distribution pattern in residual plot, indicating a smaller deviation of the fitted value from the original data and a random distribution of error (appendix F). Thus, the Elovich model was found to be a better model for describing the adsorption kinetics of SMX. Similar analyses were applied to other contaminants to obtain the best kinetic model. The adsorption of Fe and Cu were best represented by pseudo-second order model, giving the highest R^2 and lowest RSS values among all the kinetic models studied. The kinetic model of Cu determined in this study agrees with the other authors when studying different biochars at various Cu concentrations (Chen et al. 2011; Pellera et al. 2012). The adsorption of Fe on biochar was rarely reported, but this model is commonly used for metal

cation adsorption on biochar (Mohan et al. 2014). The initial adsorption rate of SMX was calculated to be 40 ppm/h, while the rate for Fe was 187 ppm/h and the rate for Cu was 9.8 ppm/h.

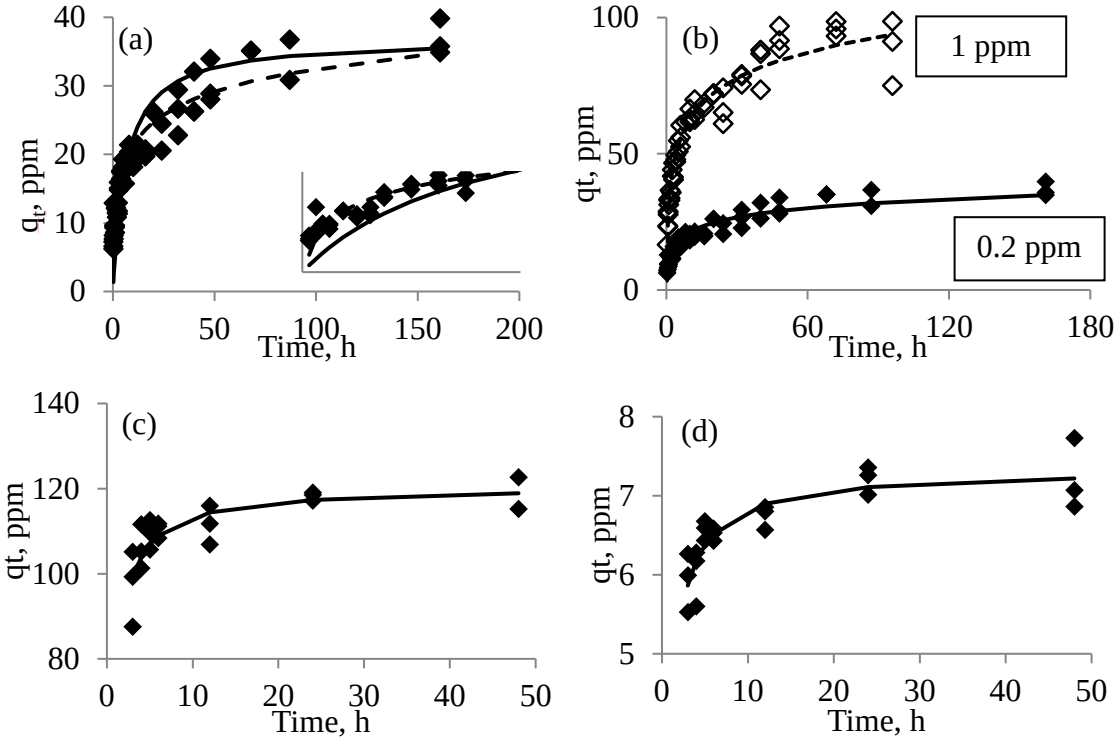

Figure IV-5. Adsorption kinetic models of SMX, Fe and Cu on biochar in wastewater. Diamond dots represent the actual data points. The solid line is Pseudo-second order model line and the dashed line is the Elovich model line. (a) SMX adsorption at 0.2 ppm. The enlarged figure showed the early phase of adsorption process, which was described more accurately by Elovich model; (b) SMX adsorption at 0.2 ppm and 1 ppm (c) Fe adsorption; (d) Cu adsorption.

It was often proposed that the adsorption of Cu on biochar could be through electrostatic interaction, cation exchange and cation-π interactions (Gao et al. 2009; Tong et al. 2011; Wu et al. 2012). At the pH of the mixed solution in this study (~7.5), Cu mainly exist as Cu^{2+}, and some existed as $Cu(OH)^{+}$ and $Cu(OH)_2$ (Rao et al. 2007; Wu et al. 2012). Electrostatic interaction was favored due to the negatively charged biochar. The pseudo-second order model indicated the adsorption under studied condition was mainly limited by chemical sorption. Thus, electrostatic interaction was not considered to be the rate-determining step for the adsorption process. Cation exchange is the specific interaction with surface functional groups,

such as the carboxylic and hydroxyl groups. The FT-IR result of this biochar provided evidence of the presence of the carboxylic group, which might be the main interaction sites for Cu adsorption. Considering the H^+ concentration was less than Cu^{2+} by two orders of magnitude at the studied pH range, the potential competition to Cu^{2+} from H^+ in solution was limited for cation exchange. Moreover, Raman spectroscopy confirmed the presence of π electrons in the graphene-like structure of the studied biochar, which could adsorb Cu^{2+} via cation-π interaction. Wu et al. (2012) suggested that the cation-π interaction could be stronger than the others, which made it especially important at low concentration of Cu.

Table IV-4. Summary of adsorption kinetic models of SMX, Fe and Cu on biochar in wastewater

Compound	Model	R^2	RSS	Initial concentration (ppm)	Initial rate (ppm/h)	Parameters
SMX	Elovich	0.920	384	0.200	39.6	α=39.6 ppm/h; β=0.206 ppm^{-1}
	Elovich	0.949	1410	1.00	130	α=130 ppm/h; β=0.0726 ppm^{-1}
Fe	Pseudo-second	0.994	392	0.511	187	q_e=120 ppm; k_{p2}=0.013 $ppm^{-1}h^{-1}$
Cu	Pseudo-second	0.996	1.41	0.036	9.8	q_e=7.33 ppm k_{p2}=0.18 $ppm^{-1}h^{-1}$

The adsorption of SMX at the pH range of this study was mainly related to the interaction between the predominant SMX^- and biochar, most likely via π-π interaction of the benzene rings (Zhang et al. 2010). The adsorption kinetics at higher concentration of SMX was also studied (figure IV-5b). Results showed that SMX at higher concentration also followed a similar pattern to that at low concentration, which was best described by Elovich model. Equilibrium was also achieved within the 48 hr contact time, but at a higher initial adsorption rate of 130 ppm/h.

The interaction between SMX, Cu and biochar was more complex. Cation bridging of biochar-Cu-SMX and cation-π binding of biochar-SMX-Cu were the two previously discussed mechanisms (Sheng et al. 2010; Wu et al. 2012; Morel et al. 2014). Wu et al. (2012) reported increased adsorption of Cu or SMX with the presence of the other at high concentrations. However, at low concentrations of Cu, the biochar-SMX-Cu complexation was expected to be dominant and Cu was interacting with the benzene ring of absorbed SMX. To the knowledge of the author, the adsorptive interaction between Fe, SMX and biochar has not been reported. Fe(II)-SMX complex was reported by binding to the negatively charged –NH- and isoxazolic-N of SMX^- (Bouchoucha et al. 2013). However, according to Irving-Williams Series, Fe (II) is a weaker chelating agent than Cu(II), and weaker complexation with SMX is expected (Irving and Williams 1953). Thus, we expect electrostatic interaction would be the main mechanism for Fe adsorption.

Desorption information was important for treatment application of adsorbents, which allows people to evaluated the leaching risk of the adsorbed contaminants. Results of the SMX adsorption-desorption experiment showed that after the treating with fresh wastewater, small amounts of adsorbed SMX were released into aqueous phase after adsorption treatment. Only 6 % of adsorbed SMX were leached into aqueous phase for BC. This finding indicted that the leaching risk of the application of BC for SMX adsorption was low.

4.3.1.3 Effectiveness of biochar for SMX removal in soil

Commercial biochar was mixed with soil at different loading rates to examine the application of biochar in soil remediation. The 1 % and 2 % loading rates were used and adsorption isotherms were studied and compared with those of pure biochar and pure soil. Results are presented in figure IV-6a. The adsorption data were fitted using linear, Freundlich and Langmuir models respectively. However, the Langmuir model failed to capture the feature of the data in the range of concentrations of this study. Results of the linear and Freundlich modeling were presented in table IV-5.

The highest R^2 values were obtained with the Freundlich model. Except for the soil, the difference of the R^2 values between the linear model and Freundlich model was not significant. A linear model was considered to be adequate for quick estimation for SMX adsorption on

biochar and soil/biochar mixtures. The effective distribution coefficient (K_d^{eff}) values for SMX at the lowest equilibrium concentration (C = 25 ppb for all the samples) were higher than the corresponding K_d values due to the low concentration used for K_d^{eff} calculation. The nonlinearity of all the isotherms found from Freundlich model was low, with N values ranging from 0.80 to 0.94.

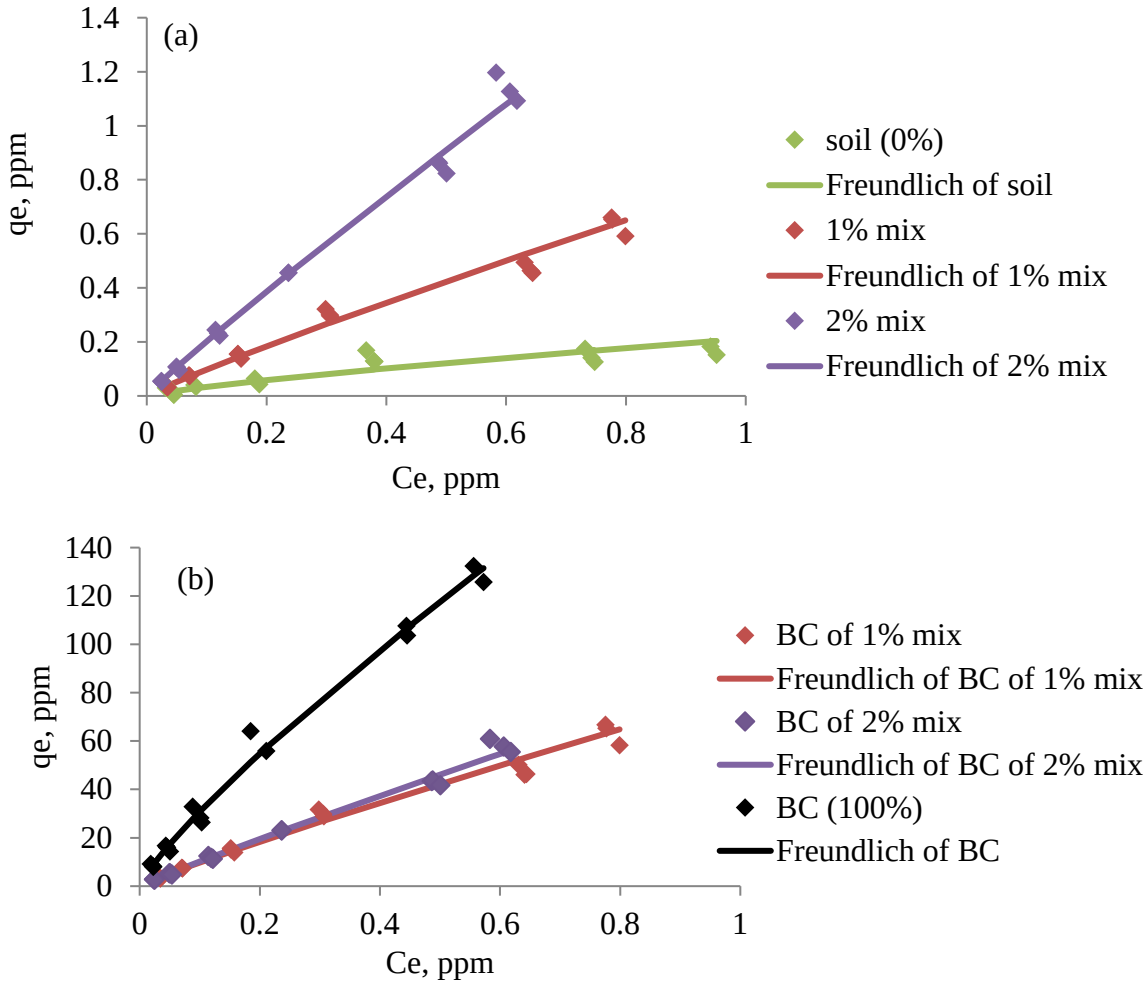

Figure IV-6. Adsorption isotherms of SMX removal on soil mixtures amended with different percentage of biochar. (a) adsorption isotherms of soil and soil mixtures. (b) adsorption isotherms of BC and BC in the mixtures.

Table IV-5 Parameters of Freundlich model for SMX sorption by different soil mixtures

Sorbents	Linear model		Freundlich model			
	K_d	R^2	K_F , ppm^{1-N}	N	R^2	K_d^{eff}
Soil	0.211	0.678	0.217	0.80	0.742	0.45
1% mix	0.805	0.939	0.797	0.91	0.991	1.12
2% mix	1.84	0.989	1.74	0.94	0.997	2.17
BC	239	0.974	209	0.83	0.984	391
BC of 1% mixture	80.5	0.970	79.5	0.91	0.992	111
BC of 2% mixture	93.3	0.988	88.3	0.94	0.997	110

$K_d^{eff} = K_F C_e^{N-1}$, using the estimated lowest equilibrium aqueous concentration of C_e = 25 ppb.

The distribution coefficient of SMX sorption on soil was found to be low (K_d^{eff} = 0.45), and K_d^{eff} of biochar was higher by two orders of magnitude (K_d^{eff} = 391). Adding biochar to soil increased the overall K_d^{eff} values, but did not have a marked effect on the overall sorption non-linearity. Recent studies on SMX sorption on soil revealed K_F values that ranged from 0.28 to 2.37 and N valuea that ranged from 0.66 to 0.75 at pH conditions close to those for this study (Drillia et al. 2005; Srinivasan and Sarmah 2015). The sorption isotherms of biochar were also reported with K_d values over a wide range of 2-10500, varying with the biochar feedstock and preparation temperature (Ji et al. 2011; Yao et al. 2012; Han et al. 2013; Lian et al. 2014; Srinivasan and Sarmah 2015). Soil amendments with biochar were recently reported by Srinivasan and Sarmah (2015), in which enhanced SMX sorption was also observed with addition of biochar in soil. However, these studies were completed in a DI water matrix, with or without addition of electrolyte. A single point sorption experiment was performed and results are shown in figure IV-7. SMX sorption in DI water was much higher than that in wastewater, which contained 21 mg/L DOC and other constituents (table IV-1). The dissolved organic matter (DOM) in wastewater could reduce SMX sorption via to competition for sorption sites or formation of complexes between DOM and organic contaminants, like sulfonamides (Seol and Lee 2000; Thiele-Bruhn and Aust 2004; Zhang et al. 2014).

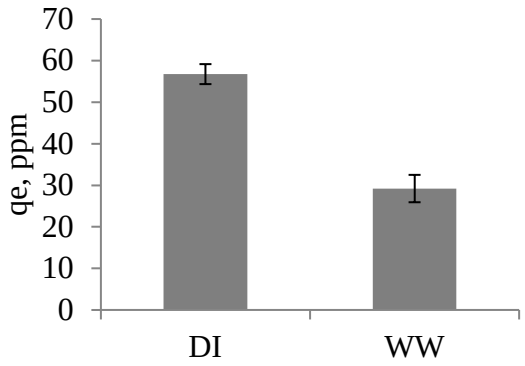

Figure IV-7. Sorption of SMX on biochar in the matrix of DI water and wastewater. The initial concentration of SMX was 200 ppb. Error bars represent sample standard deviations (n=3).

Note that the effect of biochar amendment on the K_d^{eff} was lower than the expected value that could be expected based on a mathematical calculation. If soil and biochar acted independently when mixed, the calculated K_d^{eff} would be 4.36 and 8.26, for 1 % mix and 2 % mix respectively. Considering the limited adsorption on soil, it is reasonable to assume that biochar was the main contributor for SMX sorption. Based on this assumption, new sorption isotherm models were obtained only considering biochar in the mix (figure IV-6b) and results were presented in table IV-5. Lower K_d^{eff} values were found for biochar in the soil/biochar mix, which confirmed the diminished sorption capability of biochar in mixture. Srinivasan and Sarmah (2015) also reported that biochar amendments do not lead to a marked increase in overall SMX sorption for most studied biochar samples. However, the sorption isotherms of pure biochar were not included - thus quantificational assessment on the effect of biochar amendment could not be performed. The results implied that presence of soil interferes with the adsorption of SMX onto biochar. It is possible that fine particles from soil could block the micro-pores of biochar, or the material released by the soil could be competing with SMX for sorption sites.

In summary, SMX was used as a model compound to study the effectiveness of biochar in the application in wastewater remediation in actual scenario by considering the complexity of co-existing components in wastewater. Cu, Fe and SMX were effectively removed by biochar, while nutrients (N and P), the heavy metal Zn and exchangeable cations were not significantly affected. The spectroscopic study revealed the presence of functional groups and molecular arrangements, which played important roles in the interactions between biochar and contaminants. The functional groups could facilitate the removal of Cu through cation

exchange, while the graphitic structure could enhance SMX and Cu adsorption through interacting with π-electrons. To achieve higher removal efficiency, we suggest engineering biochars with higher aromaticity and surface functional groups. However, the high content of surface functional groups is usually obtained at low pyrolysis temperature, which could sacrifice aromaticity and surface area of material. Thus, further study is needed to explore different feedstock materials and pyrolysis temperatures to achieve a biochar structure optimizing the removal performance.

4.3.2 Lab engineered biochars and their application in SMX adsorption

4.3.2.1 Characterization of Lab engineered biochars

Physicochemical properties

The chemical properties of the lab engineered biochars are presented in table IV-6. The biochar yields were all below 50% and the yields decreased with increasing pyrolysis temperature. The yield drop of pinecone biochars was not as marked as those of pine sawdust and woodchips. Measurements of pH indicated that woodchip biochars and pine sawdust were acidic while pinecone biochars were alkaline, which could be used to reduce soil acidity when applied for soil amendment. Except for pine sawdust biochars (P350 and P500), biochars produced at higher temperature resulted in higher pH value for all samples. The pH trend with pyrolysis temperature was also observed for other wood-based biochars and sewage sludge biochars (Yao et al. 2012; Srinivasan and Sarmah 2015). It could be due to the decomposition of acidic organic matter of the feedstock.

Table IV-6 also shows the total contents of trace metals in commercial and lab engineered biochar samples measured by the acid-extract method with ICP-MS analysis. The contents of the metals were higher when pyrolysis temperature increased, which revealed the metals were retained and enriched during the pyrolysis process. The accumulation of mineral components in the biochar samples could also led to the pH increase (Yuan et al. 2011; Enders et al. 2012; Zhang et al. 2015). The accumulation of heavy metals in biochar is of concerns for its application in wastewater and soil remediation because of its potential leaching risk with environmental pH changes. The heavy metal contents of biochars studied in this work were

lower than those prepared from sludge and were comparable to other wood-based biochars (Srinivasan and Sarmah 2015; Zhang et al. 2015). They were also lower than, if not comparable to, the heavy metals contents found in soil (Gough et al. 1988; Bradford et al. 1996; Castro et al. 2013). The metallic composition of biochar samples varied with different feedstock. Total metallic content of lab engineered biochar followed the trend of woodchip > pinecone > pinewood, with highest metallic concentration in woodchip-derived biochars and lowest in pinewood-derived biochars. Note that iron concentrations of woodchip-derived biochars were comparable to the commercial biochar, which were greater than others by one order of magnitude.

Table IV-6. Physicochemical properties of commercial biochar (BC) and lab engineered biochars

Biochar	Yield	pH	SSA	Exchangeable cation, ppm					Heavy metals, ppm			
	wt%		m^2/g	Na	Mg	Al	K	Ca	Fe	Mn	Cu	Zn
BC		8.7	171	450	648	323	1.8E3	586	1.2E3	204	2.3	33
P350	44	4.3		24	231	142	717	128	26	20	1.1	13
P500	21	4.3	340	26	392	522	1154	199	172	29	7.2	20
C350	28	7.4		235	957	483	4568	126	65	18	5.3	15
C500	26	9.1		321	857	451	5139	156	106	19	5.7	16
W350	32	5.0		189	602	836	1612	1257	1321	24	4.0	19
W500	23	6.9	370	208	718	1128	2190	1379	1379	25	5.4	22

Surface functional groups

Surface functional groups of the lab engineered biochar samples were characterized by FT-IR. The results are shown in figure IV-8. The spectra of lab engineered BCs showed broad adsorption bands between 3200-3600 cm^{-1}, which were absent in activated carbon, commercial biochar and air-dried soil. These bands were more likely associated with structural –OH groups in lab engineered biochars because free water were evaporated during the pyrolysis process. The structural hydroxyl groups were stable under 500 ˚C.

As observed in commercial biochar, the bands at 1695-1710 cm^{-1} are also observed in lab engineered biochar samples, indicating the presence of aromatic carboxyl/carbonyl C=O bonds (Chun et al. 2004; Sitko et al. 2013). The bands at 1580-1610 cm^{-1} could be assigned to the vibration of C=C of non-oxidized graphitic domain (Sitko et al. 2013; Jindo et al. 2014) or aromatic –COO- anti-symmetric stretching (Cheng et al. 2008; Qiu et al. 2008; Yuan et al. 2011). The two groups of adsorption bands exhibited the same trend as biochars prepared from different feedstock. The bands of woodchip biochars were close to those of pine sawdust and pinecone biochar samples, which were at higher wavenumbers than commercial and bamboo biochars. The difference in the adsorption bands of biochars implies that the surface functional groups could retain the feature of their feedstock. For the bands at 1580-1610 cm^{-1}, a value of 10 cm^{-1} to the lower wavenumbers was observed for all the lab engineered biochar samples at higher pyrolysis temperature. It could be explained by the enhanced conjugated effect from extended of graphitic network formed at higher pyrolysis temperature. In the wave numbers between 1350 and 1450 cm^{-1}, one adsorption band was observed in wood-based biochar samples, which shifted to lower wavenumbers with temperature increase. However, bamboo biochar exhibited two adsorption bands in this region, the one at lower wavenumber could be associated with the deviational vibration and symmetric stretching of carboxylate (-COO-) group (Cheng et al. 2008; Fu et al. 2009; Lammers et al. 2009; Yuan et al. 2011), while the band at higher wavenumber was related to the in-plane bending of carbonyl groups (Chun et al. 2004; Cheng et al. 2008; Yuan et al. 2011).

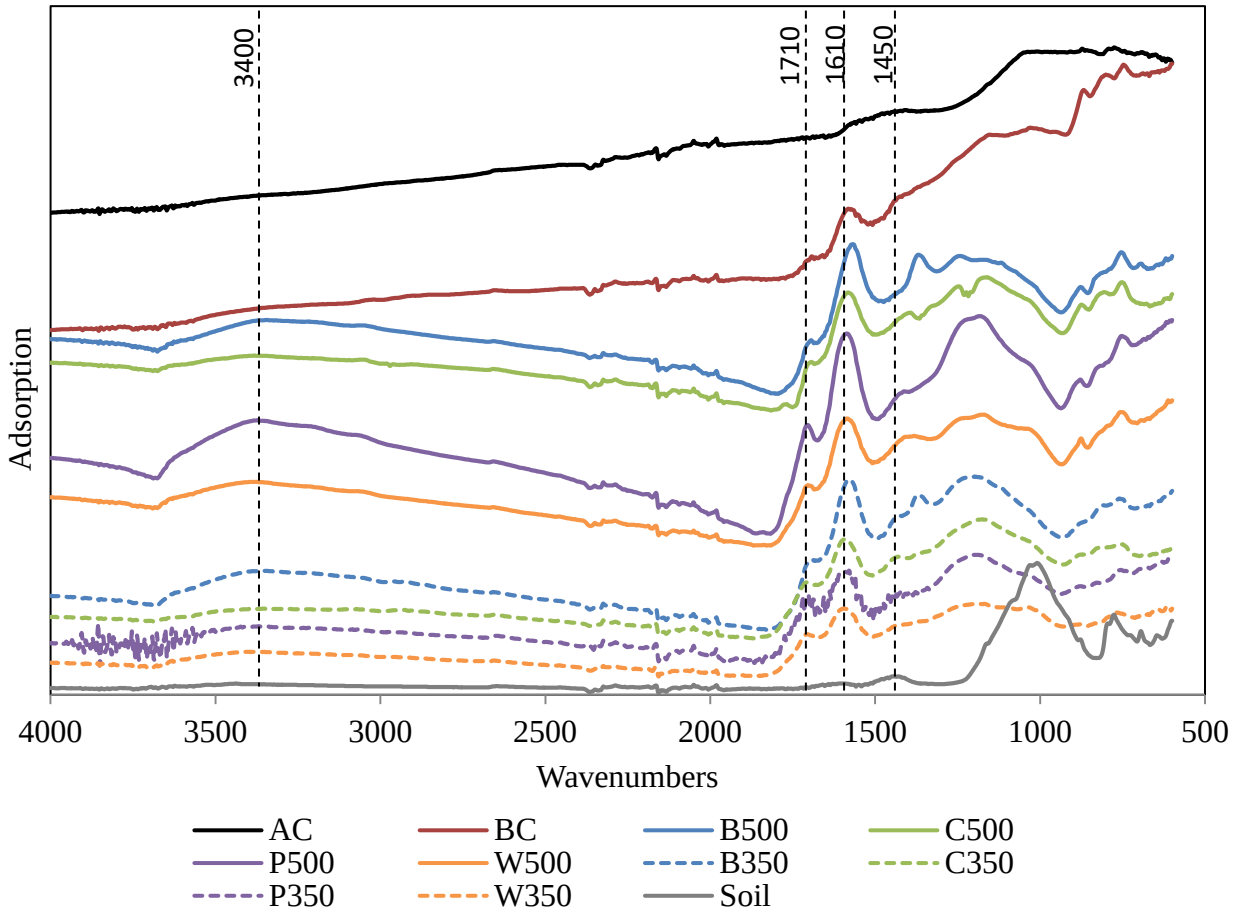

Figure IV-8. FT-IR spectra of lab engineered biochars, commercial biochar, activated carbon and MASSTC soil.

The change in the intensity for the functional groups of BCs was not notable. Previous studies reported the functional groups gradually disappear with the rise of pyrolysis temperature, but considerable amount of functional groups were still present at 500 ˚C (Chun et al. 2004; Yuan et al. 2011; Jindo et al. 2014). Aliphatic –CH, -CH2, -CH3 adsorption was reported at 2855 cm^{-1} and 2925 cm^{-1} from vibration and at 2120 cm^{-1} from stretching, but it was the same as commercial biochar, and they were not observed for lab engineered biochars as well (Sitko et al. 2013; Zhang et al. 2015).

Unlike biochar samples, the spectra of AC and soil didn't show significant bands of the functional groups. The existence of surface functional groups in biochar samples could facilitate SMX adsorption through various ways, which will be discussed in section 3.3.2.4.

Analysis of Raman spectra

The Raman technique was used to examine the microstructure of the lab engineered biochar materials, commercial biochar and activated (figure IV-9). The Raman spectra were fitted using a Gaussian function and the results were summarized in table IV-7. The changes in the structural features of lab engineered biochars were quantified by structural ratios, I_D/I_G and I_V/I_D.

Similar to the Raman spectrum of commercial biochar, two broad Raman bands were observed around 1340-1380 cm^{-1} and 1570-1600 cm^{-1} for the lab engineered biochar materials and commercial activated carbon, which correspond to the D band and G band. Compared to AC and BC, the band positions of the lab engineered biochar samples shifted to higher wavenumbers for the D band and shifted to lower wavenumbers for the G band. In addition, the D bands shifted to lower wavenumbers for all four feedstocks when pyrolysis temperature increased. For all of the biochars except for the biochar prepared from woodchips, the G band of the biochars shifted to higher wavenumbers with increased pyrolysis temperature.

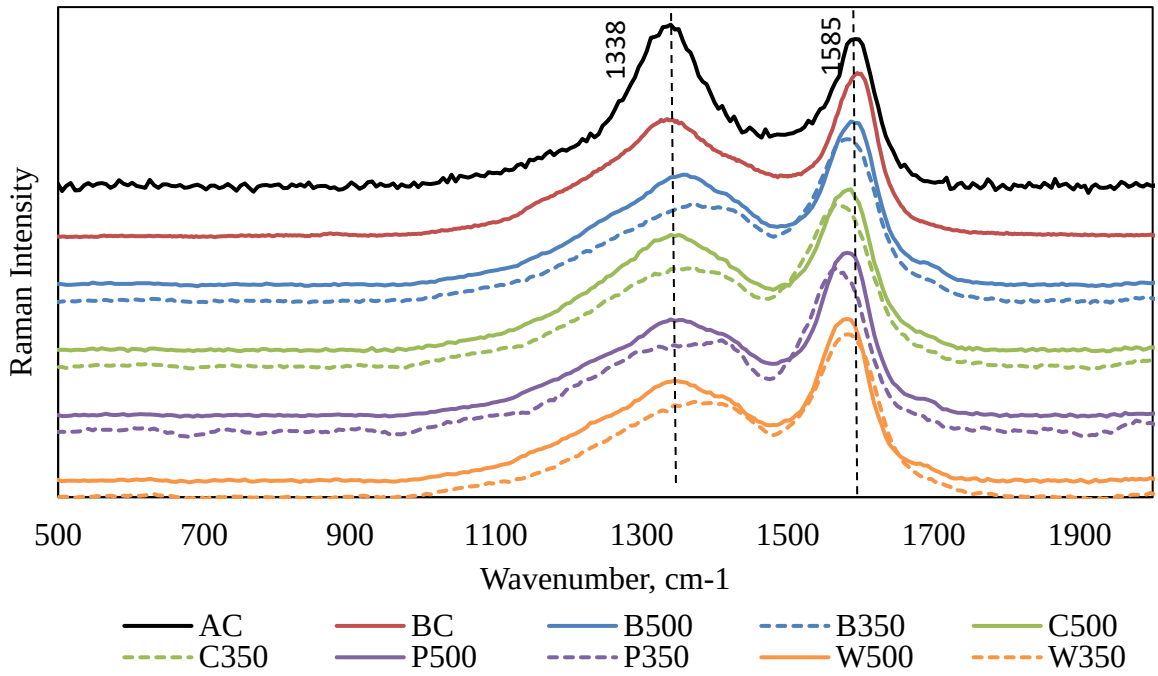

Figure IV-9. Raman spectra of lab engineered biochars, commercial biochar and activated carbon. The spectra were the averaged results of 5 spots of lab engineered biochar samples and 3 spots of commercial biochar and activated carbon.

The ratio of the intensities calculated from the results of Gaussian fitting, I_D/I_G, revealed the highest graphite degree for AC. The graphite degree of all biochar materials were found to be lower than 1, which was not the case for AC. The values of I_D/I_G of lab engineered biochars were close to that of the commercial BC. No significant difference or trend was observed for I_D/I_G values and pyrolysis temperatures in the range of studied temperatures. An increase of I_D/I_G with the increasing temperature was reported in the literature for wood derived biochars, at temperatures rising from 500 ˚C to higher temperatures (Asadullah et al. 2010; Keiluweit et al. 2010; Guizani et al. 2017). At low temperature, the I_D/I_G value was nearly constant, which agreed with our findings. A mechanism of converting small aromatic ring systems (3-5 fused rings) to larger ones (not less than 6 fuse rings) was proposed for the structural evolution (Asadullah et al. 2010; Keiluweit et al. 2010). However, the effect of pyrolysis temperature was variable with the properties of feedstock. Zhang et al. (2015) observed that the I_D/I_G ratio (3.8 - 8.3) decreased when temperature increased from 300 ˚C to 900 ˚C by using sewage sludge as feedstock, indicating the increase of crystallographic order. Rhim et al. (2010a) also studied the graphite degree of biochars prepared at different pyrolysis temperatures using microcrystalline cellulose. An increase in the I_D/I_G ratio was reported with increasing temperature from 300 ˚C to 650 ˚C, and then a decrease in the ratio (2.6 to 0.0) was reported when temperature increased further to 2000 ˚C. The results of this study revealed low degree of condensed aromatic structure in AC. The condensation was not significant for the wood-derived biochars studied in this work when pyrolysis temperature increased from 350 ˚C to 500 ˚C.

Table IV-7. The D band and G band parameters of lab engineered biochars, commercial biochar and activated carbon

Sorbents	D band, cm^{-1}	G band, cm^{-1}	I_D/I_G	I_V/I_D
W350	1379.0 ± 5.1	1585.3 ± 2.2	0.68 ± 0.01	0.68 ± 0.05
W500	1353.6 ± 2.7	1579.0 ± 1.2	0.65 ± 0.02	0.59 ± 0.03
B350	1381.5 ± 2.5	1584.9 ± 2.9	0.71 ± 0.02	0.69 ± 0.04
B500	1357.5 ± 2.5	1589.6 ± 0.8	0.71 ± 0.03	0.56 ± 0.02
C350	1363.3 ± 9.0	1574.2 ± 4.3	0.71 ± 0.07	0.70 ± 0.09

Table IV-7. Continued

C500	1347.7 ± 2.9	1581.1 ± 1.4	0.76 ± 0.08	0.55 ± 0.04
P350	1360.1 ± 3.8	1571.7 ± 0.6	0.63 ± 0.01	0.60 ± 0.04
P500	1353.8 ± 0.4	1581.1 ± 0.5	0.62 ± 0.01	0.59 ± 0.03
AC	1337.8 ± 1.1	1585.4 ± 0.6	1.03 ± 0.02	0.36 ± 0.02
BC	1344.4 ± 9.5	1592.1 ± 0.5	0.72 ± 0.11	0.59 ± 0.04

The I_V/I_D values reflect the content of amorphous carbon structure in the biochar material. The results showed that the lowest value of I_v/I_D was in AC. This indicated that AC was highly order with least amorphous carbon. The I_v/I_D ratios of biochars were in the range of 0.55 to 0.70. Lower I_v/I_D ratios were obtained for biochars prepared at high temperatures. The decrease of valley region with increasing temperature was also reported in literatures, suggesting the char ordering from amorphous carbon to condensed aromatic structures (Li et al. 2006; Asadullah et al. 2010; Guizani et al. 2017). The findings from the analysis of Raman spectra were then used for understanding the SMX adsorption on biochar from the aspect of potential molecular interactions between SMX and biochars.

4.3.2.2 Adsorption of SMX in wastewater

The adsorption performance of SMX by lab engineered biochar samples was characterized using closed bottle experiments in DI and MASSTC septic effluent, respectively. The results were compared with commercial biochar and activated carbon. These results are presented in figure IV-10.

For all sorbent samples, more SMX was adsorbed for per unit weight of sorbent in DI water than in MASSTC septic effluent. The same effect was also observed for commercial biochar and activated carbon, which is probably due to the competing or complexation effect of DOM in wastewater as discussed in section 3.3.1.3. The hindering effect of wastewater for woodchip and pinecone biochars was not as significant as those observed for commercial biochar, activated carbon and pine sawdust biochar, where the q_e values in DI water were greater than those in wastewater by one order of magnitude. The q_e values of bamboo sawdust biochar in wastewater were not included in the analysis. The SMX sorption by bamboo sawdust biochars

were not quantified because the leachate of organic components from biochar introduced extra peaks in the region of SMX peak in LC-MS spectrum, which made it difficult to integrate.

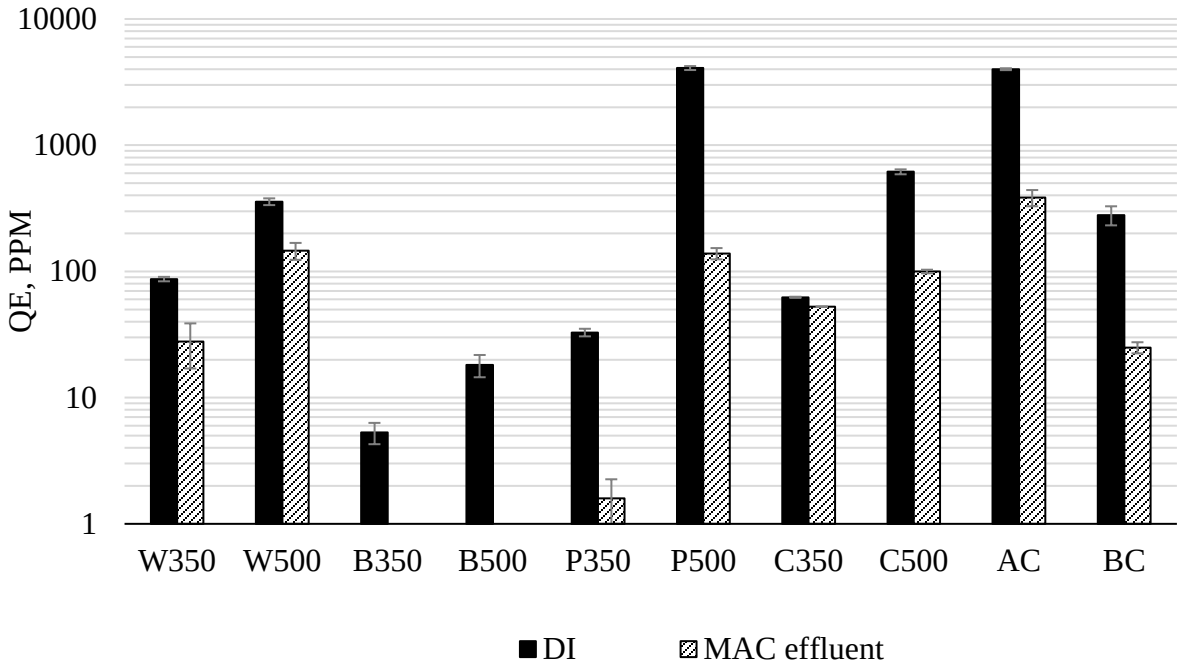

Figure IV-10. Adsorption capacity of SMX on lab engineered biochars, commercial biochar and activated carbon in DI water and MASSTC septic effluent. The initial SMX concentration was 200 ppb. Error bars represent sample standard deviation (n = 3).

Higher q_e values were achieved for biochar samples prepared at the higher pyrolysis temperature. The biggest qe increase with elevated pyrolysis temperature was obtained for biochars prepared using pine sawdust. The value of q_e for P500 was greater than P350 by two orders of magnitude. All lab engineered biochar samples prepared at 500°C showed comparable q_e values to commercial biochar, which was produced at similar pyrolysis temperature. The highest q_e was obtained by P500 in DI water, the q_e of which was 4088 ppm, which is comparable to that of activated carbon (4002 ppm).

Adsorption isotherm experiments were performed with lab engineered biochar samples, except for the biochar prepared from bamboo sawdust. Isotherms for P350 were not included, because the low adsorption lead to high variations in q_e values, which led to poor correlation when developing the models. All the isotherms were fitted using linear, Langmuir and Freundlich

models. The Langmuir model was not able to describe the feature of sorption isotherms and thus only the results of linear and Freundlich models are presented in figure IV-11 and the corresponding parameters are summarized in table IV-8.

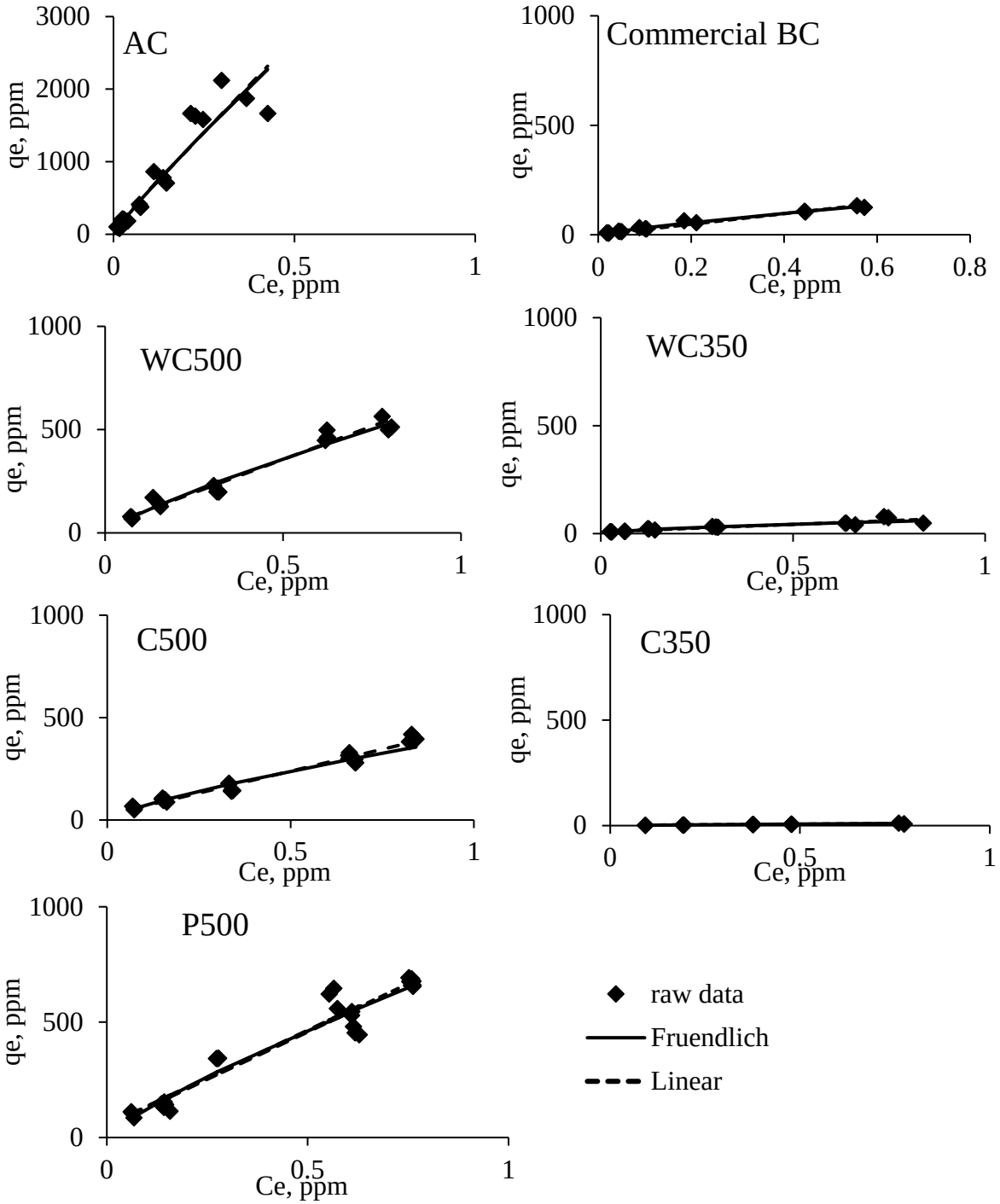

Figure IV-11. Adsorption isotherms of SMX removal on lab engineered biochars, commercial biochar and activated carbon.

Table IV-8. Parameters of Freundlich model for SMX sorption by lab engineered biochars, commercial biochar and activated carbon

	K_d	R^2	K_F, ppm^{-N}	N	R^2	K_d^{eff}
AC	5204	0.8691	4922	0.91	0.9524	6860
P500	821	0.9351	822	0.82	0.9405	1595
WC500	644	0.9683	635	0.82	0.9666	1234
C500	427	0.9723	406	0.76	0.9633	977
BC	239	0.9736	209	0.83	0.9844	391
WC350	90.3	0.9307	80.4	0.67	0.9511	262
C350	10.9	0.9597	12.0	0.78	0.9538	26.5

$K_d^{eff} = K_F C_e^{N-1}$, using the estimated lowest equilibrium aqueous concentration of C_e = 25 ppb.

The highest adsorption isotherms were observed for the AC with the highest values of the non-linear coefficient N. Compared to the biochars prepared at 500 ˚C, biochars prepared at low temperature (350 ˚C) exhibited lower adsorption isotherms with higher non-linearity and more heterogeneous adsorption. This finding could be explained by the findings in Raman analysis. When pyrolysis temperature increases, there are less heterogeneous sites present due to loss of functional groups and amorphous carbon ordering to aromatic structure.

The correlation between the SMX sorption coefficient K_d^{eff} and the physical-chemical properties of biochars was also examined (appendix G). A negative correlation was found between K_d^{eff} and the I_V/I_D ratio (figure IV-12a). 52.7 % of the variance of K_d^{eff} could be statistically explained by the changes in I_V/I_D ratio. This result indicated that the structural evolution of biochar from amorphous carbon through small aromatic ring systems to larger ones favored the SMX sorption. However, the correlation between K_d^{eff} and N, I_D/I_G ratio was weak (figure IV-12b and c).

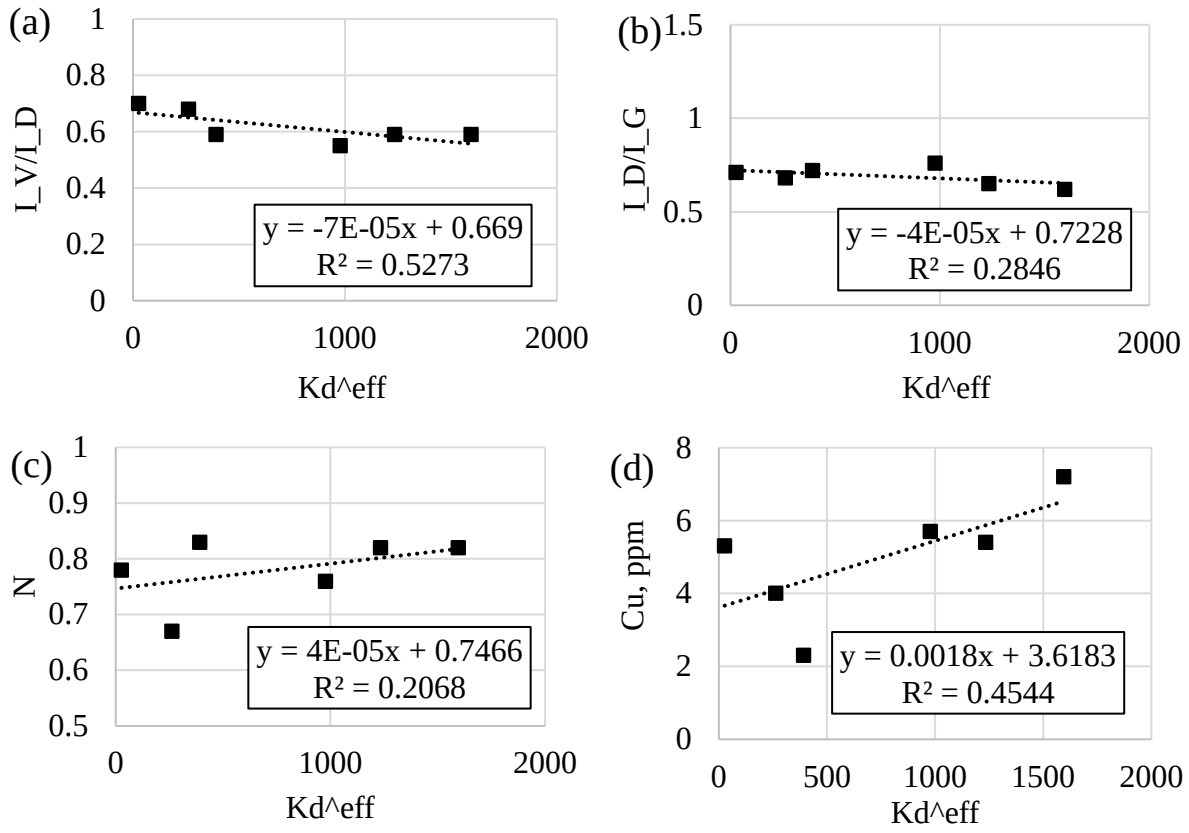

Figure IV-12. The correlation between between (a) K_d^{eff} and I_V/I_D ratio (b) K_d^{eff} and I_D/I_G ratio (c) K_d^{eff} and N in biochar (d) K_d^{eff} and Cu in biochars.

The presence of aromatic carbon was also confirmed by FT-IR analysis. The resulting aromatic ring structure could facilitate the SMX adsorption through π-π interactions of the aromatic structure in SMX and graphitic carbon of biochar. Other than the effect of aromatic structure, the existence of the functional groups, such as carbonyl and carboxylate groups as observed in FT-IR, could also inhibit SMX adsorption by increasing surface hydrophilicity. These functional groups were not eliminated at temperature of 500 ˚C. However, the concentration of the functional groups could not be obtained from the FT-IR results, but it was reasonable to presume less functional groups at higher temperature as often reported by other researchers (Chun et al. 2004; Yuan et al. 2011; Jindo et al. 2014).

Other features of biochar could also play a role in determining SMX adsorption. The high pH values for biochars prepared as higher temperature could influence SMX adsorption via altering SMX charges. However, the pH values after wastewater addition all fell within the

region where SMX^- dominated (pH = 7.5-8). Thus, the pH variation had limited effect on SMX adsorption in wastewater. The correlation between pH and K_d^{eff} was weak, with a low R^2 of 0.0895 (figure A-IV-4). However, the low pH of P500 (pH = 4.3) could contribute to the remarkably high SMX removal in DI water.

Low metallic content could inhibit SMX via increasing the hydrophilicity of the sorbents, but it could on the other hand facilitate SMX^- sorption through electrostatic interaction and cation-π interactions. No significant correlation between metallic contents of Na, K, Mg, Al, Zn, Mn, Fe, Ca, and SMX sorption was observed for the biochars of this study (appendix G). The changes in K_d^{eff} of biochar samples was explained by the intrinsic Cu concentration by the percentage of 45.4 % (figure IV-12). K_d^{eff} and Cu were positively related. The increased adsorption of SMX with increasing Cu in biochar could be explained by the formation of Cu bridge between SMX and biochar at low concentration of Cu. This result agreed with the findings reported by Wu et al. (2012). The π-cation interaction between Cu and SMX was found to be stronger than other interactions at low Cu concentration (Wu et al. 2012).

4.4 Conclusions

The ubiquitous occurrence of antibiotics in environment posed potential threats to humans and to the environment. Biochar, because of its benefits such as sustainability and cost-effectiveness, were widely used for water and soil remediation. This study used SMX as a model compound to study the effectiveness of biochar in the application in wastewater remediation in actual scenario by considering the complexity of co-existing components in wastewater. Cu, Fe and SMX were effectively removed by biochar, while nutrients (N and P), heavy metal Zn and exchangeable cations were not significantly affected. Soil application of biochar was examined with different soil/biochar mixing rates. A biochar amendment could enhance the overall removal of SMX from septic effluent. However, the presence of the soil diminished the SMX removal performance of biochar and lower K_d values were obtained as compared to the theoretical values. DOM in wastewater and from soil could also inhibit SMX removal by biochar, probably due to competition and blocking effect.

To achieve higher removal efficiency, we prepared biochar materials from different feedstocks at different pyrolysis temperatures. The resulted biochar materials varied in physicochemical

properties with feedstock and pyrolysis temperatures. Improved SMX adsorption was obtained with increased temperature and the highest removal was obtained with pine sawdust-derived biochar. Metallic content and Ph could influence the SMX removal by biochars; however, weak correlation between these properties and adsorption coefficients were observed. On the other hand, the effective Kd value calculated from adsorption isotherms using Freundlich model was well correlated with I_V/I_D and I_D/I_G from Raman spectroscopy, suggesting the important effect of the structural evolution of aromatic region on SMX adsorption. This implied that the π-π interactions between biochar and SMX could be one major mechanism for SMX removal from septic effluent.

The soil application of biochar is a promising technique with wide applications, such as drain fields of septic system, bank filtration beds for municipal wastewater treatment plants, farmland that is irrigated with reclaimed water, and even regular farmland. However, to test the applicability and effectiveness of biochar in antibiotic removal in soil, additional analyses are needed to study the contaminant transport and examine the performance of biochar in a dynamic scenario. A column test, completed for this purpose, is described in the next chapter. In addition, to obtain more insights of the SMX interactions with carbonaceous absorbents, the correlation of adsorption capacities and Raman I_V/I_D and I_D/I_G results could be assessed for other materials that are enriched with aromatic carbons, such as activated carbons, hydro chars and carbon nanotubes.

References

Ahmad, M., Lee, S. S., Oh, S. E., Mohan, D., Moon, D. H., Lee, Y. H. and Ok, Y. S. (2013). "Modeling adsorption kinetics of trichloroethylene onto biochars derived from soybean stover and peanut shell wastes." *Environmental Science and Pollution Research* 20(12), 8364-8373.

Ahmad, M., Rajapaksha, A. U., Lim, J. E., Zhang, M., Bolan, N., Mohan, D., Vithanage, M., Lee, S. S. and Ok, Y. S. (2014). "Biochar as a sorbent for contaminant management in soil and water: A review." *Chemosphere* 99, 19-33.

Ahmaruzzaman, M. (2008). "Adsorption of phenolic compounds on low-cost adsorbents: A review." *Advances in Colloid and Interface Science* 143(1-2), 48-67.

Alberti, G., Amendola, V., Pesavento, M. and Biesuz, R. (2012). "Beyond the synthesis of novel solid phases: Review on modelling of sorption phenomena." *Coordination Chemistry Reviews* 256(1-2), 28-45.

Asadullah, M., Zhang, S. and Li, C. Z. (2010). "Evaluation of structural features of chars from pyrolysis of biomass of different particle sizes." *Fuel Processing Technology* 91(8), 877-881.

Barnes, K. K., Kolpin, D. W., Furlong, E. T., Zaugg, S. D., Meyer, M. T. and Barber, L. B. (2008). "A national reconnaissance of pharmaceuticals and other organic wastewater contaminants in the United States - I) Groundwater." *Science of the Total Environment* 402(2-3), 192-200.

Beesley, L., Moreno-Jimenez, E. and Gomez-Eyles, J. L. (2010). "Effects of biochar and greenwaste compost amendments on mobility, bioavailability and toxicity of inorganic and organic contaminants in a multi-element polluted soil." *Environmental Pollution* 158(6), 2282-2287.

Beesley, L., Moreno-Jimenez, E., Gomez-Eyles, J. L., Harris, E., Robinson, B. and Sizmur, T. (2011). "A review of biochars' potential role in the remediation, revegetation and restoration of contaminated soils." *Environmental Pollution* 159(12), 3269-3282.

Bornemann, L. C., Kookana, R. S. and Welp, G. (2007). "Differential sorption behaviour of aromatic hydrocarbons on charcoals prepared at different temperatures from grass and wood." *Chemosphere* 67(5), 1033-1042.

Bouchoucha, A., Terbouche, A., Zaouani, M., Derridj, F. and Djebbar, S. (2013). "Iron and nickel complexes with heterocyclic ligands: Stability, synthesis, spectral characterization, antimicrobial activity, acute and subacute toxicity." *Journal of Trace Elements in Medicine and Biology* 27(3), 191-202.

Boxall, A. B. A., Blackwell, P., Cavallo, R., Kay, P. and Tolls, J. (2002). "The sorption and transport of a sulphonamide antibiotic in soil systems." *Toxicology Letters* 131(1-2), 19-28.

Boxall, A. B. A. and Sinclair, C. J. (2001). "Assessment of the environmental properties and effects of pesticide degradation products." *Pesticide Behaviour in Soils and Water*(78), 113-118.

Bradford, G. R., Change, A. C., Page, A. L., Bakhtar, D., Frampton, J. A. and Wright, H. (1996). "Background concentrations of trace and major elements in california soils" Available: https://www.waterboards.ca.gov/water_issues/programs/compost/docs/kearney1996.pdf [Accessed 11/20/2017]

Brown, J. R. (1998). Recommended chemical soil test procedures for the North Central Region. Missouri Agricultural Experiment Station, University of Missouri--Columbia.

Brown, K. D., Kulis, J., Thomson, B., Chapman, T. H. and Mawhinney, D. B. (2006). "Occurrence of antibiotics in hospital, residential, and dairy, effluent, municipal wastewater, and the Rio Grande in New Mexico." *Science of the Total Environment* 366(2-3), 772-783.

Castiglioni, S., Bagnati, R., Fanelli, R., Pomati, F., Calamari, D. and Zuccato, E. (2006). "Removal of pharmaceuticals in sewage treatment plants in Italy." *Environmental Science & Technology* 40(1), 357-363.

Castro, J. E., Fernandez, A. M., Gonzalez-Caccia, V. and Gardinali, P. R. (2013). "Concentration of trace metals in sediments and soils from protected lands in south Florida: background levels and risk evaluation." *Environmental Monitoring and Assessment* 185(8), 6311-6332.

Chen, H., Gao, B., Li, H. and Ma, L. Q. (2011). "Effects of pH and ionic strength on sulfamethoxazole and ciprofloxacin transport in saturated porous media." *Journal of Contaminant Hydrology* 126(1-2), 29-36.

Cheng, C.-H., Lehmann, J. and Engelhard, M. H. (2008). "Natural oxidation of black carbon in soils: changes in molecular form and surface charge along a climosequence." *Geochimica et Cosmochimica Acta* 72(6), 1598-1610.

Cheung, C. W., Porter, J. F. and McKay, G. (2000). "Elovich equation and modified second-order equation for sorption of cadmium ions onto bone char." *Journal of Chemical Technology and Biotechnology* 75(11), 963-970.

Chun, Y., Sheng, G. Y., Chiou, C. T. and Xing, B. S. (2004). "Compositions and sorptive properties of crop residue-derived chars." *Environmental Science & Technology* 38(17), 4649-4655.

Drillia, P., Stamatelatou, K. and Lyberatos, G. (2005). "Fate and mobility of pharmaceuticals in solid matrices." *Chemosphere* 60(8), 1034-1044.

Du, B., Price, A. E., Scott, W. C., Kristofco, L. A., Ramirez, A. J., Chambliss, C. K., Yelderman, J. C. and Brooks, B. W. (2014). "Comparison of contaminants of emerging concern removal, discharge, and water quality hazards among centralized and on-site wastewater treatment system effluents receiving common wastewater influent." *Science of the Total Environment* 466, 976-984.

Edgell, K. (1989). USEPA method study 37 SW-846 method 3050 acid digestion of sediments, sludges, and soils. US Environmental Protection Agency, Environmental Monitoring Systems Laboratory.

Enders, A., Hanley, K., Whitman, T., Joseph, S. and Lehmann, J. (2012). "Characterization of biochars to evaluate recalcitrance and agronomic performance." *Bioresource Technology* 114, 644-653.

Focazio, M. J., Kolpin, D. W., Barnes, K. K., Furlong, E. T., Meyer, M. T., Zaugg, S. D., Barber, L. B. and Thurman, M. E. (2008). "A national reconnaissance for pharmaceuticals and other organic wastewater contaminants in the United States - II) Untreated drinking water sources." *Science of the Total Environment* 402(2-3), 201-216.

Fu, P., Hu, S., Xiang, J., Sun, L. S., Li, P. S., Zhang, J. Y. and Zheng, C. G. (2009). "Pyrolysis of Maize Stalk on the Characterization of Chars Formed under Different Devolatilization Conditions." *Energy & Fuels* 23, 4605-4611.

Gao, Z. M., Bandosz, T. J., Zhao, Z. B., Han, M. and Qiu, J. S. (2009). "Investigation of factors affecting adsorption of transition metals on oxidized carbon nanotubes." *Journal of Hazardous Materials* 167(1-3), 357-365.

Gelband, H., Miller-Petrie, M., Pant, S., Grandra, S., Levinson, J., Barter, D., White, A. and Laxminarayan, R. (2015). "State of the World's Antibiotics, 2015" Available: [Accessed

Gell, K., van Groenigen, J. W. and Cayuela, M. L. (2011). "Residues of bioenergy production chains as soil amendments: Immediate and temporal phytotoxicity." *Journal of Hazardous Materials* 186(2-3), 2017-2025.

Gough, L. P., Severson, R. C. and Shacklette, H. T. (1988). "Element concentrations in soils and other surficial materials of Alaska." Professional Paper 1458. http://pubs.er.usgs.gov/publication/pp1458 [Accessed

Gros, M., Petrovic, M. and Barcelo, D. (2007). "Wastewater treatment plants as a pathway for aquatic contamination by pharmaceuticals in the ebro river basin (northeast spain)." *Environmental Toxicology and Chemistry* 26(8), 1553-1562.

Guizani, C., Haddad, K., Limousy, L. and Jeguirim, M. (2017). "New insights on the structural evolution of biomass char upon pyrolysis as revealed by the Raman spectroscopy and elemental analysis." *Carbon* 119, 519-521.

Hameed, B. H. (2008). "Equilibrium and kinetic studies of methyl violet sorption by agricultural waste." *Journal of Hazardous Materials* 154(1-3), 204-212.

Han, X., Liang, C. F., Li, T. Q., Wang, K., Huang, H. G. and Yang, X. E. (2013). "Simultaneous removal of cadmium and sulfamethoxazole from aqueous solution by rice straw biochar." *Journal of Zhejiang University-Science B* 14(7), 640-649.

Heberer, T. (2002). "Occurrence, fate, and removal of pharmaceutical residues in the aquatic environment: a review of recent research data." *Toxicology Letters* 131(1-2), 5-17.

Hirsch, R., Ternes, T., Haberer, K. and Kratz, K. L. (1999). "Occurrence of antibiotics in the aquatic environment." *Science of the Total Environment* 225(1-2), 109-118.

Ho, Y. S. and McKay, G. (1998). "Sorption of dye from aqueous solution by peat." *Chemical Engineering Journal* 70(2), 115-124.

Homem, V. and Santos, L. (2011). "Degradation and removal methods of antibiotics from aqueous matrices - A review." *Journal of Environmental Management* 92(10), 2304-2347.

Irving, H. and Williams, R. J. P. (1953). "The stability of transition-metal complexes." *Journal of the Chemical Society (Resumed)*(0), 3192-3210.

Ishimaru, K., Hata, T., Bronsveld, P., Nishizawa, T. and Imamura, Y. (2007). "Characterization of sp2- and sp3-bonded carbon in wood charcoal." *Journal of Wood Science* 53(5), 442-448.

Ji, L. L., Wan, Y. Q., Zheng, S. R. and Zhu, D. Q. (2011). "Adsorption of Tetracycline and Sulfamethoxazole on Crop Residue-Derived Ashes: Implication for the Relative Importance of Black Carbon to Soil Sorption." *Environmental Science & Technology* 45(13), 5580-5586.

Jindo, K., Mizumoto, H., Sawada, Y., Sanchez-Monedero, M. A. and Sonoki, T. (2014). "Physical and chemical characterization of biochars derived from different agricultural residues." *Biogeosciences* 11(23), 6613-6621.

Kahle, M. and Stamm, C. (2007). "Time and pH-dependent sorption of the veterinary antimicrobial sulfathiazole to clay minerals and ferrihydrite." *Chemosphere* 68(7), 1224-1231.

Keiluweit, M., Nico, P. S., Johnson, M. G. and Kleber, M. (2010). "Dynamic Molecular Structure of Plant Biomass-Derived Black Carbon (Biochar)." *Environmental Science & Technology* 44(4), 1247-1253.

Khoo, K. H., Culberson, C. H. and Bates, R. G. (1977). "Thermodynamics of Dissociation of Ammonium Ion in Seawater from 5 to 40degreesc." *Journal of Solution Chemistry* 6(4), 281-290.

Kolpin, D. W., Furlong, E. T., Meyer, M. T., Thurman, E. M., Zaugg, S. D., Barber, L. B. and Buxton, H. T. (2002). "Pharmaceuticals, hormones, and other organic wastewater

contaminants in US streams, 1999-2000: A national reconnaissance." *Environmental Science & Technology* 36(6), 1202-1211.

Lagergren, S. (1898). "Zur theorie der sogenannten adsorption gelöster stoffe." *Kungliga Svenska Vetenskapsakademiens. Handlingar* 24(4), 1-39.

Lammers, K., Arbuckle-Keil, G. and Dighton, J. (2009). "FT-IR study of the changes in carbohydrate chemistry of three New Jersey pine barrens leaf litters during simulated control burning." *Soil Biology & Biochemistry* 41(2), 340-347.

Li, X., Hayashi, J.-i. and Li, C.-Z. (2006). "FT-Raman spectroscopic study of the evolution of char structure during the pyrolysis of a Victorian brown coal." *Fuel* 85(12), 1700-1707.

Lian, F., Sun, B. B., Song, Z. G., Zhu, L. Y., Qi, X. H. and Xing, B. S. (2014). "Physicochemical properties of herb-residue biochar and its sorption to ionizable antibiotic sulfamethoxazole." *Chemical Engineering Journal* 248, 128-134.

Lucida, H., Parkin, J. E. and Sunderland, V. B. (2000). "Kinetic study of the reaction of sulfamethoxazole and glucose under acidic conditions - I. Effect of pH and temperature." *International Journal of Pharmaceutics* 202(1-2), 47-61.

Mohan, D., Sarswat, A., Ok, Y. S. and Pittman, C. U. (2014). "Organic and inorganic contaminants removal from water with biochar, a renewable, low cost and sustainable adsorbent - A critical review." *Bioresource Technology* 160, 191-202.

Morel, M. C., Spadini, L., Brimo, K. and Martins, J. M. F. (2014). "Speciation study in the sulfamethoxazole-copper-pH-soil system: Implications for retention prediction." *Science of the Total Environment* 481, 266-273.

Ozcimen, D. and Ersoy-Mericboyu, A. (2010). "Characterization of biochar and bio-oil samples obtained from carbonization of various biomass materials." *Renewable Energy* 35(6), 1319-1324.

Pellera, F. M., Giannis, A., Kalderis, D., Anastasiadou, K., Stegmann, R., Wang, J. Y. and Gidarakos, E. (2012). "Adsorption of Cu(II) ions from aqueous solutions on biochars prepared from agricultural by-products." *Journal of Environmental Management* 96(1), 35-42.

Qiu, Y. P., Cheng, H. Y., Xu, C. and Sheng, D. (2008). "Surface characteristics of crop-residue-derived black carbon and lead(II) adsorption." *Water Research* 42(3), 567-574.

Rao, G. P., Lu, C. and Su, F. (2007). "Sorption of divalent metal ions from aqueous solution by carbon nanotubes: A review." *Separation and Purification Technology* 58(1), 224-231.

Rhim, Y., Zhang, D., Fairbrother, D., Wepasnick, K., Livi, K., Bodnar, R. and Nagle, D. (2010a). "Changes in electrical and microstructural properties of microcrystalline cellulose as function of carbonization temperature." *Carbon* 48(4), 1012-1024.

Rhim, Y. R., Zhang, D. J., Fairbrother, D. H., Wepasnick, K. A., Livi, K. J., Bodnar, R. J. and Nagle, D. C. (2010b). "Changes in electrical and microstructural properties of microcrystalline cellulose as function of carbonization temperature." *Carbon* 48(4), 1012-1024.

Seol, Y. and Lee, L. S. (2000). "Effect of dissolved organic matter in treated effluents on sorption of atrazine and prometryn by soils." *Soil Science Society of America Journal* 64(6), 1976-1983.

Sheng, G. D., Li, J. X., Shao, D. D., Hu, J., Chen, C. L., Chen, Y. X. and Wang, X. K. (2010). "Adsorption of copper(II) on multiwalled carbon nanotubes in the absence and presence of humic or fulvic acids." *Journal of Hazardous Materials* 178(1-3), 333-340.

Sitko, R., Turek, E., Zawisza, B., Malicka, E., Talik, E., Heimann, J., Gagor, A., Feist, B. and Wrzalik, R. (2013). "Adsorption of divalent metal ions from aqueous solutions using graphene oxide." *Dalton Transactions* 42(16), 5682-5689.

Smith, M. W., Dallmeyer, I., Johnson, T. J., Brauer, C. S., McEwen, J. S., Espinal, J. F. and Garcia-Perez, M. (2016). "Structural analysis of char by Raman spectroscopy: Improving band assignments through computational calculations from first principles." *Carbon* 100, 678-692.

Srinivasan, P. and Sarmah, A. K. (2015). "Characterisation of agricultural waste-derived biochars and their sorption potential for sulfamethoxazole in pasture soil: A spectroscopic investigation." *Science of the Total Environment* 502, 471-480.

Tan, I. A. W., Ahmad, A. L. and Hameed, B. H. (2008). "Adsorption of basic dye on high-surface-area activated carbon prepared from coconut husk: Equilibrium, kinetic and thermodynamic studies." *Journal of Hazardous Materials* 154(1-3), 337-346.

Ternes, T. A. (1998). "Occurrence of drugs in German sewage treatment plants and rivers." *Water Research* 32(11), 3245-3260.

Thiele-Bruhn, S. and Aust, M. O. (2004). "Effects of pig slurry on the sorption of sulfonamide antibiotics in soil." *Archives of Environmental Contamination and Toxicology* 47(1), 31-39.

Tong, X. J., Li, J. Y., Yuan, J. H. and Xu, R. K. (2011). "Adsorption of Cu(II) by biochars generated from three crop straws." *Chemical Engineering Journal* 172(2-3), 828-834.

Wu, D., Pan, B., Wu, M., Peng, H. B., Zhang, D. and Xing, B. S. (2012). "Coadsorption of Cu and sulfamethoxazole on hydroxylized and graphitized carbon nanotubes." *Science of the Total Environment* 427, 247-252.

Xu, W. H., Zhang, G., Li, X. D., Zou, S. C., Li, P., Hu, Z. H. and Li, J. (2007). "Occurrence and elimination of antibiotics at four sewage treatment plants in the Pearl River Delta (PRD), South China." *Water Research* 41(19), 4526-4534.

Yao, Y., Gao, B., Chen, H., Jiang, L. J., Inyang, M., Zimmerman, A. R., Cao, X. D., Yang, L. Y., Xue, Y. W. and Li, H. (2012). "Adsorption of sulfamethoxazole on biochar and its impact on reclaimed water irrigation." *Journal of Hazardous Materials* 209, 408-413.

Yu, L., Fink, G., Wintgens, T., Melina, T. and Ternes, T. A. (2009). "Sorption behavior of potential organic wastewater indicators with soils." *Water Research* 43(4), 951-960.

Yuan, J. H., Xu, R. K. and Zhang, H. (2011). "The forms of alkalis in the biochar produced from crop residues at different temperatures." *Bioresource Technology* 102(3), 3488-3497.

Zhang, J., Lu, F., Zhang, H., Shao, L., Chen, D. and He, P. (2015). "Multiscale visualization of the structural and characteristic changes of sewage sludge biochar oriented towards potential agronomic and environmental implication." *Scientific Reports* 5.

Zhang, X., Pan, B., Yang, K., Zhang, D. and Hou, J. (2010). "Adsorption of sulfamethoxazole on different types of carbon nanotubes in comparison to other natural adsorbents." *Journal of Environmental Science and Health Part a-Toxic/Hazardous Substances & Environmental Engineering* 45(12), 1625-1634.

Zhang, Y. L., Lin, S. S., Dai, C. M., Shi, L. and Zhou, X. F. (2014). "Sorption-desorption and transport of trimethoprim and sulfonamide antibiotics in agricultural soil: effect of soil type, dissolved organic matter, and pH." *Environmental Science and Pollution Research* 21(9), 5827-5835.

Zheng, H., Wang, Z. Y., Zhao, J., Herbert, S. and Xing, B. S. (2013). "Sorption of antibiotic sulfamethoxazole varies with biochars produced at different temperatures." *Environmental Pollution* 181, 60-67.

Chapter V. SMX removal in columns with soil and biochar amendments.

5.1 Introduction

The occurrence of antibiotics and their metabolites in aquatic environment has been widely reported (Kolpin et al. 2002; Barnes et al. 2008; Focazio et al. 2008). The emerging concerns of the risks to the environment and ecosystems have presented research challenges. Antibiotics can enter the subsurface through direct pathways (e.g. field treatment of wastewater, livestock farming, leak of sewage system, etc.) and indirect pathways (e.g. bank filtration of wastewater treatment plant discharges and septic effluent). Sulfamethoxazole (SMX), a sulfonamide antibiotic, was used as a model compound in this study due to its wide usage, common occurrence in the environment and resistance to natural attenuation.

The transport of SMX in the subsurface is a complex process involving a wide range of transport behaviors (including advection, dispersion and a variety of reactions). Due to the complexity of the subsurface and large *in-situ* variations, the various interactions between SMX and soil particles, and between SMX and microorganisms make the transport of SMX difficult to predict in the subsurface. Batch experiments in previous studies showed that SMX could be removed through biodegradation and biochar amendments could overcome the limited adsorption of SMX on the soil. However, batch experiments are limited without considering the effect of transport behaviors and dynamic interactions between soil and the aqueous solution flowing through it. Therefore, the behavior of SMX in the subsurface and the effectiveness of biochar amendment in subsurface applications still need to be assessed.

Compared to batch experiments, column studies provide a good estimate for SMX transport in the subsurface by allowing for consideration of transport behavior and local interactions in the soil media. The objectives of the study in this chapter were to understand the influence of adsorption and biodegradation and to access the effect of biochar amendments for mitigating SMX transport. To this end, three soil columns were constructed with soil/biochar mixtures of different biochar percentages. The columns were flushed with the same solution prepared by spiking septic effluent with SMX and a conservative bromide tracer. Concentrations of the

conservative tracer and SMX in the effluent were measured and evaluated to characterize physical transport and transformations.

5.2 Materials and methods

5.2.1 Materials

The soil and wastewater used in this study were collected from Massachusetts Alternative Septic System Test Center (MASSTC). The wastewater was sampled at the effluent of a septic tank and stored 4 °C before use. Soil samples were air dried and stored at room temperature in a capped container. The soil characterization was performed and the results are presented in appendix A. Before use, the wastewater was filtered through Whatman grade 4 filter paper and the soil was passed through 2300 μm sieve.

The commercial biochar (BC) used in this study was obtained from Biochar Now US, which was generated by pyrolysis at around 500 °C from wood-based feedstock. SMX (analytical standard) was purchased from Sigma Aldrich, Australia.

The physicochemical properties of soil, wastewater and BC were characterized and reported in previous chapters.

5.2.2 Soil column setup

The setup of soil column experiments is shown in figure V-1. The acrylic columns were 60 cm high with inner diameters of 0.73 cm. The two ends of the capped with rubber stoppers. The top stoppers were open to the air with center holes, while the bottom stoppers were attached to effluent tubes which were joined together after the sampling ports and connected to the same effluent tank to maintain the same pressure head at the bottom of the three columns. Stainless steel meshes were placed on the bottom stopper and then loaded with 2 cm of glass beads to prevent the soil from entering the effluent tubing. Soils were mixed with commercial biochar at 0 %, 1 % and 2 % by mass and wet-packed into column to a height of 50 cm (detailed packing method was described below). Another layer of glass beads were added on top of the soil to prevent disturbance of soil from the inflow. The schematic of packed soil column is shown in figure V-2.

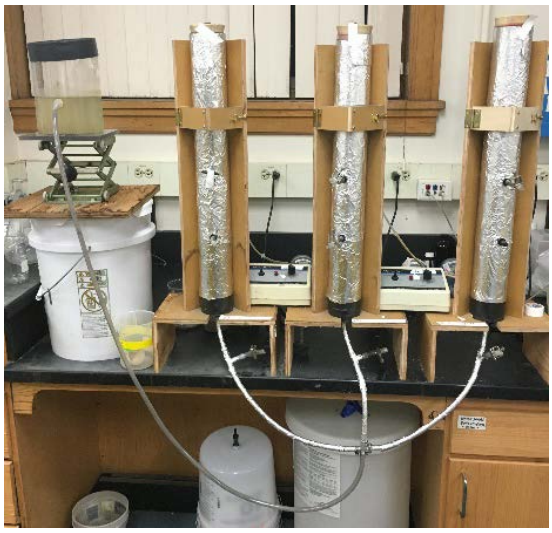

Figure V-1. Experiment setup for soil column study.

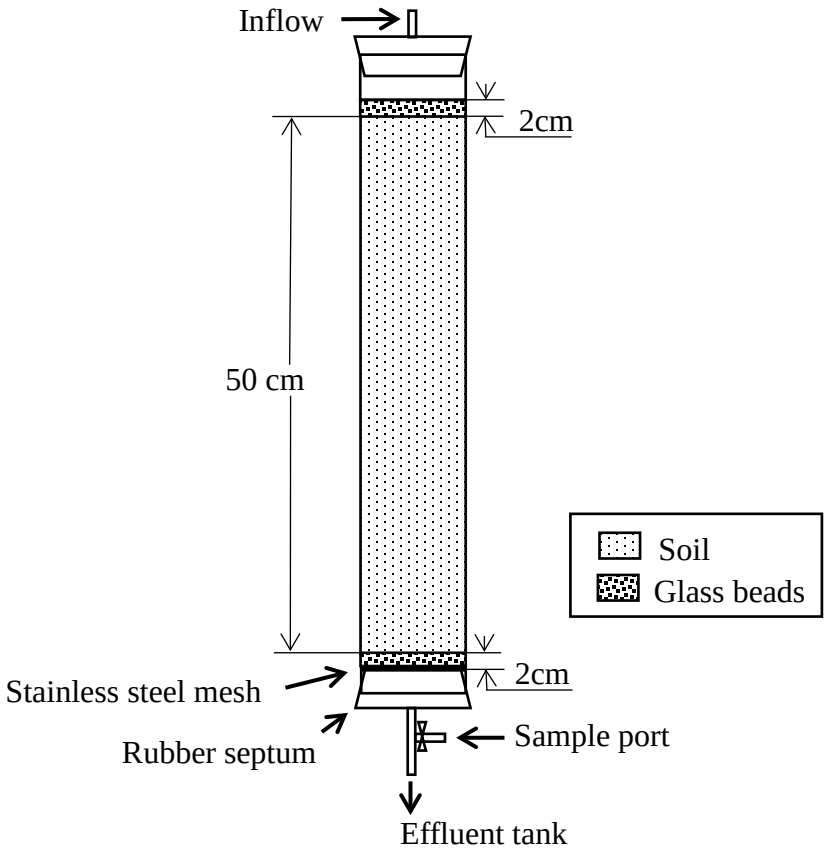

Figure V-2. Schematics of soil column.

The packing method was adjusted from the procedure described by Tian et al. (2010). The effluent tank was filled with wastewater and then a water layer was maintained at a height of

2 cm above the media by adjusting the height of the effluent tank. To saturate porous media, a small amount of the soil/biochar mixture was poured gently into the water layer until the soil surface was 0.5 cm below the water level. Approximately 10 ml of wastewater was added to each column followed by soil slurry made with soil mixture and wastewater. Sides of columns were gently tapped remove air bubbles. A 0.5-cm-high water layer was maintained after each addition of soil slurry. This procedure was repeated several times until the column was packed to a height of 50 cm for each of the soil mixtures. Columns were wrapped with aluminum foil to limit photodegradation. The height of effluent tank was adjusted accordingly to maintain the water levels after each addition in the columns. All the three soil columns were operated simultaneously using same input solution. Loading rates were controlled by adjusting the height of effluent tank, which maintained the head differences in the columns. Loading rates within each column fluctuated and varied between columns due to the differences of the substrates, which led to different pore volumes (table V-1).

Table V-1. Properties of the columns

	0 % column	1 % column	2 % column
Length L, cm	50	50	50
Diameter d, cm	0.73	0.73	0.73
Total dry mass of solids[a], kg	3.50	3.50	3.45
Total dry mass of soil, kg	3.50	3.47	3.38
Total dry mass of biochar, g	0	35	70
Total pore volume PV[b], ml	600	650	725
Total porosity n[c]	0.31	0.34	0.39

[a] total mass of soil and biochar

[b] volume of solution used for preparing saturated column

[f] calculated from pore volume derived by total volume of the column

5.2.3 Breakthrough experiment and characterization

Wastewater was added from the top of columns at certain time intervals with the same head in each of the three columns. The flowrate was adjusted by changing the height of effluent tank. After three weeks' acclimation, the same aqueous solution was introduced into each column.

The solution was prepared by adding SMX and potassium bromide (KBr) to the septic effluent. A sample volume of 7 ml was collected at each time interval and then analyzed for SMX, dissolved anions, pH and total ammonia. Sample volumes were limited to ensure that the sampling process did not adversely affect experiments. The characterization procedure was described in previous chapters and detailed procedures can be found in appendix B.

The column experiment consisted of three steps (table V-2):

- Step 0: Preparation/acclimation with low wastewater loading
- Step 1: Low wastewater loading with tracer and SMX addition
- Step 2: High wastewater loading with tracer and SMX addition

After three weeks' acclimation (step 0), the three columns were initially treated with 500 ppb of bromide and 800 ppb of SMX at same loading rates of approximately 2 cm/day (step 1). After 40 days of operation, the solution was replaced with septic effluent of higher concentrations of bromide (2000 ppb) and SMX (1000 ppb) (step 2). The loading rates were also increased by lowering the height of the effluent tank. The loading rate was about 7 cm/day for 0 % and 1 % columns, and 9 cm/day for 2 % column. The detailed plot of loading rate over time can be found in figure V-3.The loading rates were well maintained at step 1 at low loading rate. However, the loading rate kept decreasing during step 2 when the loading rates were increased.

Table V-2. Characteristics of the steps of column experiments

Step	Starting time, day	Duration, days	Designed loading rate, cm/day	Concentration of bromide, ppb	Concentration of SMX, ppb
0	5	13	2	0	0
1	18	40	2	500	800
2	58	16	8	2000	1000

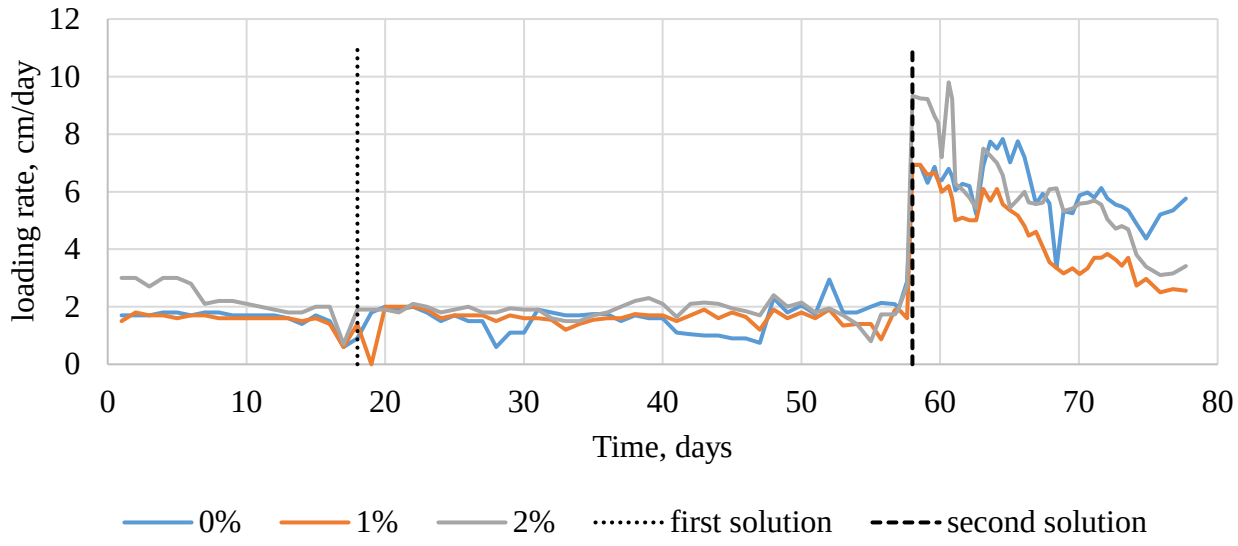

Figure V-3. Loading rates for the three soil columns throughout the experiment time.

5.2.4 Data analysis and modeling

The concentrations of bromide and SMX were adjusted by subtracting out the background concentrations, and were then normalized to their input concentrations (c/c_0), which were plotted against pore volume of the column (V/V_0).

The transport parameters of bromide and SMX were estimated by breakthrough curve fitting code known as CXTFIT 2.0 (Toride et al. 1995; Tang et al. 2010). The transport of solutes is described by the convective-dispersive equation (CDE):

$$R\frac{\partial c_r}{\partial t} = D\frac{\partial^2 c_r}{\partial x^2} - v\frac{\partial c_r}{\partial x} - \mu c_r \qquad (5.1)$$

where R is the retardation factor, c_r [ML^{-3}] is the resident concentration of the liquid phase, t is the time, D [L^2T^{-1}] is the dispersion coefficient, x [L] is the distance, v [LT^{-1}] is the averaged pore water velocity, μ [T^{-1}] is the first-order decay coefficient (Toride et al. 1995). This equation was developed assuming steady-state flow in a homogeneous soil. The adsorption of the solutes by the solid phase follows linear isotherms. The first-order decay degradation presents the general removal of a variety of processes such as metabolism, redox reactions and hydrolysis. Equation 5.1 can be rewritten in a reduced form with dimensionless parameters as:

$$R\frac{\partial C_r}{\partial T} = \frac{1}{P}\frac{\partial^2 C_r}{\partial Z^2} - \frac{\partial C_r}{\partial Z} - \mu^E C_r \quad (5.2)$$

where C_r is the normalized volume-averaged solute concentration (= c/c_0), Z is the dimensionless space variable (= x/L), T is the dimensionless time (= vt/L = pore volume), μ^E is a first-order decay coefficient (= Lμ/v). P is the Peclet number (= vL/D). The normalization of time using pore volume helps by correcting the variation of the flowrate (Banzhaf et al. 2012). Since a layer of glass beads were added on top of the soils, the distribution is considered to be uniform on the influent end and the flow through the studied soils were assumed to be uniform throughout the cross sections. Therefore, transversal dispersion was assumed to be negligible. The longitudinal dispersion is related to longitudinal dispersivity with formula:

$$D_L = D^* + \alpha_L \cdot v \quad (5.3)$$

Where D^* [L^2T^{-1}] is the molecular diffusion. Mechanical dispersion is presented by the term of $\alpha_L \cdot v$. In saturated water flow, diffusion is usually dominated by mechanical dispersion, and thus D^* is assumed to be 0. Equation 5.3 can be rewritten as:

$$D_L = \alpha_L \cdot v \quad (5.4)$$

in which case the Peclet number can be written as $P = L/\alpha_L$.

The modeling was first performed with breakthrough curves of tracer bromide. Porosities of the columns were fitted with normalized concentration distributions by minimizing sum of squared residuals (SSR) (Tang et al. 2010). The total porosity obtained from the experiment was set as a starting value. The retardation factor was set to 1 and μ^E was set to 0. The effective pore volume (PV) was then calculated with the resulting porosity. The α_L was then fitted using the breakthrough curve of normalized bromide concentration vs effective pore volume with 1.0 as a starting value.

The second step was the fitting of the CDE to the normalized breakthrough curve of SMX. The normalized concentrations of SMX were plotted against the effective pore volume obtained from the conservative tracer modeling. The fitted value of α_L were used as fixed parameter to fitted the retardation factor R and μ^E.

5.3 Results and discussions

The concentrations of conservative bromide tracer and SMX were measured over time and presented in appendix H. The results were discussed and modeled in step 1 and step 2, separately. Since no replicates were included for each column, Statistical variations cannot be estimated. and the differences between columns could be a reflection of variation. Therefore, there is no statistical meaning that can be derived by making comparisons between columns. However, the magnitudes of values and their changes during the column operation could help for understanding the properties of the columns, the development of column conditions, and transport and transformation processes of SMX.

5.3.1 Transport and modeling of the conservative tracer bromide

The breakthrough curves of bromide were presented in figure V-4 and figure V-5 with blue dots. Concentrations of bromide (as indicated by one-half of the influent concentration) showed up at about one pore volume in all the cases, which was expected for a conservative tracer. The bromide concentrations reached a constant concentration at later times with regional decreases of sequential data. These sequential decreases were due to the decreasing signal responses of ion chromatography on samples in sequences (appendix I). The breakthrough curves didn't change much between the two loading rates for 0 % and 1 % columns The breakthrough curves for 2 % column in step 2 (figure V-5c) were much steeper than in step 1 (figure V-4c).

The hydraulic conditions of the column are important for interpretation of the SMX transport. The hydraulic parameters were estimated using the breakthrough curve of conservative tracer bromide (figure V-4 and V-5).

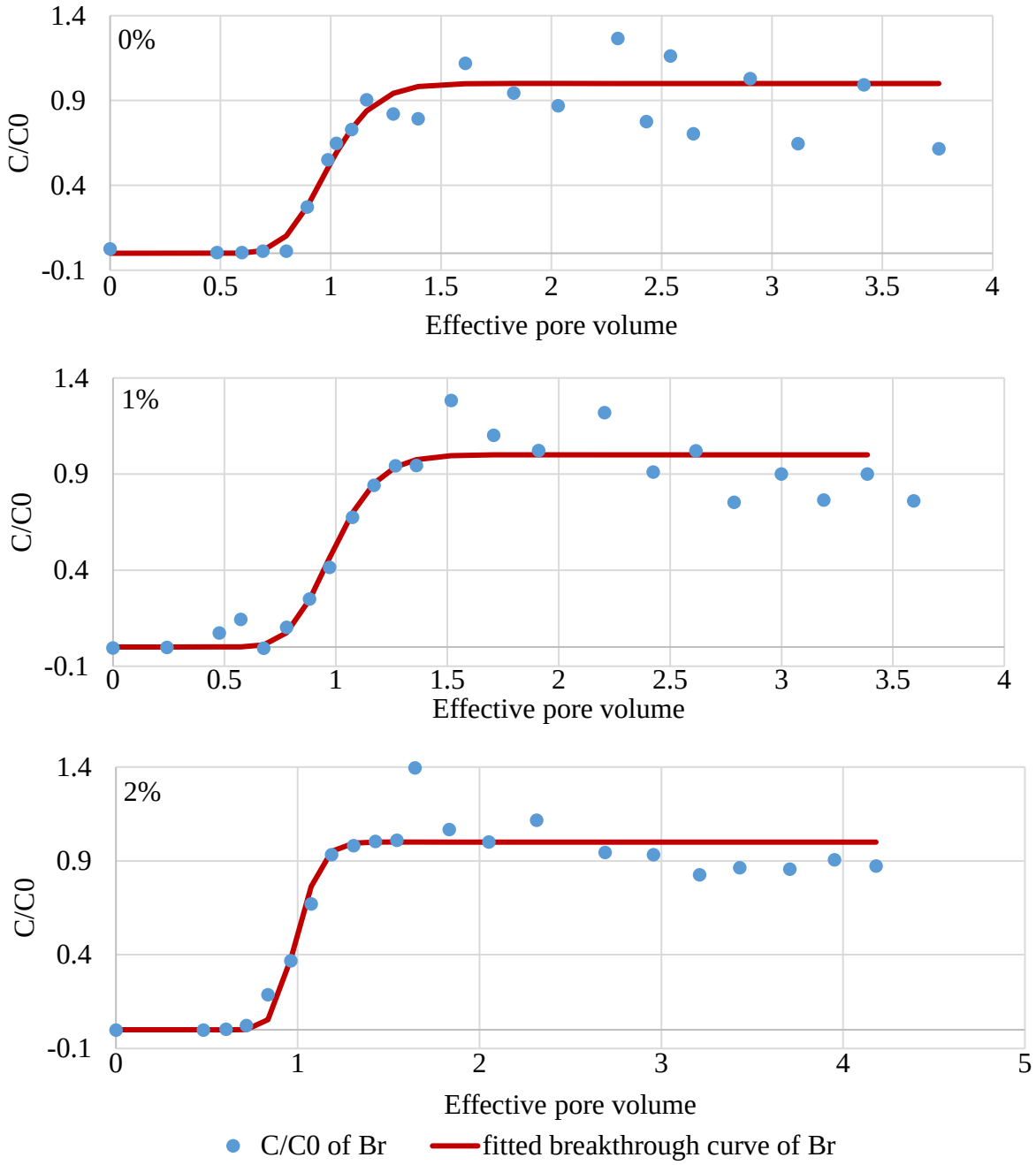

Figure V-4. Normalized breakthrough curves (C/C_0) of conservative tracer bromide at step 1 of low loading rate.

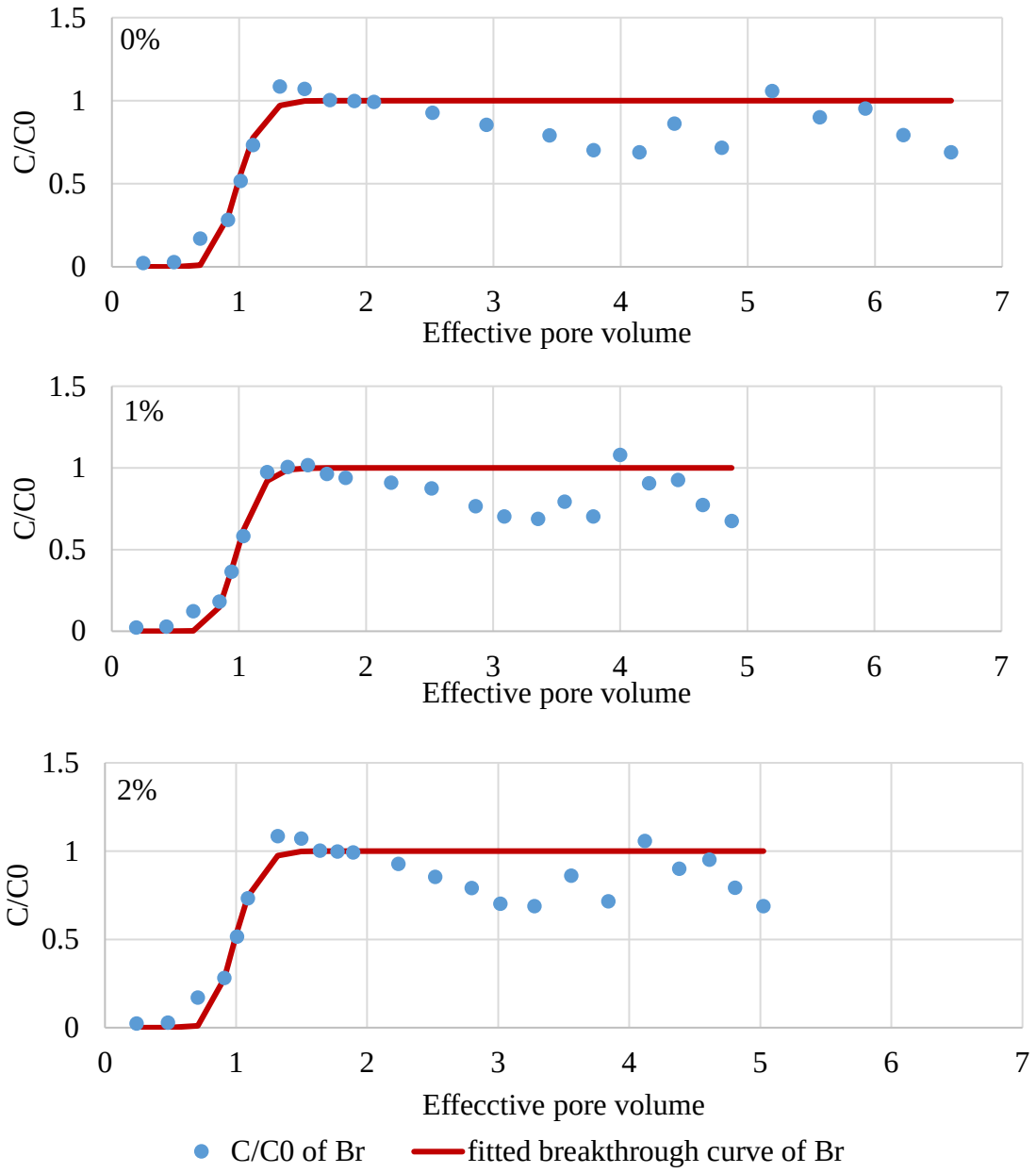

Figure V-5. Normalized breakthrough curves (C/C_0) of conservative tracer bromide at step 2 of high loading rate.

The fitted parameters were presented in table V-3. The measure porosities were the total porosity, the fitted porosities presents the effective porosity, which is the porosity that is available for transport. The fitted porosities in the 0 % and 1 % columns were consistent with the measured porosities in step 1. The slight reduction in porosity in 2 % column could due to a compression effect during the acclimation and the clogging of the pore sites. The values of

longitudinal dispersivity ranged from 0.29 cm to 0.70 cm. These values fell in the reasonable range of modeled α_L values published in literatures. Schulze-Makuch (2005) reported a α_L of 0.11 cm, but for smaller scales of about 20 cm length and well-sorted sands. In a study of three sand columns for similar scales of 41 cm length and 7.6 cm diameter, the calculated α_L values from modeling was from 0.37 cm to 0.41 cm (Hebig et al. 2017).

The porosities didn't change between the two steps for the 0 % column and 1 % column. On the other hand, the longitudinal dispersivities for the 0 % and 1 % columns decreased, probably due to the chronic clogging with the development of biomass in the column. Direct evidence for biomass growth within the columns was not available. However, significant amounts of biomass were observed in the aqueous layers at the top and effluent tubes at the bottom during the acclimation. It is very likely that biomass growth also occurred within the columns. Note that the porosity increased from 0.32 to 0.44 for 2 % column. The breakthrough curves for 2 % column in step 2 was much steeper than in step 1 (figure V-4 and figure V-5). The longitudinal dispersivity for 2 % column also exhibited significant increase between the two steps. The increased dispersivity could indicate that more preferential pathways was developed after the flow increase, when some pores sites could be freed up with particles fractured from high shear stress and as a result small constituents got flushed out of the pores (Langner et al. 1998).

Table V-3. Transport parameter determined by fitting of the breakthrough curves of the conservative tracer bromide. Retardation factor R and first-order decay coefficient μ^E were fixed to be 1.0 and 0, respectively during the modelling.

	Step 1			Step 2		
	0 %	1 %	2 %	0 %	1 %	2 %
Retardation factor, R	1.0	1.0	1.0	1.0	1.0	1.0
First-order decay coefficient, μ^E	0	0	0	0	0	0
Effective pore volume PV_e, ml	612	637	616	621	636	834
Measured porosity, n	0.31	0.34	0.39	0.31	0.34	0.39
Fitted porosity, n_e	0.32	0.33	0.32	0.33	0.33	0.44
Fitted longitudinal dispersivity α_L, cm	0.699	0.680	0.289	0.59	0.56	0.531
Adjusted R^2	0.837	0.925	0.922	0.872	0.881	0.874

5.3.2 Transport of contaminant SMX.

The concentrations of SMX in effluent were monitored over time. The breakthrough curves of SMX in the three soil columns are presented in figure V-6. The normalized SMX concentrations were plotted against the effective pore volumes derived from the fitted results of bromide breakthrough curves. The concentration of SMX in the effluent samples at step 1 was below detection limit of liquid chromatography-mass spectrometry (LC-MS), and thus no plots were generated for step 1.

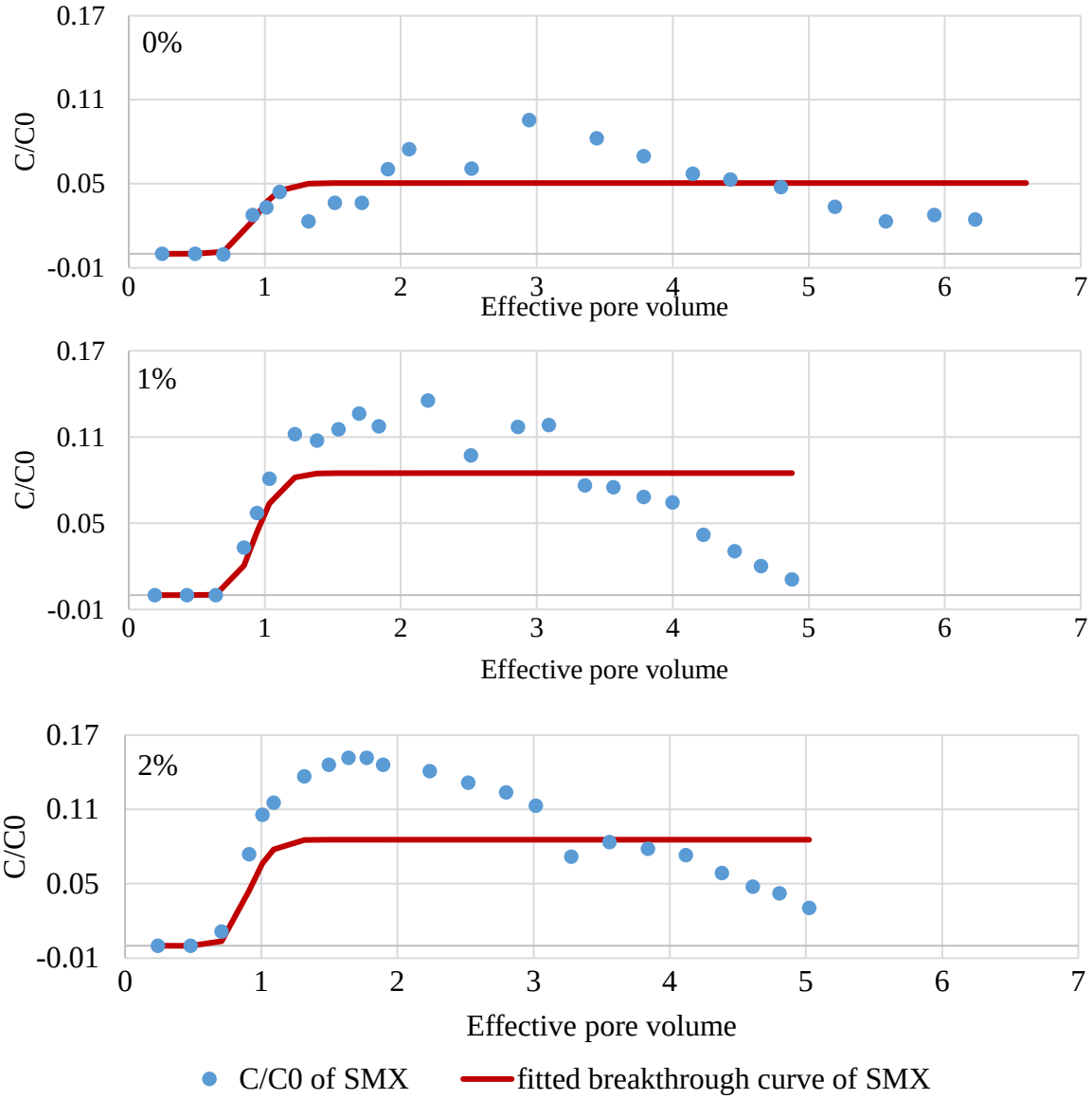

Figure V-6. Normalized breakthrough curves (C/C_0) of conservative tracer bromide at step 2 of high loading rate.

SMX was detected in the effluent for the three columns in step 2, but it was still at much lower concentrations than expected (figure V-6). The highest SMX concentration was observed in 2 % column and the lowest concentration was observed in 0 % column. The SMX concentrations in all the three columns started to decrease after a maxima was reached. Hebig et al. (2017) also observed the SMX decrease before the decrease of conservative tracer in a column filled with sand of high organic carbon fraction.

SMX was strongly degraded in the soil columns in this project. The SMX had previously been reported to be persistent in soil soils (Godfrey et al. 2007; Ternes et al. 2007; Gruenheid et al. 2008; Chen et al. 2011; Muller et al. 2013), which was not consistent with the results of our investigation. However, for a number of investigations, remarkable degradation was reported in saturated columns and microbial activities were believed to play an important role(Baumgarten et al. 2011; Banzhaf and Hebig 2016; Hebig et al. 2017).

The changes of nitrate, total ammonia and sulfate in effluent flows were also monitored to provide some insight into the redox condition for the three columns (figure V-7).

The concentrations of sulfate were reduced by over 90 % after column treatment. Removal of sulfate could resulted from precipitation with cations and reduction reaction by microorganism. Among the exchangeable cations of the soil used in this project, the cation that was high in concentrations and could precipitate with sulfate was calcium. However, the total exchangeable calcium was too low to maintain a sulfate concentration as low as 500 ppb for the whole operation (detailed calculation could be found in appendix J). Therefore, we think a sulfate-reducing condition was developed in column and caused the sulfate reduction as shown in figure V-7b. SMX degradation was expected in nitrate-reducing and sulfur-reducing conditions, through bacterial-assisted abiotic processes, which was in agreement with the results of our batch experiments on biodegradation in chapter III (Banzhaf et al. 2012; Nodler et al. 2012). In addition, a purple color was developed in the effluent tubing during the operation. This purple phenomenon is likely caused by the blooming of purple sulfur bacteria, which could reduce sulfate in anoxic condition (Belila et al. 2013).

The nitrate concentration of the solutions also decreased after column attenuation, suggesting that a nitrate-reducing condition exists in the columns. The reduction of nitrate could involve

denitrification and nitrate ammonification. Total ammonia was also reduced in the effluent and it slowly restored to its influent value at step 2. The reduction of ammonia could have resulted from cation exchanges of ammonium. The exchangeable cations of the soil were presented in appendix J, which were low compared to total ammonium in wastewater. With the continuous feeding of influent, fewer exchangeable sites may have been available as time progressed, until the sites became completely saturated, leading to the slow recovery of total ammonia in the effluent. Since the nitrate concentration was smaller than the changes of total ammonia by two orders of magnitude, nitrate ammonification was an insignificant contributor, if it occurred, to the ammonia recovery.

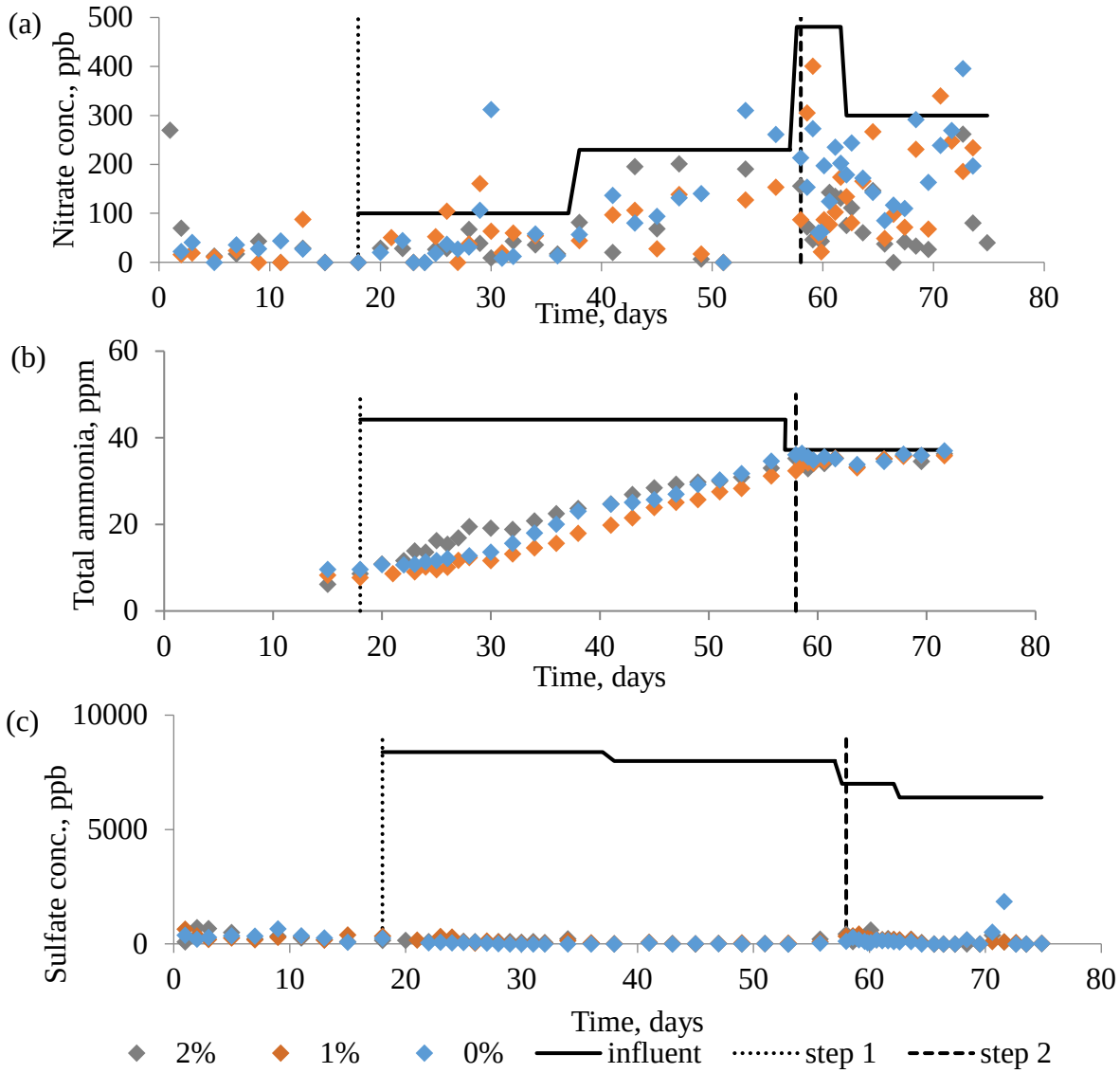

Figure V-7. Effluent concentrations of nitrate, total ammonia, and sulfate.

Apart from the redox condition of the column and microorganisms (which could not investigated in the study), dissolved organic carbon (DOC) in aqueous phase and the fraction of organic carbon (f_{OC}) in soil had also been reported to contribute to SMX degradation (Baumgarten et al. 2011; Banzhaf et al. 2012; Hebig et al. 2017). The septic effluent used in this study was enriched with DOC (46 ppm) and the f_{OC} of the soil was measured to be 0.75 %. Hebig et al. (2017) reported only 31 % and 5 % mass recoveries for sands of f_{OC} equals 0.06 % and 5 %, respectively. Therefore, high DOC and f_{OC} could foster the degradation of SMX by supporting microbial activity.

To summarize, the SMX was strongly degraded in the soil column. The analysis of the column properties suggests that a biodegradation favored environment was established within the soil columns. The redox conditions (nitrate-reducing and sulfate-reducing) in the columns supported SMX biodegradation, as found in biodegradation batch experiments discussed in chapter III. The soil f_{OC} and influent DOC could benefit the degradation by fostering microbial activity. The higher degradation observed in step 1 than in step 2 was very likely due to a longer resident time at the lower loading rate (Langner et al. 1998; Haest et al. 2011).

5.3.3 Modeling of the transport of SMX.

Since no SMX was detected in step 1, modeling analysis was only applied to the data in step 2. The fitted α_L values from the modeling of bromide breakthrough curves were used as a constant for the modeling of SMX breakthrough curves. The fitted results of retardation factor R and the dimensionless first-order decay coefficient μ^E can be found in table V-4.

The CDE model with constant μ^E didn't describe the feature of the breakthrough curve of SMX in step 2 (figure V-5). The constant μ^E assumption resulted in curve plateaus for all the columns. However, the SMX concentration decreased after reaching the maximum value. As a result, low adjusted R^2 values were obtained for all the cases (table V-4). This inconsistency was rooted in the assumption of steady-state flow, where the velocity doesn't change overtime. However, a decrease of flow was observed at step 2, probably due to the clogging of the columns (figure V-3). As $\mu^E = L\mu/v$, decreases in velocities would result in the increase of μ^E, which matched with the reduction of SMX concentrations in the breakthrough curve.

Table V-4. Transport parameters determined by fitting of the breakthrough curves of SMX. R_{batch} was calculated with the K_d values from batch experiments in chapter IV. R_{batch} was calculated with the K_d values from batch experiments in chapter IV; μ_{fitted} was calculated using by the definition of dimensionless equation ($\mu^E_{fitted}=L\mu_{fitted}/v$), where L is column length, v is pore velocity (=initial loading rate at step 2 /fitted porosity n^e); μ_{batch} was the first-order coefficient estimated using the degradation data in the chapter III. The influence of small amount of biochar on biodegradation was assumed negligible. $C_{estimated\ for\ step\ 1}$ was calculated for the SMX concentration at the effluent during step 1 assuming the same first order decay as step 2 (=$C_0\ e^{-\mu_{fitted}L/v}$).

	0%	1%	2%
R_{batch}	2.43	6.35	9.94
R_{fitted}	1.0	1.0	0.96
μ^E_{fitted}	3.09	2.53	2.52
$\mu_{fitted,\ d}{}^{-1}$	1.31	1.08	1.03
$\mu_{batch,\ d}{}^{-1}$	0.0453	0.0453	0.0453
Adjusted R^2	0.547	0.450	0.417
$C_{estimated\ for\ step\ 1}$, ppb	0.06	0.26	0.48

In addition, the fitted first-order decay coefficients (μ^E) were not consistent with the estimated values from batch experiments in chapter III. The fitted μ^E values were higher than the estimated values by two orders of magnitude. Complete removal of SMX was observed in the three columns in step 1, which was not expected with the estimation from batch experiments.

As discussed in section 5.3.2, biodegradation was contributing to the removal of SMX in the soil columns, which was supported by the non-zero value of dimensionless first-order decay coefficient. The higher value of μ^E in columns due to the limitation of constant assumption. The actual μ^E was expected to change with the growth of microorganisms in the columns. An advanced CDE equation (equation 5.6) could be developed by incorporating the logistic model (equation 5.5) describing microbial growth (Langner et al. 1998).

$$\frac{dX}{dt} = k_L c_r X \tag{5.5}$$

$$R\frac{\partial c_r}{\partial t} = D\frac{\partial^2 c_r}{\partial x^2} - v\frac{\partial c_r}{\partial x} - \frac{k_L X}{Y}c_r \quad (5.6)$$

where X [ML^{-3}]is the microbial biomass, Y is the yield of compounds converted to biomass during biodegradation and k_L is the logistic rate constant. Therefore, μ is related to biomass X by $\mu = (k_L/Y)X$.

The different experiment designs between batch and column experiments could result in big differences in microbial biomass. First, there was a longer time span in column experiment than batch reactions. The acclimation times for the columns were twice as those in batch experiments, which allows more time for microbial growth. Second, the amount of soil used in the column was larger than that in batches by a factor of 50. Results in chapter III showed soil was the major contributor for the biodegradation in the system. Larger amount of soil could enhance the biodegradation by providing more sites for biomass growth on solid phase. Third, the experiment period in column experiments were much longer than batch experiments, allowing more biomass accumulating with columns. As a result, biomass was observed during the acclimation period in the aqueous layer at the top and in the effluent tubes at the bottom, which was never seen in batch experiments.

Moreover, the fitted values of retardation factor R didn't agree with the data estimated from batch experiment in chapter IV (table V-4). SMX was expected to retard in the columns with highest retardation in the 2 % column and lowest in the 0 % column. However, the elution of SMX was detected almost at the same time as the conservative tracer bromide in all the three columns and no retardation occurred based on fitted R values. As found in chapter IV, high DOC of the aqueous phase could inhibited the SMX adsorption through competition and pore blocking. With the increased amount of soil and enhance growth of biomass in the columns, an even more sever inhibition was expected for SMX adsorption. With the 40 days of feeding of septic effluent, consists of high contents of organic and inorganic compounds, the adsorption sites could be saturated, leading to no adsorption of SMX in step 2. The concentrations of SMX in the effluent at low flowrate were calculated for the three columns by assuming a same first order decay coefficient μ as that of the high flowrate. The estimated concentrations were less than 1 ppb, which were below the detection limit (4.01 ppb), and is consistent with our observations.

Therefore, the design of column experiment indicated that the biodegradation was the dominant process during the SMX transport in soil columns. The contribution of the limited adsorption was insignificant and not observed during step 1. The large amount of filtered solutions during the long operation time could result in the saturation of adsorption sites, leading to no retardation of SMX at step 2.

5.4 Conclusions

SMX has be considered as a compound of emerging concerns with occurrences frequently reported in the environment. Biodegradation and adsorption were considered to be the two main processes for SMX removal in the subsurface. Limited adsorption on soil was found to be enhanced with the amendment of a green and cost-effective adsorbent, biochar. The objectives of this study were to understand the contribution of biodegradation and adsorption to the SMX transport and to assess the effectiveness of biochar amendment in the soil columns.

Biodegradation was found to be the dominant process for SMX transport in saturated column. The anoxic conditions (nitrate-reducing and sulfate-reducing) developed in the columns supported the bacteria-assisted degradation of SMX. The high organic carbon content in soil and solution, as well as the design of the column experiment (with large soil amounts and long operation times) could enhance biodegradation by benefiting microbial growth and accumulation. Adsorption could be inhibited with long-term operation and became a minor factor for SMX transport.

The breakthrough curves of the columns appeared to similar and closely fitted results were obtained from the models. However, no statistical conclusion could be drawn due to the low elute concentrations of SMX and lack of replicates. Future work is needed to: (1) get good fit of the SMX breakthrough curve, (2) address the effects of biochar amendments, and (3) expand the application of the finding to other soil textures and wastewater types. To improve the fit to the breakthrough curve, a new model needs to be developed that incorporates a more advanced approach than model used for this analysis. This model may include a more advanced analysis of the first-order decay coefficient (e.g. with consideration of velocity and microbial biomass) or a Michaelis-Menton approach. In addition, column replications could be conducted to enable the statistical analysis. To make the effect of adsorption can be evaluated,

biodegradation inhibitors could be added to reduce the SMX degradation, such that retardation factor could be modeled.

The column study was not very successful in assessing the effectiveness of biochar amendments, but the findings still provide useful information for understanding the effect of biodegradation and adsorption to SMX transport in the subsurface. Since the heavy wastewater of septic effluent was used in this study, these findings could have direct relevance to the practices such as septic systems, livestock farming and irrigation of treated wastewater.

References

Banzhaf, S. and Hebig, K. H. (2016). "Use of column experiments to investigate the fate of organic micropollutants - a review." *Hydrology and Earth System Sciences* 20(9), 3719-3737.

Banzhaf, S., Nodler, K., Licha, T., Krein, A. and Scheytt, T. (2012). "Redox-sensitivity and mobility of selected pharmaceutical compounds in a low flow column experiment." *Science of the Total Environment* 438, 113-121.

Barnes, K. K., Kolpin, D. W., Furlong, E. T., Zaugg, S. D., Meyer, M. T. and Barber, L. B. (2008). "A national reconnaissance of pharmaceuticals and other organic wastewater contaminants in the United States - I) Groundwater." *Science of the Total Environment* 402(2-3), 192-200.

Baumgarten, B., Jaehrig, J., Reemtsma, T. and Jekel, M. (2011). "Long term laboratory column experiments to simulate bank filtration: Factors controlling removal of sulfamethoxazole." *Water Research* 45(1), 211-220.

Belila, A., Abbas, B., Fazaa, I., Saidi, N., Snoussi, M., Hassen, A. and Muyzer, G. (2013). "Sulfur bacteria in wastewater stabilization ponds periodically affected by the 'red-water' phenomenon." *Applied Microbiology and Biotechnology* 97(1), 379-394.

Chen, H., Gao, B., Li, H. and Ma, L. Q. (2011). "Effects of pH and ionic strength on sulfamethoxazole and ciprofloxacin transport in saturated porous media." *Journal of Contaminant Hydrology* 126(1-2), 29-36.

Focazio, M. J., Kolpin, D. W., Barnes, K. K., Furlong, E. T., Meyer, M. T., Zaugg, S. D., Barber, L. B. and Thurman, M. E. (2008). "A national reconnaissance for pharmaceuticals and other organic wastewater contaminants in the United States - II) Untreated drinking water sources." *Science of the Total Environment* 402(2-3), 201-216.

Godfrey, E., Woessner, W. W. and Benotti, M. J. (2007). "Pharmaceuticals in on-site sewage effluent and ground water, western Montana." *Ground Water* 45(3), 263-271.

Gruenheid, S., Huebner, U. and Jekel, M. (2008). "Impact of temperature on biodegradation of bulk and trace organics during soil passage in an indirect reuse system." *Water Science and Technology* 57(7), 987-994.

Haest, P. J., Philips, J., Springael, D. and Smolders, E. (2011). "The reactive transport of trichloroethene is influenced by residence time and microbial numbers." *Journal of Contaminant Hydrology* 119(1-4), 89-98.

Hebig, K. H., Groza, L. G., Sabourin, M. J., Scheytt, T. J. and Ptacek, C. J. (2017). "Transport behavior of the pharmaceutical compounds carbamazepine, sulfamethoxazole, gemfibrozil, ibuprofen, and naproxen, and the lifestyle drug caffeine, in saturated laboratory columns." *Science of the Total Environment* 590, 708-719.

Kolpin, D. W., Furlong, E. T., Meyer, M. T., Thurman, E. M., Zaugg, S. D., Barber, L. B. and Buxton, H. T. (2002). "Pharmaceuticals, hormones, and other organic wastewater contaminants in US streams, 1999-2000: A national reconnaissance." *Environmental Science & Technology* 36(6), 1202-1211.

Langner, H. W., Inskeep, W. P., Gaber, H. M., Jones, W. L., Das, B. S. and Wraith, J. M. (1998). "Pore water velocity and residence time effects on the degradation of 2,4-D during transport." *Environmental Science & Technology* 32(9), 1308-1315.

Muller, E., Schussler, W., Horn, H. and Lemmer, H. (2013). "Aerobic biodegradation of the sulfonamide antibiotic sulfamethoxazole by activated sludge applied as co-substrate and sole carbon and nitrogen source." *Chemosphere* 92(8), 969-978.

Nodler, K., Licha, T., Barbieri, M. and Perez, S. (2012). "Evidence for the microbially mediated abiotic formation of reversible and non-reversible sulfamethoxazole transformation products during denitrification." *Water Research* 46(7), 2131-2139.

Schulze-Makuch, D. (2005). "Longitudinal dispersivity data and implications for scaling behavior." *Ground Water* 43(3), 443-456.

Tang, G. P., Mayes, M. A., Parker, J. C. and Jardine, P. M. (2010). "CXTFIT/Excel-A modular adaptable code for parameter estimation, sensitivity analysis and uncertainty analysis for laboratory or field tracer experiments." *Computers & Geosciences* 36(9), 1200-1209.

Ternes, T. A., Bonerz, M., Herrmann, N., Teiser, B. and Andersen, H. R. (2007). "Irrigation of treated wastewater in Braunschweig, Germany: An option to remove pharmaceuticals and musk fragrances." *Chemosphere* 66(5), 894-904.

Tian, Y. A., Gao, B., Silvera-Batista, C. and Ziegler, K. J. (2010). "Transport of engineered nanoparticles in saturated porous media." *Journal of Nanoparticle Research* 12(7), 2371-2380.

Toride, N., J. Leij, F. and Van Genuchten, M. (1995). The CXTFIT Code for Estimating Transport Parameters from Laboratory or Field Tracer Experiments.

Chapter VI. Conclusions and Future Work

5.1 Conclusions

The ubiquitous occurrence of antibiotics in the environment poses threats to humans and to the environment. The commonly used antibiotic, sulfamethoxazole (SMX), is believed to be persistent in the subsurface. Biodegradation and adsorption have been considered to be the two main processes governing the natural attenuation of SMX in the subsurface. However, SMX generally shows weak affinity to soils, and the biodegradation rate of SMX has been found to be low and highly variable depending on in-situ conditions in the subsurface. The purpose of this thesis was to improve our understanding of these processes.

This thesis evaluated the soil remediation of SMX in septic effluent in terms of biodegradation and adsorption. Nutrient and matrix effects were evaluated under aerobic and anoxic conditions for the biodegradation of SMX in soil/wastewater systems (chapter III). The effectiveness of the use of biochar amendments in soils was assessed for SMX adsorption (chapter IV). The analyses included assessment of the influence of biochar production conditions, pyrolysis temperature and feedstock types in relation to SMX adsorption. Finally, the one-dimensional transport of SMX in the subsurface was estimated in soil column studies. Adsorption and degradation contributions to SMX transport was analyzed using the breakthrough curve fitting code CXTFIT, which was based on convective-dispersive equation that incorporates the effects of retardation and first order decay (chapter V).

The major results from the biodegradation experiments (chapter III) are as follows:

1. Under aerobic conditions, SMX degradation was enhanced by DOC addition but was not affected by ammonia and sulfate addition. Under nitrate reducing conditions, SMX degradation was not influenced by the addition of ammonium and sulfate. SMX degradation was likely heterotrophic and could be co-metabolized with DOC. However, the nitrifying bacteria may be non-degraders for SMX. (chapter III)

2. SMX was persistent in wastewater and the highest degradation was achieved for wastewater in soil systems. Soil was the main contributor for SMX dissipation by

providing DOC for aerobic conditions and creating a stronger reducing condition (a sulfate-reducing condition) for the anoxic experiments. (chapter III)

The major results from the soil and biochar sorption experiments (chapter IV) are as follows:

1. Cu, Fe and SMX were effectively removed by biochar, while nutrients (N and P compounds), the heavy metal Zn, and exchangeable cations were not significantly affected. (chapter IV)
2. Both the Freundlich model and linear model provided a good fit to SMX sorption on biochars. The R^2 values for Freundlich model were slightly higher than for the linear model. However, linear adsorption was recommended for the purposes of quick estimation in practice. (chapter IV)

3. A biochar amendment could enhance the overall removal of SMX from septic effluent. Dissolved organic carbon in wastewater and from soil leachate could also inhibit SMX adsorption by biochar, probably due to competition and blocking effects. (chapter IV)

4. Improved SMX adsorption was obtained with an increased pyrolysis temperature and the highest removal was obtained with pine sawdust-derived biochar. (chapter IV)

5. The different production conditions led to variations in physicochemical properties of biochars. Adsorption coefficients showed weak correlation with pH and metallic content of the biochars. However, moderate correlation was achieved between adsorption coefficients and I_V/I_D and I_D/I_G values from Raman spectroscopy, suggesting the important effect of the structural evolution of aromatic region on SMX adsorption. It was thus concluded that π-π interactions between biochar and SMX could be one major mechanism for SMX removal from septic effluent. (chapter IV)

The major results from the column experiments (Chapter V) are as follows:

1. Measured SMX concentrations were lower than expected based on the batch results. Biodegradation was found to be the dominant process for SMX transport in the saturated column. The anoxic conditions (i.e. nitrate-reducing and sulfate-reducing conditions) developed in the columns supported the bacteria-assisted degradation of

SMX. The high organic carbon content in soil and solution, as well as the design of the column experiment (which included a large soil amount and long operation time) could enhance biodegradation by benefiting microbial growth and accumulation. Adsorption could be inhibited after a long-term operation and was found to be a minor factor for SMX transport for the column experiment.

2. The breakthrough curves appeared to similar among the columns with different biochar content. The constant first order decay coefficient failed to provide a good fit to SMX data. No statistical comparison could made between columns due to the low effluent concentrations of SMX and the lack of replicates.

5.2 Future work

Detailed next steps for the batch degradation study, batch adsorption study and soil column study were discussed at the end of each chapter. Future work for the study from a broader perspective is included here.

The conclusions drawn from the results of this thesis showed importance of biodegradation for the SMX attenuation in the subsurface. Therefore, the recommend future studies would include

1. the analysis and determination of the biodegradation intermediates to understand the degradation pathways from the perspective of SMX transformation
2. the analysis of bacterial growth and identification of microorganisms to understand the biodegradation from the perspective of microbiology

The research in this thesis provides a basis for these and other future investigations to characterize the transport of SMX in the environment.

Appendix A. Characterization of the soil sample.

Table A-1. Characterization of soil sample, standard deviation was calculated for a sample volume of 3.

Properties	Average ± SD
pH [a]	7.96±0.02
Water content [b], %	7.8±0.2
Fraction of organic carbon [a], %	0.755±0.006
Particle density [c], g/ml	2.64±0.004
D60, mm	0.55
D30, mm	0.30
D10, mm	0.14
C_u	3.9
C_c	1.2
Liquid limit [d], LL	39.0
Plasticity Index [d], PI	7.90
Soil classification (USCS)	SP-SM, poorly grained sand with silt
Exchangeable cation, with nitric acid digestion, ppm	
Na	381±101
Mg	1886±364
Al	6541±921
Ca	2182±299
K	837±403
Fe	68174±892
Cr	12±2
Ni	8.1±0.9
Cu	12±5
Zn	8.6±8.4
As	8.6±3.6
Cd	0.07±0.02

Table A-1. Continued

Exchangeable cation with 1N ammonium acetate extraction at pH =7[a], ppm	
Na	11.1±2.1
Mg	16.7±1.1
Al	6.9±4.2
Ca	1127.7±8.1
K	23.2±1.2
Fe	4.7±2.3

[a.] method reference: Recommended Chemical Soil Test Procedures for the North Central Region (Brown 1998).

[b.] Standard method ASTM D2216-10.

[c.] Adapted from standard method ASTM D854-14

[d.] Atterberg limits test. Standard test method ASTM D4318-17

Appendix B. Experiment procedure and analytical analysis

B1. Biodegradation experiment in aerobic condition

70 g of soil was weighed into 250 ml glass amber bottles to reach a soil layer of 2 cm in depth. 150 ml of filtered wastewater was measured using graduated cylinder and added. A headspace of air was remained.

The bottles were capped and inverted vigorously to mix the soil with wastewater. Two needles were inserted into the headspace of each bottle to facilitate air exchange. The experiment setup was shown in figure B1-1.

Figure B1-1. Experiment setup for aerobic removal of SMX.

The systems were acclimated for one week. Each sample was then spiked with desired volume of solutions according to table A1-1. System pH was measured after mixing. The preparation of stock solutions was summarized in table A1-2. The concentrations of the ammonia, sulfate and DOC, and SMX stock solutions were verified using UV-vis spectrometer, IC, TOC analyzer and LC-MS, respectively.

Table B1-1. Experiment design for biodegradation removal of SMX

Sample	Soil, g	Aqueous phase	Volume of aqueous phase, ml	Volume of 100 ppm SMX spiked, ml	Other nutrients spiked
WW blank	70	WW	150	0	-
WW only	0	WW	150	0.75	-
WW + soil	70	WW	150	0.75	-
WW + NaN_3	70	WW	150	0.75	3 ml NaN_3 stock solution
Soil only (DI)	70	DI	150	0.75	-
DI+NH3	70	DI	150	0.75	0.75 ml of ammonia stock solution
DI+SO4	70	DI	150	0.75	0.5 ml of sulfate stock solution
DI+DOC	70	DI	150	0.75	1 ml of DOC stock solution

Table B1-2. Preparation of stock solutions for degradation experiment

Stock solution	Target concentration	Chemical	Formula weight, g/mol	Weight of chemical, g	Volume, ml
SMX stock	100 ppm SMX	Sulfamethoxazole	253.38	0.020	100
Ammonia stock	6000 ppm NH_3	NH4Cl	53.49	944.2	50
Sulfate stock	900 ppm sulfate	Na_2SO4	142.04	69.4	50
DOC stock	3000 ppm DOC	NaAc·3H2O	136.08	849.8	50
NaN_3 stock	1% NaN_3	NaN3	65.01	1.000	100

After one hour of settlement, 0.5 ml of sample were collected and diluted to 50 ml for further analysis of anion, DOC, total ammonia. Subsequent samples were taken at day 3, 5, 9, 18. Before each sampling, systems were mixed and settled for one hour. After each samples, the system was purged with air and mixed again. After the last sample of day 18, final pH values of the systems were measured again.

B2. Biodegradation experiment in anoxic condition

70 g of soil and 150 ml of filtered wastewater were added to 250 ml glass amber bottles. The bottles were capped and inverted vigorously to mix the soil with wastewater.

A bottle was half filled with water and N_2 gas was moisturized after flowing though the the water layer by inserted needle. After purging for two hours, the headspace water filled with moisturized N_2, which was then introduced to all the sample bottles through syringe needles inserted into aqueous phase of each bottle. The gas flows existed the systems through the water seal created by the water in the Erlenmeyer flask. The experiment setup was shown in figure B2-1.

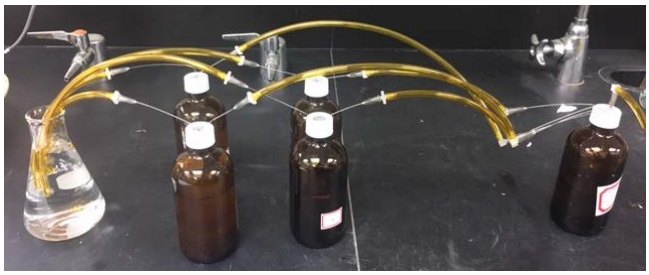

Figure B2-1. Experiment setup for anoxic removal of SMX.

The whole system was purged with N_2 for one hour to achieve an N_2 environment, which was then maintained with continuous N_2 at slow flowrate. The systems were acclimated for one week before spiking of desired solution according to table B1-1. After mixing, the pH values of all the samples were measured at high N_2 flowrate, and the systems were purged for another hour after the measure.

Samples were collected at day 0, 3, 5, 9, 18. Before each sampling, systems were mixed and settled for one hour. 0.5 ml of sample were withdrawn from each bottle using syringes and

then diluted to 50 ml for further analysis of anion, DOC, total ammonia. After each sampling, the system was sealed by applying a layer of vacuum grease and was purged with N_2 at high flowrate for an hour. Final pH values of the systems were measured again after the last sample of day 18.

B3. Adsorption experiment

100 ml of filtered wastewater was spiked with desired volume of 200 ppm SMX stock solution to achieve the designed concentration (table A3-1). 30 ml of the solutions were then added into 45 ml amber glass bottles.

Table B3-1.Preparation for SMX solutions in WW.

Desired concentration, ppb	50	100	200	400	800	1000
final volume, ml	100	100	100	100	100	100
Volume of stock solution, ml	0.025	0.05	0.1	0.2	0.4	0.5

Desired amounts of sorbents were weighed into each sample bottle. Detailed weights were as follows

- 10 g for soil;
- 0.1 g for commercial biochar and lab-engineered biochar prepared at 350 ◦C;
- 0.01 g for commercial activated carbon and lab-engineered biochar prepared at 500 ◦C.

The sample bottles were continuously mixed using the rotator shown in figure A3-1 for a certain period of time. Experiment design was summarized in table A3-2.

Figure B3-1. Rotator used for SMX sorption experiment.

Table B3-2. Experiment design for SMX sorption.

Experiment type	Sorbent	Sampling time, hours
isotherms	soil	72
	biochars	48
	Activated carbon	24
kinetics	Soil	4, 8, 12, 24, 48, 72, 96, 132, 144
	Biochars	0.25, 0.5, 0.75, 1, 1.5, 2, 2.5, 3, 4, 5, 6, 8, 10, 12, 16, 20, 24, 32, 40, 48, 68, 87, 161
	Activated carbon	0.25, 0.5, 0.75, 1, 1.5, 2, 3, 4, 6, 8, 12, 16, 20, 2

The sample bottles were centrifuged at 2350 rpm for 8 min. The aqueous phase were then decanted into 5 ml syringes and filtered through 0.45 µm filters. The resulted solutions were analyzed using methods described in Appendix B. for SMX and other constituents.

B4. Analysis of total ammonia

Total ammonia was analyzed with HACH DR3900 UV-vis spectrometer at the wavelength of 425 nm (figure B4-1).

Figure B4-1. UV-vis spectrometer used for the analysis of total ammonia and total phosphors.

Standard solutions

Standard solutions were prepared with HACH 100 ppm ammonia standard solution, according to table B4-1

Table B4-1. Preparation of standard solutions for total ammonia

Standard	1	2	3	4	5	6
Volume of stock solution, ml	0.1	0.3	0.5	1.0	3.0	5.0
final volume, ml	100	100	100	100	100	100
Desired concentration, ppm	0.1	0.3	0.5	1.0	3.0	5.0

Analysis

All the aqueous samples were filtered through Whatman No. 4 filter paper. A volume of 25 mL of filtered solution was added to glass cell, followed by 3 drops of mineral stabilizer, 3 drops of polyvinyl alcohol dispersing agent and 1 mL of Nessler reagent. After each addition of reagent, the test cell was capped with rubber stopper and inverted several times to mix the solution completely. The resulted solution was analyzed after 1 min of reaction time.

The adsorption of blank solution (DI water) was analyzed and zeroed. Adsorption of standard solutions and samples were analyzed and recorded. The total ammonium of samples were calculated from the calibration curved produced from the standard solutions.

Representative calibration curve

Standards were analyzed before every sample sequence. The total ammonia was calculated based on the function developed from the calibration curve. A representative calibration curve for total ammonia analysis was shown in figure B4-2

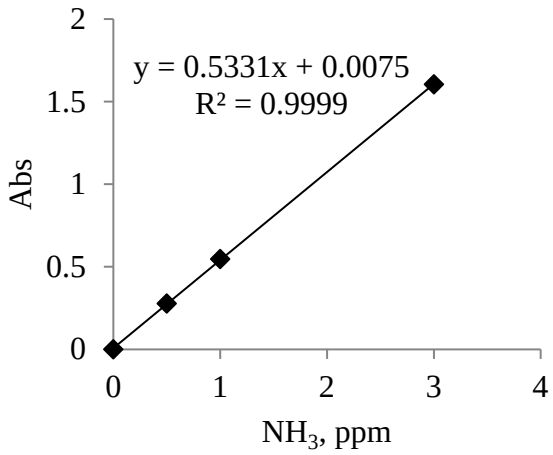

Figure B4-2. Representative calibration curve of total ammonia analysis using UV-vis spectrometer.

B5. Analysis of total phosphors

Total phosphors of samples was determined using HACH DR3900 UV-vis spectrometer at the wavelength of 400 nm (figure B4-1). Two blank solutions, standard solutions and sample solutions were digested and analyzed following the same procedure described as follows.

Standard solutions

Standard solutions were prepared with HACH 100 ppm phosphate standard solution, according to table B5-1.

Table B5-1. Preparation of standard solutions for total phosphors

Standard	1	2	3	4	5	6
Volume of stock solution, ml	0.1	0.2	0.5	1.0	2.0	3.0
final volume, ml	100	100	100	100	100	100
Desired concentration, ppm	0.1	0.2	0.5	1.0	2.0	3.0

Acid digestion

A volume of 25 ml wastewater was digested in 100 ml beaker with 5 ml of concentrated nitric acid and 1 ml of concentrated sulfuric acid. The mixed solution was heated on hot plate for

hours to concentrate down to about 1 ml. Use flame to further concentrate the solution until fume forms.

Cool down the solution and add 3 drops of H_2O_2. The solution was heated again to initiate the reaction and get rid of the excess of H_2O_2.

Analysis

The resulted solution was filtered with Whatman No. 4 filter paper. The beaker and filter paper were rinsed with DI water three times. All the solutions and rinsing water were collected in 25 ml vial.

To the 25 ml vial, 1 drop of phenolphthalein was added. The solution was neutralized by adding 6.25 N NaOH dropwise until the solution turned pink.

Dilute the resulted solution with DI water to the 25 ml line of the vial. 1 ml of Molybdovanadate was added. The UV-vis absorbance was analyzed after 3 min of reaction time at 400 nm.

Representative calibration curve

Standards were analyzed before every sample sequence. The total phosphors was calculated based on the function developed from the calibration curve. A representative calibration curve for total phosphors analysis was shown in figure B5-1,

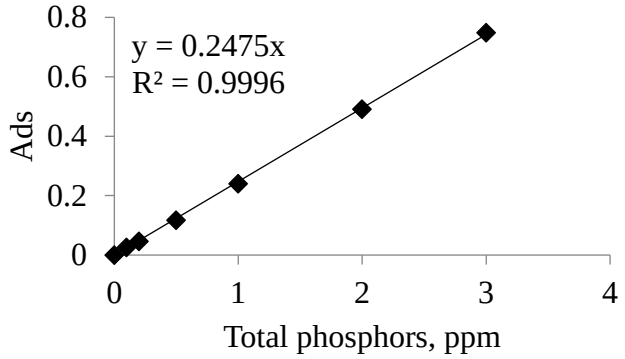

Figure B5-1. Representative calibration curve of total phosphors analysis using UV-vis spectrometer.

B6. Analysis of dissolved organic carbon

Dissolved organic carbon (DOC) was analyzed using Shimadzu TOC 5000A equipped with ASI-5000A autosampler (figure B6-1).

Figure B6-1. TOC analyzer used for DOC analysis

Standard solutions

Standard solutions were prepared from potassium hydrogen phthalate (KHP). KHP was dired in oven at 105 °C for 30 min and then cooled in dessicator for 20 min before use. 1000 ppm KHP stock solution was prepared with 0.5314 g of dried KHP dissolved to 250 ml using DI water. The stock solution was stored at 4 °C before use. It was dsicared after 3 weeks.

Working standards was prepared right before each analysis according to table B6-1. 6 N HCl was used to adjust the solution pH below 2. Calibration Curves were generated at the beginning of each sequence.

Table B6-1. Preparation of standard solutions for dissolved organic carbon

Standard	1	2	3	4
Volume of stock solution, ml	0	0.2	0.5	0.8
6N HCl, ml	0.1	0.1	0.1	0.1
final volume, ml	100	100	100	100
Desired concentration, ppm	0	2	5	8

Configuration details

- Carrier gas: compressed air
- Carrier gas pressure: 4.5 kgf/cm^2
- Carrier gas flowrate: 150 mL/min
- Sparge gas flowrate: 100 mL/min
- Purge time: 3 min
- Injection volume: 66 µL
- Furnace temperature: 680 ˚C

Representative calibration curve

Standards were analyzed before every sample sequence. The dissolved organic carbon was calculated based on the function developed from the calibration curve. A representative calibration curve for dissolved organic carbon analysis was shown in figure B6-2,

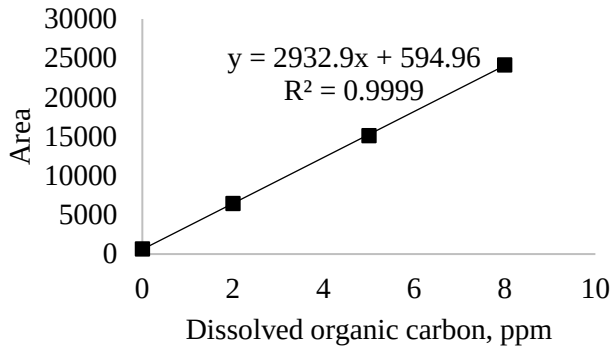

Figure B6-2. Representative calibration curve of dissolved organic carbon analysis using TOC analyzer

B7. Analysis of cations using inductively coupled plasma - mass spectroscopy (ICP-MS)

The concentrations of metallic elements in aqueous solution and acid digested soil and biochar were analyzed using ICP-MS equipped with autosampler (figure B7-1).

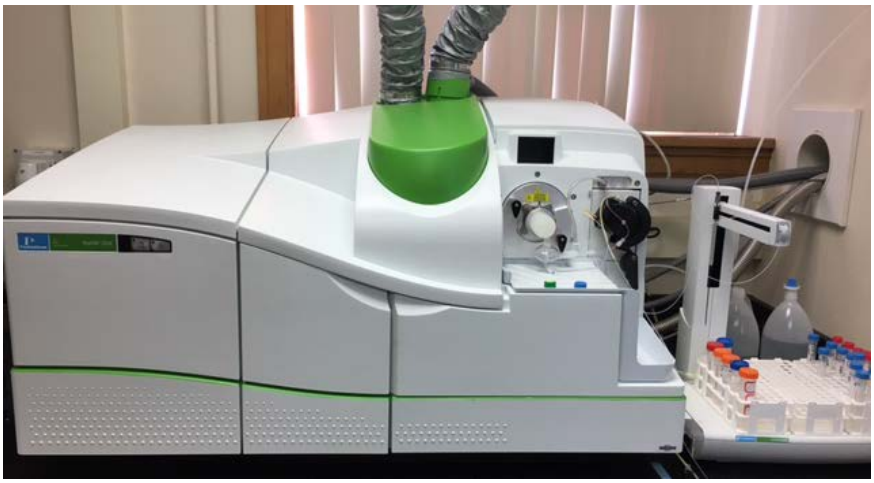

Figure B7-1. ICP-MS instrument for the analysis of metallic elements in wastewater and digested sorbents.

Standard solutions

Standard solutions were prepared with Perkin Elmer instrument calibration standard 2 solution according to table B7-1. The Perkin Elmer standard 2 solution contains 100 ppm of Ag, Al, As, Ba, Be, Ca, Cd, Co, Cr, Cu, Fe, K, Mg, Mn, Mo, Na, Ni, Pb, Sb, Se, Sn, Sr, Ti, Tl, V, Zn in 5% HNO_3 with trace tartaric acid and trace HF.

Table B7-1. Preparation of standard solutions for ICP-MS analysis

Standard	1	2	3	4	5
Volume of stock solution, ml	0.005	0.025	0.05	0.25	0.5
final volume, ml	50	50	50	50	50
Desired concentration, ppm	0.01	0.05	0.1	5.0	1.0

Acid digestion

US EPA 3050B method was used to digest sorbents for ICP-MS analysis.

One gram of sorbents were weighed into 100 ml beakers and then 10 ml of HNO_3 (1:1) solution was added. The slurry was mixed and heated on hot plate for an hour without boiling.

The solution was cooled down and 2ml of DI water and 3 ml of 30% H_2O_2 was added. Heat the solution for an hour until no effervescence was observed.

After cooling, the resulted solution was diluted to 100 ml using 100 ml volumetric flask. Samples and sample blank solutions were filtered with 0.45 µm syringe filter before analysis.

Sample solutions were further diluted 100 times for the analysis of Na, K, Ca, Mg. No dilution were performed for the analysis of Al, Fe, Mn, Zn, Cu.

Configuration details

- Sampling:
    - Sample flush: 50 sec at -48 rpm
    - Read delay: 25 sec at -20 rpm
    - Analysis: -20 rpm
    - Wash: 55 sec at -24 rpm
- Processing
    - Detector: Dual
    - Process spectral peak: average
    - Blank subtraction: after internal standard
    - Process signal profile: average
    - Apply smoothing factor = 5
    - QID: on
    - Isotope ratio mode: off
- Timing
    - 25 sweeps per reading
    - 1 reading per replicate
    - 3 replicates
    - Scan mode: peak hopping
    - Dwell time: 50 per AMU (ms)
    - RPa = 0
    - RPq = 0.25

B8. Analysis of anions using ionic chromatography system

Anion concentrations in aqueous samples including F^-, Cl^- , Br^-, SO_4^{2-}, NO_3^-, NO_2^-, PO_4^{3-} were analyzed using DIONEX ICS-2100 equipped with DIONEX 0688 AS-DV autosampler, AERS 500 anion electrolytically regenerated suppressor, CRD 200-2mm and DS6 heated conductivity cell, and controlled by a computer running DIONEX Chromeleon software (figure B8-1).

Figure B8-1. IC system for the dissolved anion analysis

Standard solutions

Desired concentration of standard solutions were prepared by diluting Dionex Seven Anion Standard II solution according to the table B8-1. The Dionex standard II solution contains 20 ppm F^-, 100 ppm Cl^- , Br^-, SO_4^{2-}, NO_3^-, NO_2^-, and 200 ppm PO_4^{3-}. Calibration Curved were generated at the beginning of each sequence.

Table B8-1. Preparation of standard solutions for IC analysis

Standard		1	2	3	4	5	6	7
Volume of stock solution, ml		0.025	0.05	0.1	0.2	0.3	0.75	1.25
Desired concentration, ppb	F^-	10	20	40	80	120	300	500
	Cl^-	50	100	200	400	600	1500	2500
	Br^-	50	100	200	400	600	1500	2500
	SO_4^{2-}	50	100	200	400	600	1500	2500
	NO_2^-	50	100	200	400	600	1500	2500
	NO_3^-	50	100	200	400	600	1500	2500
	PO_4^{3-}	100	200	400	800	1200	3000	5000

Configuration details:

- Pump Pressure: 2300 psi
- Pump Flowrate: 0.25 ml/L
- Column temperature: 30 ℃
- Column: AS153 X 250 mm
- Guard column: IonPac AG 2 x 50 mm
- Cell temperature: 35 ℃
- Delivery speed: 4.0 ml/min
- Delay volume: 125 μL
- Flush factor: 2
- Column flowrate: 1.20 ml/min
- Suppressor current: 113 mA
- Eluent generate cell: 38.00 mM KOH

B9. Analysis of SMX using liquid chromatography-mass spectrometry

Concentration of SMX were analyzed using by Agilent 1200 series liquid chromatography equipped with G1379B degasser, G1312A bin pump, G1367B autosampler, G1316A thermostatted column compartment and G130 quadrupole mass spectrometry (figure B9-1).

Figure B9-1. LC-MS instrument for the analysis of SMX concentration in aqueous samples.

Standard solutions

20 mg of SMX powder was added to a 100 ml beaker with 40 ml of DI water. The beaker was then covered by a watch glass and wrapped with aluminum foil. The solution was stirred with magnetic stir bar overnight to dissolve all the SMX.

The solution was transferred into a 100 ml volumetric flask and add DI to 100 ml. The volumetric flask was then sealed with parafilm and inverted 5 times to mix the solution. The resulted concentration of the stock solution is 200 ppm.

Desired concentration of standard solutions were prepared by dilution stock solution according to the table B9-1. Calibration Curves were generated at the beginning of each sequence.

Table B9-1. Preparation of standard solutions for LC-MS analysis

Standard	1	2	3	4	5	6
Volume of stock solution, ml	0.025	0.05	0.1	0.2	0.4	0.5
final volume, ml	100	100	100	100	100	100
Desired concentration, ppb	50	100	200	400	800	1000

Configuration details

- Injection volume: 75 μL
- Needle wash: 10 sec
- Column: Epic C18 MSO 2.3μ 150Å 5cm x 2.1mm column
- Column temperature: 30 °C
- Column flowrate: 0.300 ml/min
- Column pressure: 140-150 psi
- UV lamp: 277.16 nm with reference = 360.30 nm
- Drying gas: N_2
- Drying gas flowrate: 12.0 L/min
- Gas temperature: 350 °C
- High vacumm: ~$7.1e^{-6}$ Torr
- Nebulizer pressure: 40 psig

- Quadrupole temperature: 100 °C
- Rough vacume: ~2.55 Torr
- ESI+: single m/z = 254
- Solvent A: 0.1% formic acid
- Solvent B: 95% acetonitrile with 5% water and 0.1% formic acid
- Binary pump programing:
    - Time %B flow

Time	%B	flow
0	5	0.3
0.5	5	0.3
7	82.2	0.3
7.10	100	0.3
8.10	100	0.3
8.20	5.0	0.3
12.20	5.0	0.3

Representative calibration curve

Standards were analyzed before every sample sequence. The concentration of dissolved SMX was calculated based on the function developed from the calibration curve. A representative calibration curve was shown in figure B9-2,

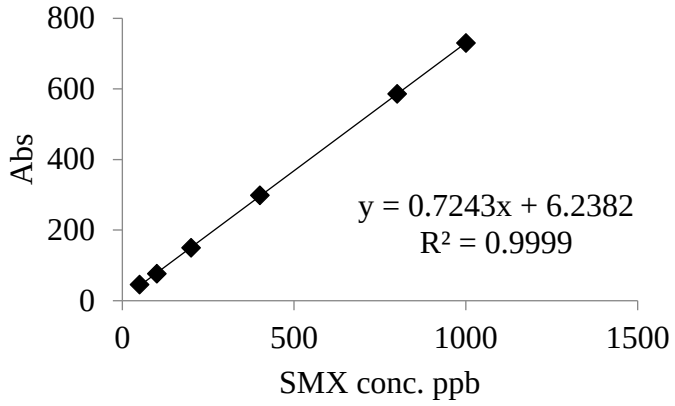

Figure B9-2. Representative calibration curve of the analysis of SMX concentrations using LC-MS. The absorbance was integrated from the spectrum at 277.16 nm. The elute time was around 6.8 min.

Appendix C. TGA data of feedstock for biochar production

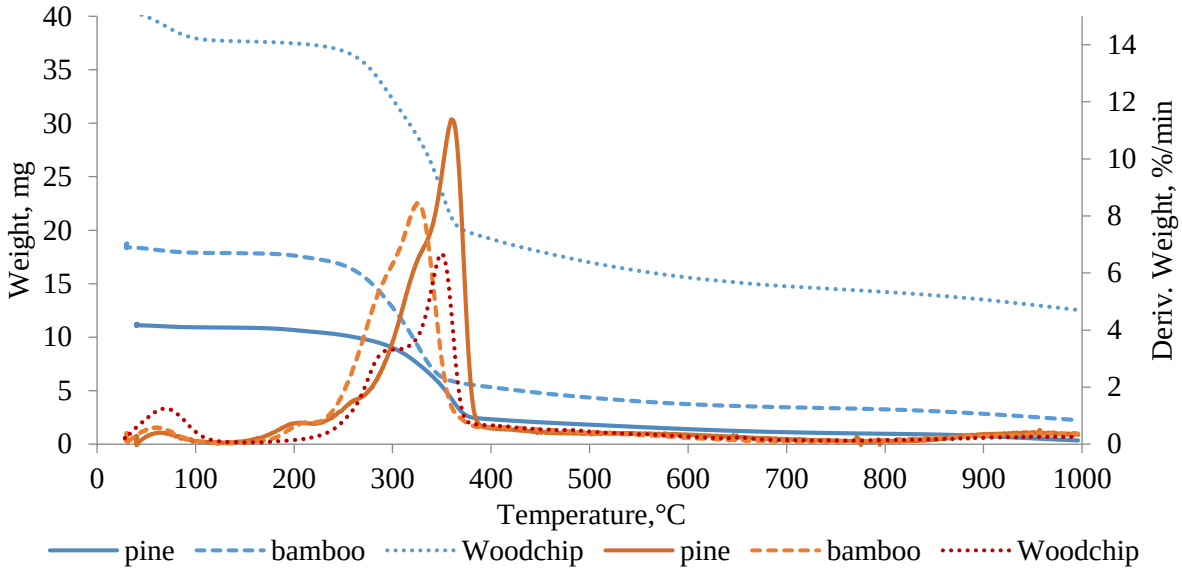

Figure C-1. TGS/DTG spectra of different types of feedstock for biochar production.

TGA/DTG measurement was taken for bamboo, pine and woodchip from 30°C to 1000°C at an increase rate of 10°C. The result is shown in figure A-III-1. The first degradation step was observed under 100°C from the three spectra due to the loss of moisture and light volatiles. Degradation of hemicellulose and cellulose was observed in the range of 200-400°C, and the peaks for pine shifted slightly to the higher temperature. Degradation of bamboo hemicellulos was in 210-300°C and cellulose in 300-360°C, while for pine sawdust hemicellulos was in 270-340°C and cellulose in 340-375°C. The following broad peak was considered to be the decomposition of lignin. Similar degradation steps were also reported by other researchers (Chaula et al. 2014; Hernandez-Mena et al. 2014). There are still several peaks unassigned so far. Those are peak of 215-260°C for pine and peak around 200°C for both pine and bamboo. Study showed that the properties of produced biochar, like pore structure, are related to the pyrolysis temperature, which were expected to be developed sufficiently at around 500 ℃ (Lee et al. 2013). From the result of TGA/DTG for pine and bamboo sawdust, pyrolysis temperature 350°C and 500°C were selected to represent two degradation phases during biochar production.

Appendix D. SMX removal at different solid to solution ratio

The SMX removal percentage at different solid to solution ratio was conducted by varying the mass of sorbents. The volume of solution was kept constant at 30 ml and septic effluent was spiked with 200 ppb SMX. The results were summarized in figure A-D-2.

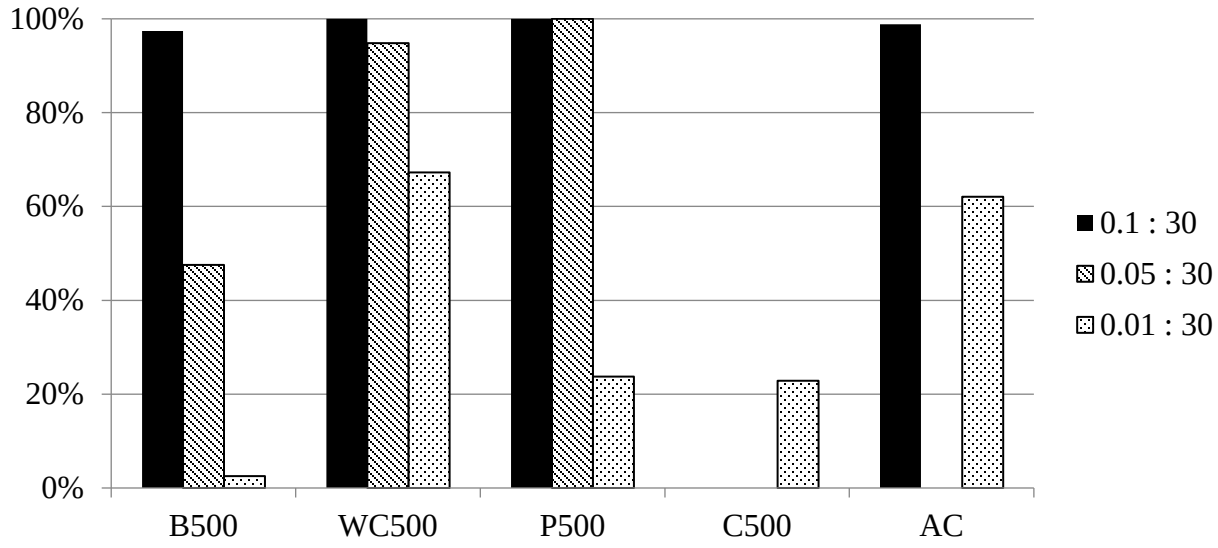

Figure D-1. Removal percentage of SMX from wastewater using different solid to solution ratio.

Appendix E. Adsorption Kinetics of SMX on activated carbon

Adsorption kinetics of SMX on activated carbon were performed with 0.01 g of AC with 30 ml of septic effluent spiked with 200 ppb of SMX. The data were fitted to the kinetics models and the two best fitting models were presented in figure E-2. The best fit with highest R^2 values and lowest SSE were shown in table E-2.

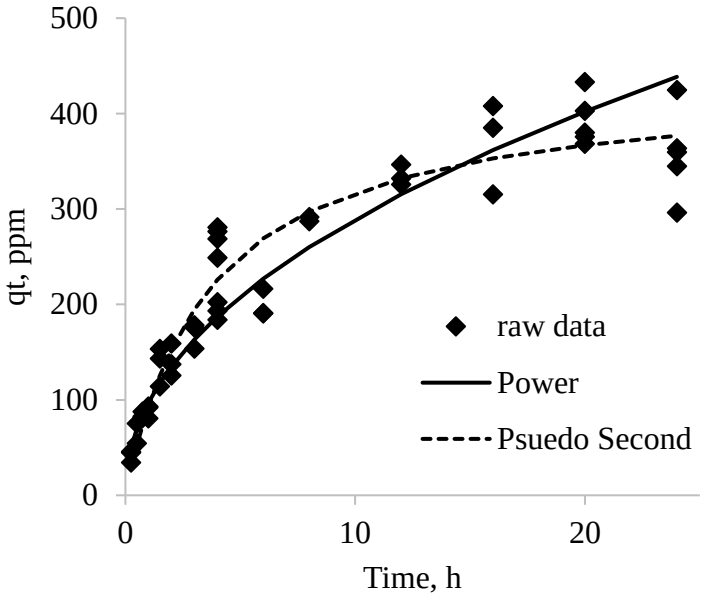

Figure E-1. Kinetics of SMX adsorption on activated carbon and the two models with lowest R^2 values.

Table E-1. Results of AC kinetics with best fit model.

Sorbents	Best Fit Model	R^2	SSE	Parameters
Commercial AC	Pseudo-Second	0.9514	54568	k_{p2}=0.27ppm^{-1}h^{-1}; q_e=4.3 x10^{2}ppm; $k_{p2}q_e^2$=5.0x10^{4}ppm/h;

Appendix F. Adsorption kinetics of SMX on commercial biochar

The modeling of the SMX adsorption kinetics on commercial biochar was conducted and residual plots were generated to examine the randomness of residuals, as shown in figure F-1.

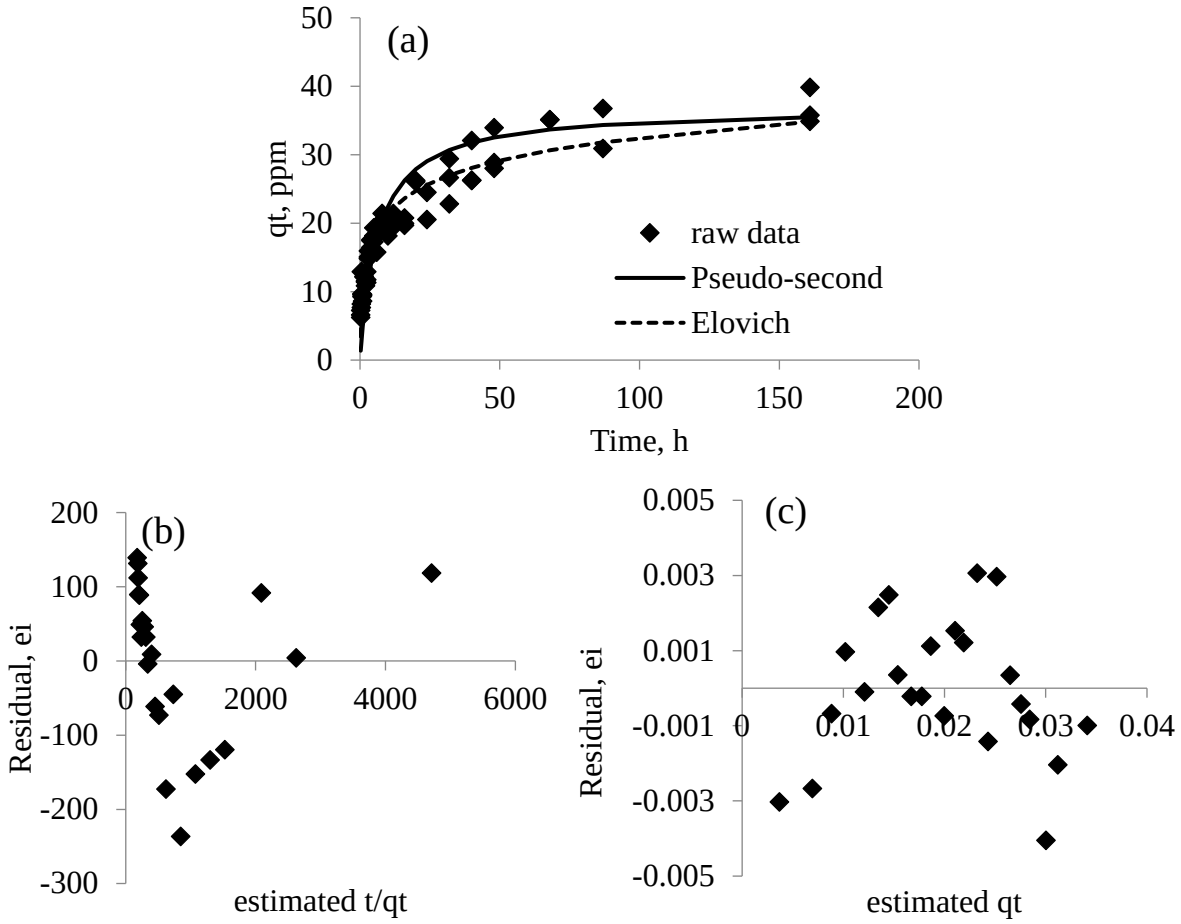

Figure F-1. Kinetics of SMX adsorption on commercial biochar. (a) Fitting of the raw data with the two models with highest R^2 values; (b) Residual plot of Pseudo-second model. R^2 = 0.9804, SSE = 1099; (c) Residual plot of Elovich model. R^2 = 0.9199, SSE =384.

Appendix G. The correlation of K_d^{eff} and the physicochemical properties of biochars.

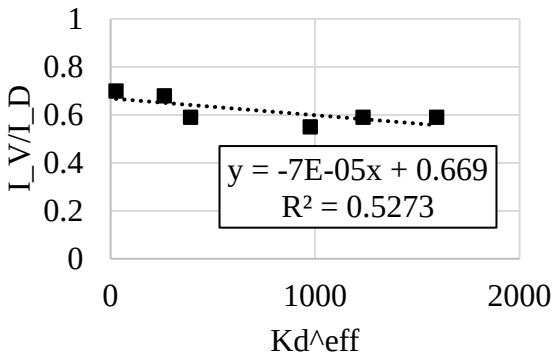

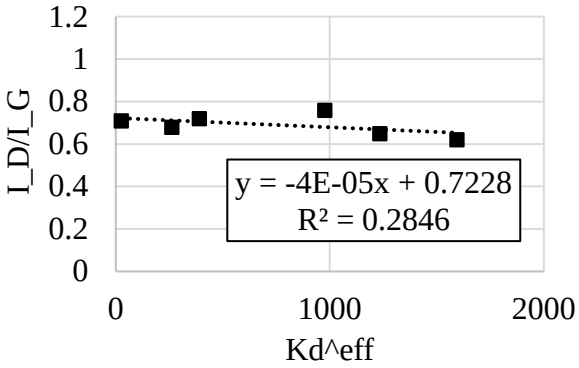

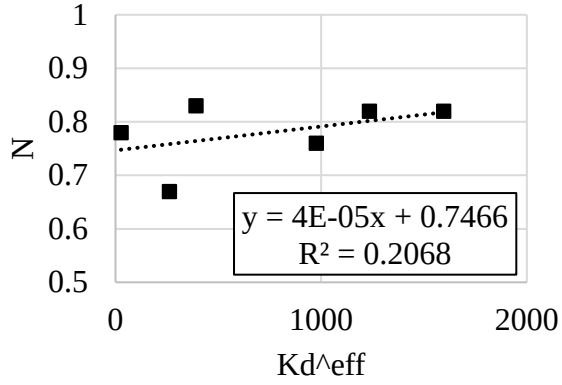

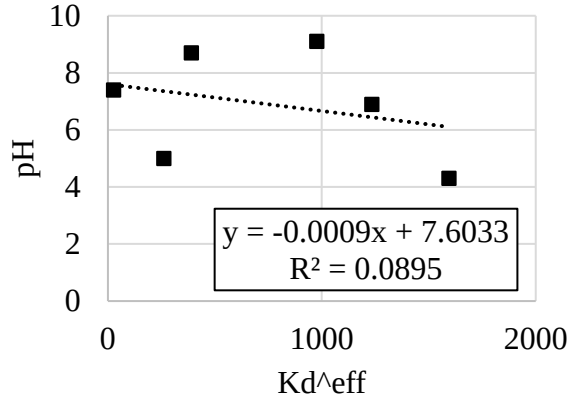

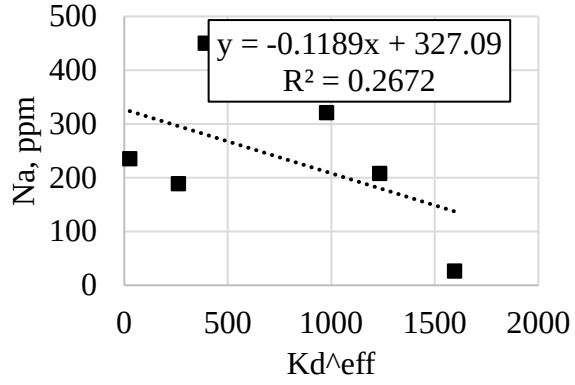

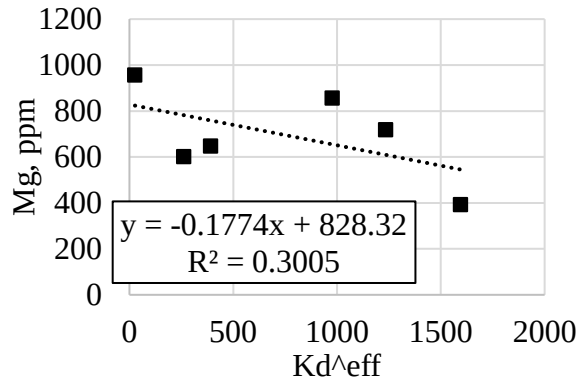

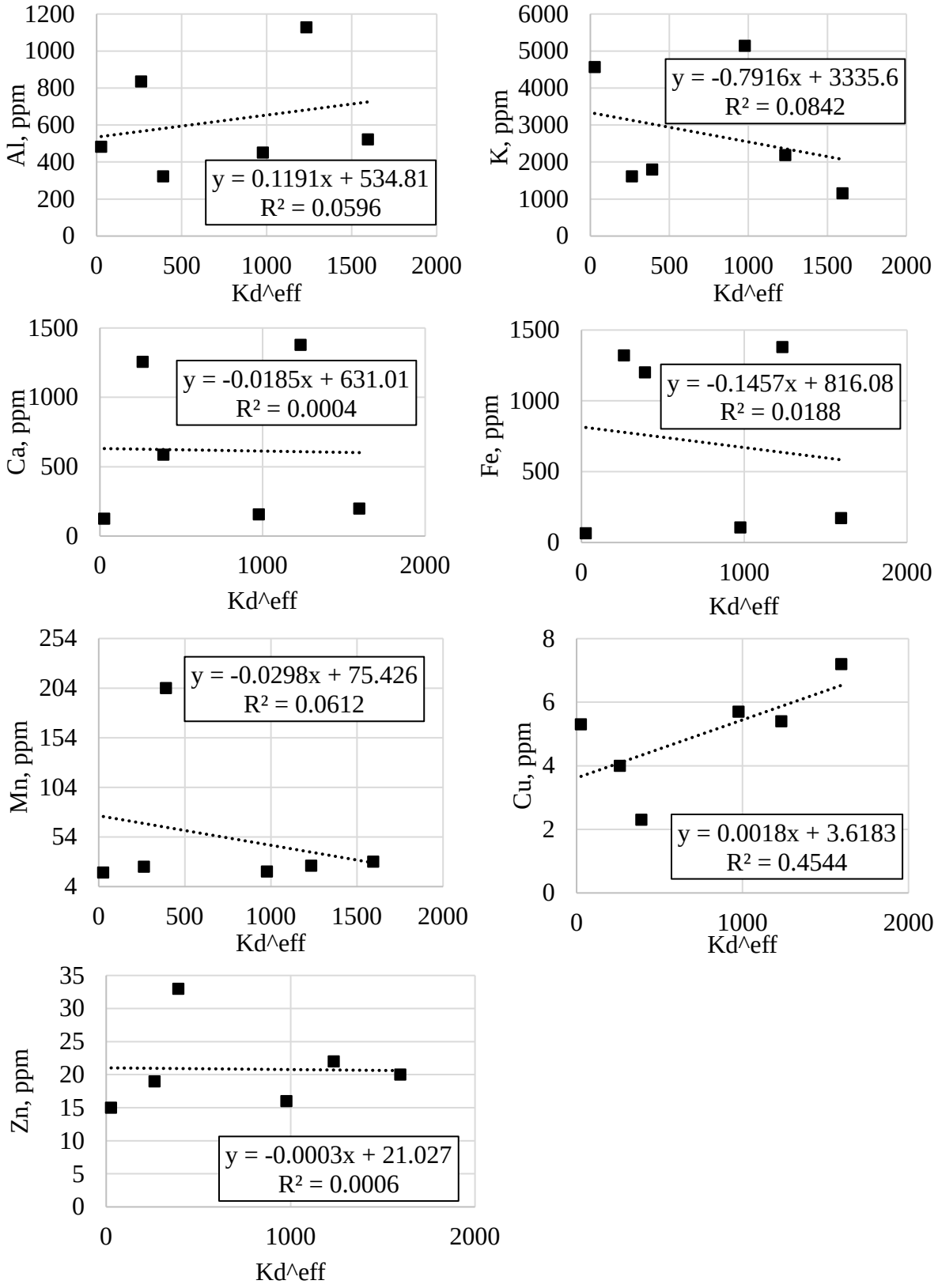

Figure G-1. Correlation of effective K_d of SMX and the physicochemical properties of biochars.

Appendix H. Transport of bromide and SMX in the three columns.

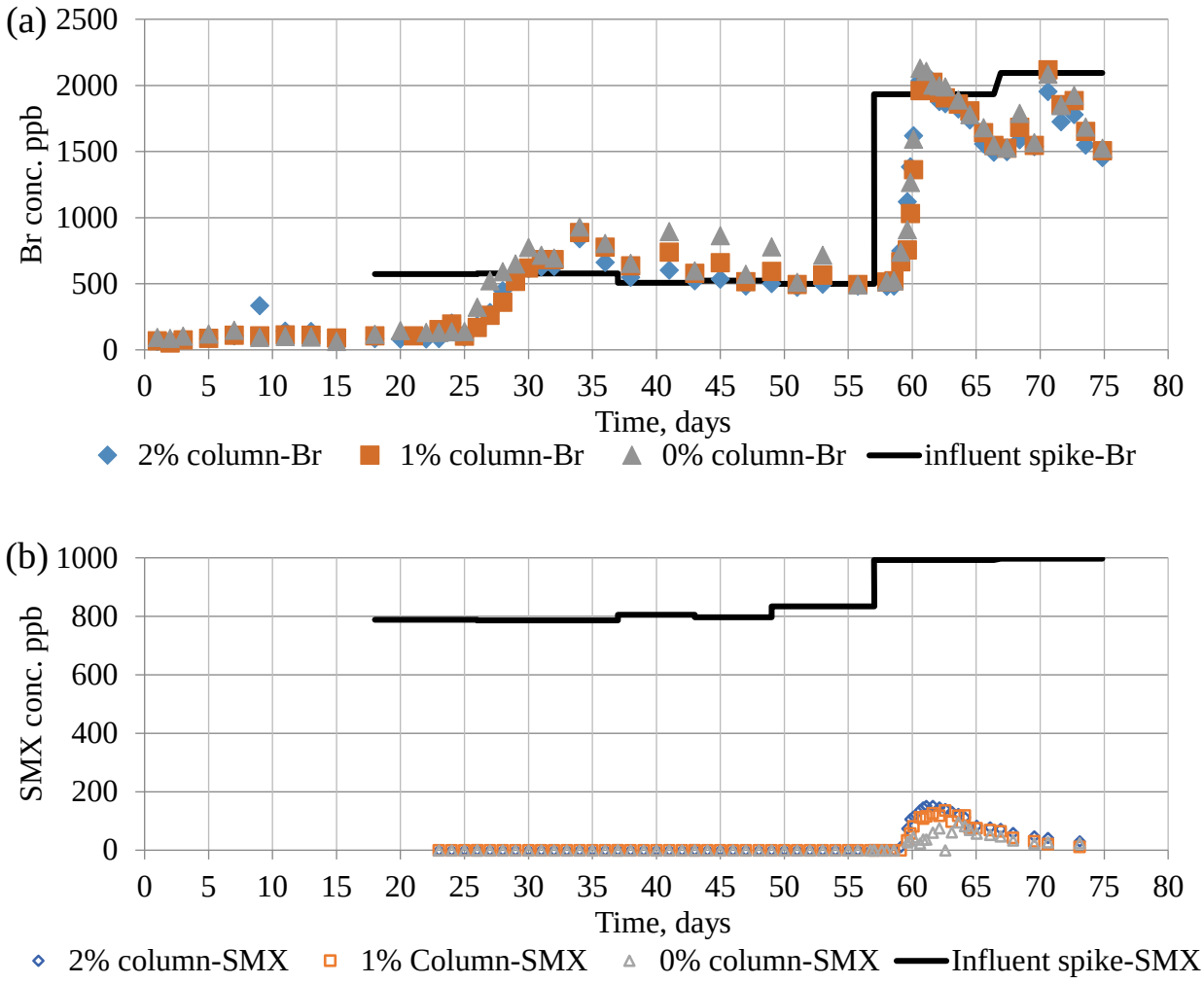

Figure H-1. Transport of bromide and SMX over time (a) bromide (b) SMX

Appendix I. Effect of analysis sequence in ion chromatography test on bromide concentration.

One sample collected at the effluent of soil column experiments was added to several IC vials and analyzed in sequence in one analysis batch with IC system. The resulted concentration derived from the same calibration curve were plotted against the order of the vial in the sequence (figure I-1).

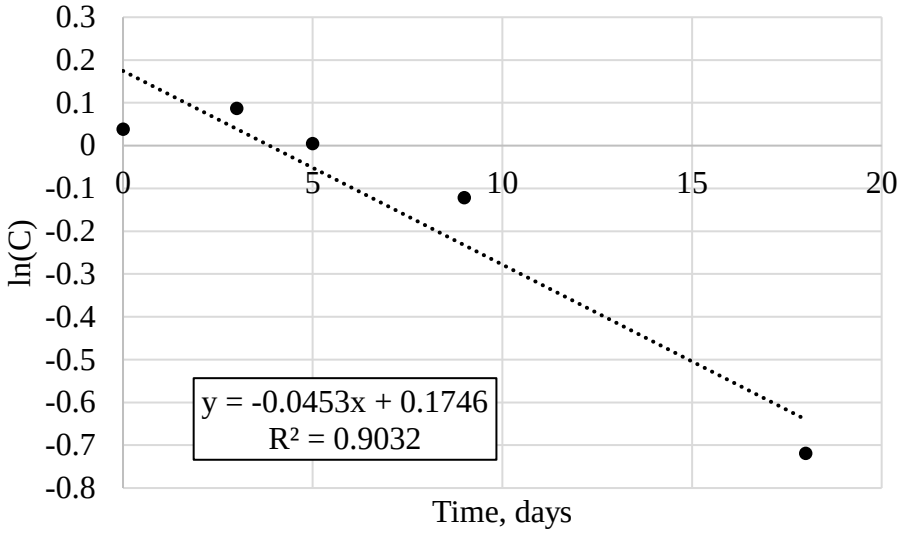

Figure I-1. First-order kinetics of the degradation of SMX in wastewater + soil sample under anoxic conditions from chapter III. k = - 0.0452 day^{-1}, ln C_0 = 0.1746. The unit of concentrations were in ppm.

Appendix J. Analysis for the contribution of calcium from soil to the reduction of sulfate in the soil column.

The exchangeable cations of soil at neutral pH was summarized in table J-1.

Table J-1. Exchangeable cations of soil at neutral pH, C_{Soil}. Unit is ppm per unit weight of soil. The standard deviation is determine for a sample volume of 3.

Na	Mg	Al	Ca	K	Fe
11.1±2.1	16.7±1.1	6.9±4.2	1127.7±8.1	23.2±1.2	4.7±2.8

To maintain a sulfate concentration $C_{sulfate}$ as low as 500 ppb, the calcium concentration $C_{calsium}$ required in the solution was calculated to be as least 9.48 mol/L (solubility constant K_{sp}= 4.93 x 10^{-5}), as shown below:

$$C_{caulsium} = \frac{K_{sp}}{C_{sulfate}} = \frac{4.93 \times 10^{-5}}{500 \times 10^{-9} ppb \times 1000 \frac{g/L}{ppb} \div 96 g/mol} = 9.48 \text{ mol/L}$$

For a total volume V of 7000 ml (total volume of effluent for the whole operation), total calcium needed would be:

$N_{calcium} = C_{caulsium} \times V = 9.47 \text{ mol/L} \times 7\text{L} = 66.4 \text{ mol.}$

However, the total exchangeable calcium for 3.5 kg soil in each column was:

$$N_{soil,calcium} = C_{calcium,\ soil} \times Mass_{soil} = 1128 ppm \times \frac{10^{-6} g/g}{ppm} \times 3500 \text{ g} = 3.9 \text{ g}$$

which is 0.1 mol. The total exchangeable cation in soil is 0.15% of the required calcium.

Therefore, sulfate precipitation by calcium from soil is not a major contributor for the sulfate reduction observed in the column experiment.

Appendix K. Effect of analysis sequence in ion chromatography test on bromide concentration.

One sample collected at the effluent of soil column experiments was added to several IC vials and analyzed in sequence in one analysis batch with IC system. The resulted concentration derived from the same calibration curve were plotted against the order of the vial in the sequence (figure K-1).

Lower bromide concentration was measure for the same solution as it was analyzed for more times. The column needs to be flushed with DI water to restored the good condition for analysis.

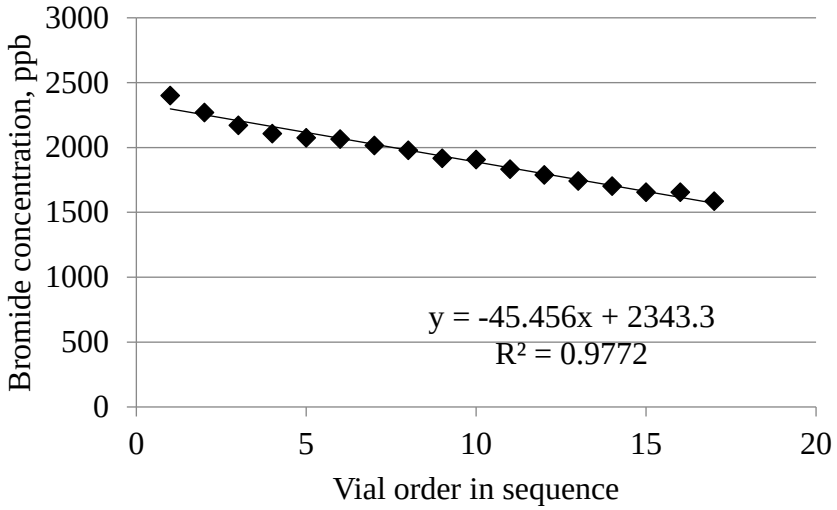

Figure K-1. Changes of detected bromide concentrations with the vial order in the sequence of IC system.

References

Brown, J. R. (1998). Recommended chemical soil test procedures for the North Central Region. Missouri Agricultural Experiment Station, University of Missouri--Columbia.

Chaula, Z., Said, M., John, G., Manyele, S. and Mhilu, C. (2014). "Modelling the Suitability of Pine Sawdust for Energy Production via Biomass Steam Explosion." *Smart Grid and Renewable Energy* Vol.05No.01, 7.

Hernandez-Mena, L. E., Pecora, A. A. B. and Beraldo, A. L. (2014). "Slow Pyrolysis of Bamboo Biomass: Analysis of Biochar Properties." *Iconbm: International Conference on Biomass, Pts 1 and 2* 37, 115-120.

Lee, Y., Park, J., Ryu, C., Gang, K. S., Yang, W., Park, Y. K., Jung, J. and Hyun, S. (2013). "Comparison of biochar properties from biomass residues produced by slow pyrolysis at 500 degrees C." *Bioresource Technology* 148, 196-201.